5-1-2009

Role of spatial organization in ErbB receptor family signaling and identification of ErbB3 as a potential anticancer target

Shujie Yang

Shujie Yang
Candidate

Biomedical Sciences
Department

This dissertation is approved, and it is acceptable in quality and form for publication on microfilm:

Approved by the Dissertation Committee:

Bridget Wilson, Chairperson

Kim Leslie MD

James N Olivier

Marie Lidke

Accepted:

Dean, Graduate School

Date

ROLE OF SPATIAL ORGANIZATION IN ERBB RECEPTOR FAMILY SIGNALING AND IDENTIFICATION OF ERBB3 AS A POTENTIAL ANTICANCER TARGET

BY

SHUJIE YANG

B.S., Biochemistray, Beijing Normal University, 1993

M.S., Biochemistry, Beijing Normal University, 1998

DISSERTATION

Submitted in Partial Fulfillment of the
Requirements for the Degree of

Doctor of Philosophy
Biomedical Sciences

The University of New Mexico
Albuquerque, New Mexico

May 2009

Acknowledgements

I sincerely give my thanks to many people during my graduate study from 2004 to 2008. I would like to thank all my colleagues in the "OWL" laboratory, especially Mary Ann Raymond-Stintz for great help of the immunoelectron microscopy data presented here. Mary helped me, supported me and cheered me up for the duration of this dissertation project. I would like to thank Nick Andrews for many helpful discussions, Marina Martinez for *in vitro* kinase assays and lab management, and Sheli Ryan for cell culture. I would also like to thank Shalini Low-Nam for help to conjugate ligands and many helpful discussions, WenXia Ying and Jun Zhang for assistance with statistical analysis and Dr. Tomas Mazel, Christy Tarleton, and Janet Pfeiffer for general help. I appreciate my committee members, Dr. Kimberly Leslie and Dr. Jeremy Edwards, for their constant support and insightful suggestions. I thank Dr. Diane Lidke for her expertise in designing the FRAP assay and for close supervision. I thank Dr. Janet Oliver for her enthusiastic support. And, most importantly, I would like to thank Dr. Bridget Wilson (my dear mentor) for accepting me into her lab and for her continued support and training thoroughout my graduate studies.

I also would like to thank people in Dr. Larry Sklar's laboratories for ligand binding affinity assays and flow cytometry usage. Dr. Bruce Edwards, Dr. Tione Buranda, Dr. Alexandre Chigaev, Susan Young, Dr. Yang Wu and Mark Carter all made useful contributions. Brandy Comyford was especially helpful for sorting cells and assistance with the use of the Flow Cytometer. Special thanks go to the people in neighboring laboratories who were always nice to me.

Special thanks goes to Dr. Marilyn Smith, University of Kansas, for generating the ErbB3 (E933Q) mutation vector that is so important to Chapter 3.

Finally, I thank my family -- my dear husband as well as my colleague, Dr. Xiangbing Meng, and my daughter Wendy Meng – for their continued support and love.

ROLE OF SPATIAL ORGANIZATION IN ERBB RECEPTOR FAMILY SIGNALING AND IDENTIFICATION OF ERBB3 AS A POTENTIAL ANTICANCER TARGET

BY

SHUJIE YANG

ABSTRACT OF DISSERTATION

Submitted in Partial Fulfillment of the
Requirements for the Degree of

Doctor of Philosophy
Biomedical Sciences

The University of New Mexico
Albuquerque, New Mexico

May 2009

Role of spatial organization of ErbB receptors family signaling and identification of ErbB3 as a potential anticancer target

by

Shujie Yang

B.S., Biochemistry, Beijing Normal University, 1993

M.S., Biochemistry, Beijing Normal University, 1998

Ph.D., Biomedical Sciences, University of New Mexico, 2009

ABSTRACT

The ErbB family of receptor tyrosine kinases plays an important role in the development and pathogenesis of many cancers and two of its members, ErbB1 and ErbB2, are already important cancer therapeutic targets. The first goal of this project was to evaluate novel aspects of ErbB signaling complexity, by studying fine-scale membrane organization of three ErbB receptors (ErbB1, ErbB2 and ErbB3) under conditions of receptor overexpression and ligand-induced signaling in breast cancer cells. We used innovative immunoelectron microscopy techniques to map the relative proximity of ErbB family members on SKBR3 breast cancer cell membrane sheets, before and after introduction of ligands. Based upon statistical evaluation of TEM images acquired from double-labeled membrane sheets, we demonstrate that ErbB receptors are predominantly involved in homo-interactions, with markedly less heterodimerization than predicted by previous studies.

A second focus was ErbB3, the ErbB family member with impaired kinase activity, that

has recently been implicated in escape from ErbB-targeted tumor therapies. Our work suggests that at least two mechanisms amplify ErbB3 signaling and render it partially independent of its preferred heterodimerizing partner, ErbB2. First, robust tyrosine kinase activity in ErbB3 immunoprecipitates from Heregulin-stimulated SKBR3 cells suggests that ErbB3 may compensate for its poor catalytic capabilities by association with an unknown cytoplasmic tyrosine kinase. Second, we discovered that SKBR3 cells express two ErbB3 alleles, the wild type form and a form with a single kinase domain substitution (E933Q). We found ErbB3 activation in SKBR3 cells, and in transfected CHO cells, is only partially blocked by the therapeutic antibody 2C4 (Pertuzumab), that blocks heterodimerization with ErbB2. Remarkably, the E933Q substitution increases ligand binding affinity and amplifies the phosphoinositol 3-kinase (PI3K)/AKT cell survival/ mitogenic pathway. These results suggest that multiple mechanisms contribute to ErbB3's critical roles in tumor survival and, further, that ErbB3 and its cytosolic partners are potential therapeutic targets.

These studies have revealed novel aspects of ErbB receptor membrane organization during signaling and provide the first description of an ErbB3 gain-of-function mutation. This work advances the understanding of the molecular, structural and biological characteristics of the ErbB family and offers insight into mechanisms underlying ErbB-targeted therapies.

Table of Contents

List of Figures

Chapter 1:

Chapter 2:

Chapter 3:

Chapter 4:

Chapter 5:

List of Tables

Chapter 1. General Introduction

1.1 The timeline of EGFR and its ErbB family members

Epidermal growth factor receptor (EGFR) and the other ErbB family members (named for their homology to the erythroblastoma viral gene product, *v-erbB*) have been studied for more than 40 years. After EGF was identified as a "tooth-lid" factor in 1962, four family members were discovered sequentially (see Figure 1.1, (Citri et al. 2006). In the mid 1990s, ErbB family members and their ligands were established to play crucial roles in epithelial cell development since ErbB receptor knockout mice die at early stage of development. ErbB family members have also been shown to contribute to cancer progression and many anticancer therapeutics targeting ErbBs are used in the clinic.

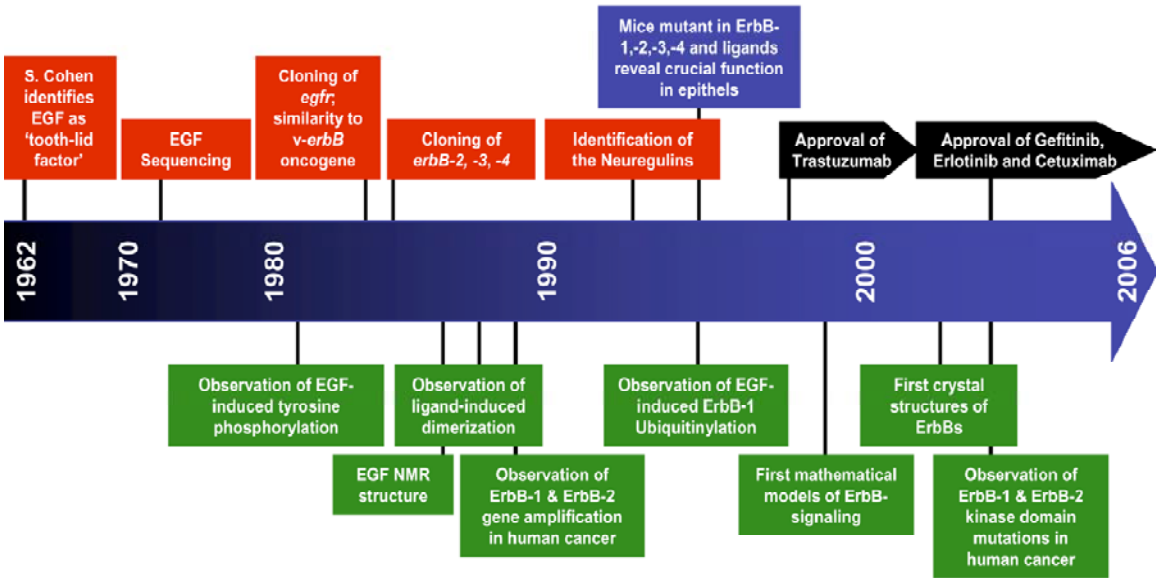

Figure 1.1 The timeline of ErbB family discovery
(from *Nature Reviews Molecular Cell Biology*, (2006) 7: 505-516)

1.2 ErbB family members and signal transduction

Receptors for growth factors mediate a variety of cellular response to the environment. The epidermal growth factor (EGF) receptor EGFR/ErbB1/Her1 and three family members (ErbB2/Her2/Neu, ErbB3/Her3, and ErbB4/Her4) continue to yield important biological and mechanistic insights that are informative for the entire receptor tyrosine kinase (RTK) field. The four ErbB receptors recognize thirteen different but structurally related growth factors and mediate processes in development, homeostasis and pathologies. Each of the receptors is a type I transmembrane protein consisting of a heavily glycosylated and disulfide-bonded ectodomain that provides a ligand binding site, a single transmembrane domain, an intracellular protein-tyrosine kinase catalytic domain and a tyrosine-containing cytoplasmic tail (Yarden et al. 2001; Linggi et al. 2006; Wieduwilt et al. 2008).

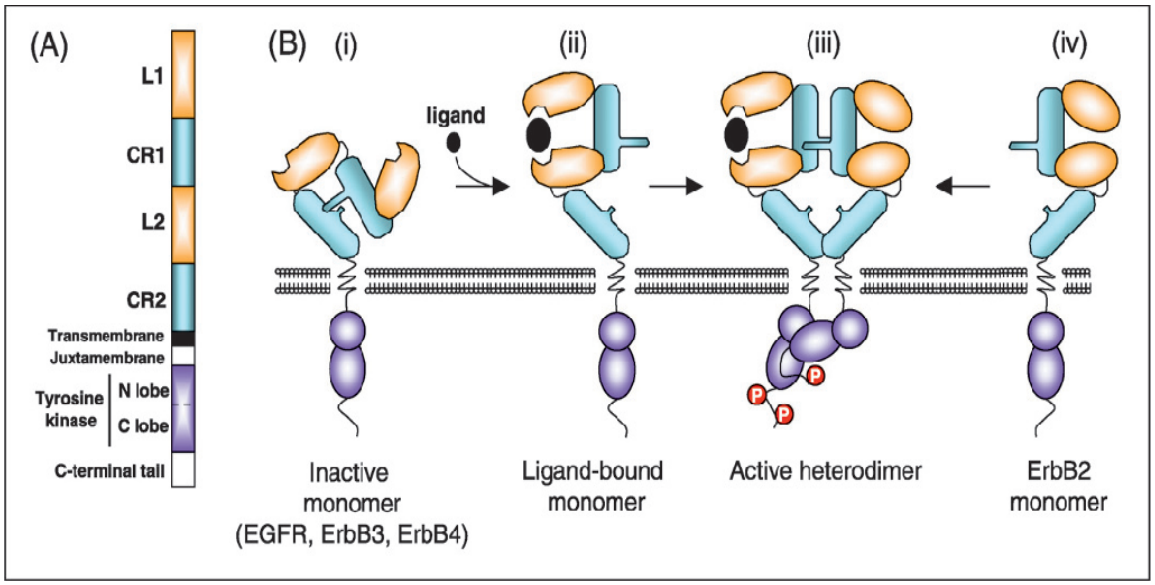

Figure 1.2 Structure diagram of ErbB family
(from *Cell. Mol. Life Sci.*, (2008) 65: 1566-1584)

Growth factor binding to the ectodomain activates the cytoplasmic tyrosine kinase, stimulating signaling pathways that direct cellular responses. Upon ligand binding, the ErbB receptors form homo- or hetero-dimers and are trans-phosphorylated on tyrosine residues in their cytoplasmic tails. Specific phosphotyrosine sites then serve as docking sites for the recruitment of cytoplasmic adaptor proteins and enzymes, initiating signaling cascades that control multiple cellular processes. Post receptor signaling by activated ErbBs includes four representative pathways: the Ras-Raf/MAP-K kinase and STATs pathways that mainly regulate cell proliferation and differentiation, the PI3K/Akt cascade that is important for cell survival and the phospholipase Cγ (PLCγ) pathway that control calcium-dependent events (Figure 1.3, (Marmor et al. 2004).

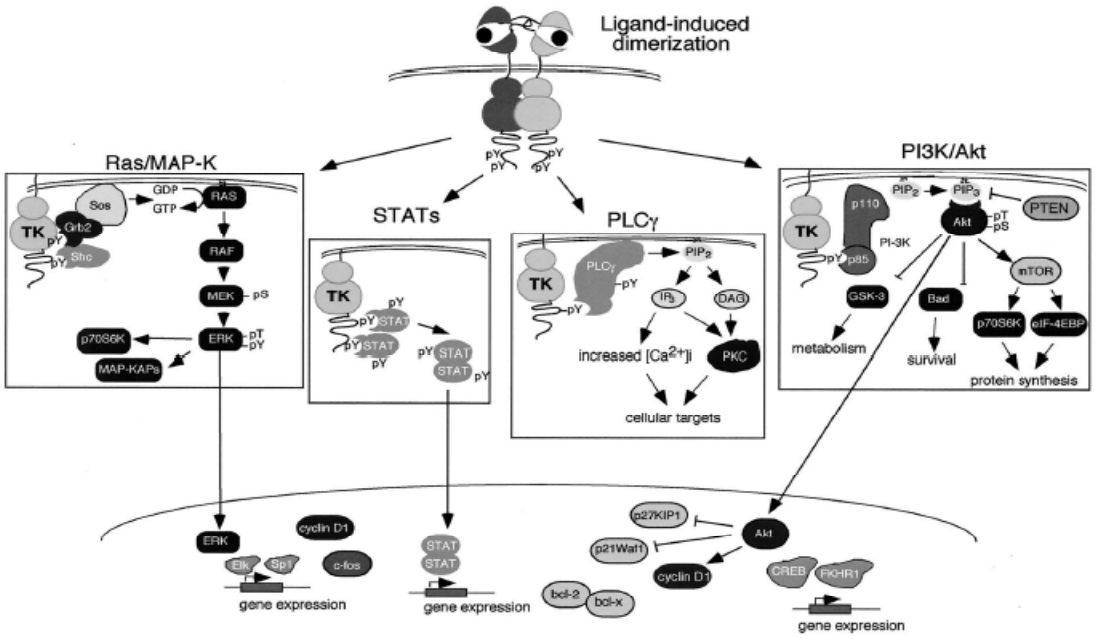

Figure 1.3 The signaling pathways initiated by ErbB family (from *Int. J. Radiation Oncology Biol. Phys.*, (2004) 58:903-913)

Although these signaling pathways are commonly attributed to all RTKs (Yarden et al. 2001; Linggi et al. 2006), the relative efficiency is highly variable and dependent upon

the strength of coupling for individual adaptor proteins to the cytoplasmic tails of individual RTKs.

1.3 ErbB receptors as target for cancer therapy

Mutations, gene amplification and protein overexpression of ErbB family members are all linked to carcinogenesis (Roskoski 2004). These aberrantly activated ErbBs are excellent candidates for selective anticancer therapies. Currently, two classes of drugs

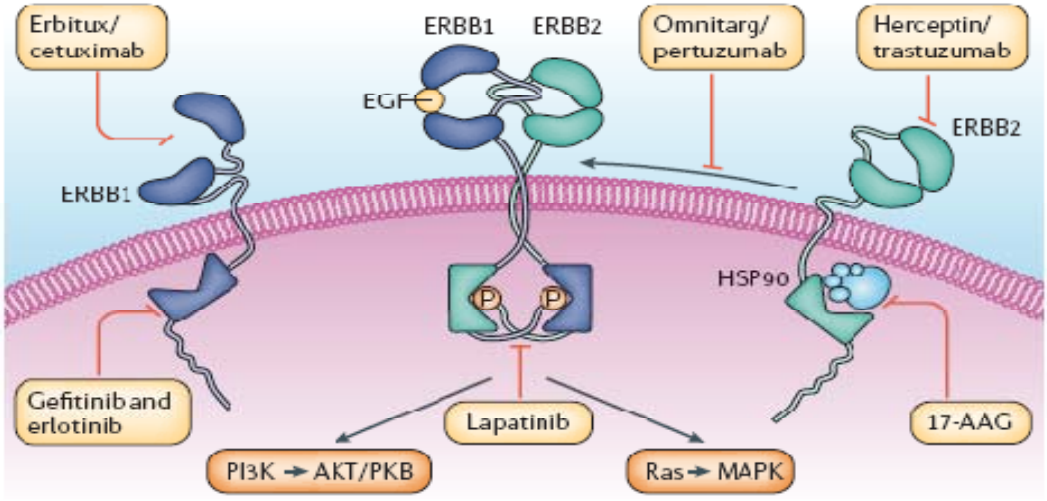

Figure 1.4 ErbB family and cancer therapy
(from *Nature Reviews Molecular Cell Biology*, 2006, 7:505-516)

that target ErbB family members are used in the clinic or in advanced preclinical developmental stages (Figure 1.4) (Citri et al. 2006). One class is a broad group of cell-permeable tyrosine kinase inhibitors (TKIs). These small molecules target the active kinase domains of ErbB1, ErbB2 and ErbB4 and typically compete with ATP binding.

Examples include: Gefitinib (Iressa), Erlotinib (Tarceva) and Lapatinib (Tykerb). Another class is based upon "humanization" of antibodies directed against the extracellular domain of ErbB1 or ErbB2. These expensive drugs must be administered by injection and are designed to prevent ErbB dimerization and/or to induce anti-tumor immune responses. This category includes Trastuzumab (Herceptin, anti-ErbB2), Cetuximab (Erbitux, anti-ErbB1) and Pertuzumab (Omnitarg; anti-ErbB2, in Phase II clinical trials) (Hynes et al. 2005). Because response to these therapies is often mixed, there is a great need for new mechanistic insights and molecular classifications that may lead to individualized therapies.

1.4 ErbB3 tyrosine kinase activity overview

ErbB3 has received less attention as a cancer therapeutic target, principally because of early studies that established it as an impaired or dead kinase. The sequence of the ErbB3 gene was first published in 1989 (Kraus et al. 1989), along with the observation that ErbB3 was overexpressed 100 fold in two mammary cell lines when compared to control cells. ErbB3 was also markedly elevated in 6 of 17 human mammary carcinomas examined. However, the ErbB3 kinase domain is only 64 and 67% identical to the kinase domains of ErbB1 and ErbB2, respectively, with important amino acid substitutions in the catalytic domain. ErbB3 kinase activity was called into question by collaborators at Cornell and Harvard in 1994 (Guy et al. 1994), who expressed intact bovine recombinant ErbB3 in insect cells and performed *in vitro* kinase assays. That study concluded that ErbB3 was poorly capable of autophosphorylation or phosphorylating an exogenous peptide substrate, with the conclusion that ErbB3 kinase activity is at least 100 fold lower

than that of ErbB1. It is notable that the Guy study could not consider the contribution of ligand binding upon ErbB3 activity, since it preceded the discovery of ErbB3 ligands. A subsequent study by Sierke (Sierke et al. 1997) completely failed to detect activity in recombinant kinase domain preparations, leading to the broadly used description of ErbB3 as a "dead kinase". While the Guy study found bovine ErbB3 capable of binding ATP analogues, Sierke concluded that rat ErbB3 completely lacked the ability to bind ATP. One other study during this period differed with these conclusions, based upon characterization of chimeric EGFR/ErbB3 proteins in transfected NIH-3T3 cells (Kraus et al. 1993). The chimeric receptor was highly expressed (0.6-1 million receptors/cell) and constitutively phosphorylated, with measurable *in vitro* kinase activity. Based upon personal communication with the senior author (Aaronson), there have been subsequent concerns about interpretations of results from the NIH-3T3 model system due to endogenous ErbB expression. To our knowledge, there have been no followup studies regarding ErbB3 kinase activity since the 1990s. Most of the current literature cites the Guy and Sierke papers and discounts the possibility of ErbB3 kinase activity.

Relevant to this are the structural studies by Zhang and colleagues (Zhang et al. 2006), who developed the asymmetrical kinase domain model for the dimerization of ErbB family members. In this model, the kinase domains of ErbBs are characterized by separate (but connected) N-lobes and C-lobes. The N-lobe of one receptor in the dimer is presumed to be responsible for activating the catalytic activity of the second receptor's C-lobe. Thus the N-lobe is an "activator", while the C-lobe functions as "acceptor" for kinase activation. Zhang proposes that ErbB3 amino acids substitution in the N-lobe should render it a poor "activator", while ErbB3 contains all key amino acids in the C-

lobe to be a good "acceptor". Figure 1.1 shows a simplified illustration of the asymmetrical kinase domain model.

1.5 ErbB3 is a critical factor in cancer progression

Despite the controversy over ErbB3 kinase activity, recent studies have shown that ErbB3 is a critical factor in the escape from therapies that target ErbB1 and ErbB2 in lung and breast cancer (Engelman et al. 2007; Sergina et al. 2007). In early 2007, ErbB3 was implicated in the escape of two breast cancer cell lines from the small molecule inhibitor, gefitinib, targeting ErbB2 and ErbB1. The authors proposed that ErbB3 phosphorylation was upregulated by "Akt-driven negative feedback signaling loops" and that this ultimately led to resistance to the TKIs (Sergina et al. 2007). Six months later, ErbB3 was shown to be trans-activated by a distantly related RTK, MET, that was amplified in ~20% of geftinib-resistant lung cancer cell lines (Engelman et al. 2007). Coprecipitation studies by Engelman led to the conclusion that ErbB3 is capable of hetero-dimerizing with MET. In addition, a wealth of information on ErbB3 expression in primary tumors and cultured cancer cells has revealed that increased ErbB3 mRNA or ErbB3 protein levels correlate with poor prognosis in multiple human cancers, including those of breast, ovaries, prostate, gastrointestinal and lung (Sithanandam et al. 2008). Therefore, understanding the pivotal role for ErbB3 in cancer should lead to new strategies for cancer therapy.

1.6 Possible ErbB3 interacting proteins

Sequence analysis of ErbB3 revealed potential binding site for Shc, Grb7, Grb2, Src and

the p85 regulatory subunit of PI3K. These proteins have been confirmed by many studies and are referred to as "traditional" ErbB3 binding proteins in Table 1.2 below. Other potential ErbB3 interacting proteins were recently suggested by yeast-two-hybrid assays and proteomics studies (Jones et al. 2006). Table 1.2 also lists these potential ErbB3 binding partners and their possible functions.

Table 1.1 ErbB3 binding partners

Traditional ErbB3 binding proteins

Interacting proteins	Molecular weight	Possible functions related to ErbB3 signaling	Reference
PI3-kinase-p85 subunit	85kD	Initiate PI3-kinase/AKT cell survival/mitogenic pathway	(Soltoff et al. 1994)
Shc	60/52/46kD	Adaptor protein role in Ras/MAP-K pathway and cell proliferation	(Prigent et al. 1994)
Grb7/Grb2	65kD/25kD	Adaptor protein role in integrin signaling and cell migration	(Fiddes et al. 1998)
Src	60kD	Oncoprotein; one study showed ErbB3 passed an anti-apoptotic signal through Src	(Contessa et al. 2006)

Other well studied ErbB3 binding proteins

Interacting proteins	Molecular weight	Possible functions related to ErbB3 signaling	Reference
NRDP1	36kD	E3 ubiquitin ligase, stimulate ErbB3 ubiquitination and rapid degradation	(Diamonti et al. 2002)
PTK6 (BRK)	48kD	Enhance phosphorylation of ErbB3 and downstream activation of Akt	(Kamalati et al. 2000)
PLCγ	150kD	Signal transducer, role in cell proliferation	(Todd et al. 1999)
EBP1	47kD	Bind unphosphorylated ErbB3, reduce cell growth and increase differentiation	(Lessor et al. 2000)

Newly identified ErbB3 binding proteins (Jones et al. 2006).

Interacting proteins	Molecular weight	Possible functions related to ErbB3 signaling
ABL2 (ARG)	145kD	Cytoplasmic tyrosine kinase
RASA1	116kD	Ras regulatory protein
SYK	80kD	Cytoplasmic tyrosine kinase with central signaling roles in hematopoietic cells and a tumor suppressor in mammary cells
CRK	36kD	Adaptor protein
CRKL	36kD	Ras/jun activator
NCK1/NCK2	47kD	Adaptor protein
JAK2	128kD	Janus family tyrosine kinase
VAV1	95kD	Oncogene and member of Rho guanine nucleotide exchange factors
TENC1	152kD	Focal adhesion molecule

1.7 ErbB3 mutations in cancer

Oncogenic mutations in ErbB1, ErbB2 and ErbB4 are well established (Paez et al. 2004; Lee et al. 2006; Soung et al. 2006). Lung adenocarcinomas harboring mutations in the ErbB1 kinase domain strongly correlate with positive clinical response to gefitinib (Iressa) and erlotinib (Tarceva) (Paez et al. 2004). ErbB2 and ErbB4 kinase domain mutations have also been detected in lung, gastric, colorectal and breast carcinomas (Stephens et al. 2004; Lee et al. 2006; Soung et al. 2006). Collectively, these studies indicate that the kinase domains of the ErbB family play important roles in human carcinogenesis.

In this work, we describe the first functional studies of an ErbB3 kinase domain mutation. We note, however, that several ErbB3 mutations and amino acid substitutions have previously been noted by others. Table 1.2 below summarizes the literature on ErbB3 mutations in primary tumors or in established cancer cell lines. Note that residues L690 through T947 correspond to the ErbB3 kinase domain.

Table 1.2 ErbB3 SNP/mutation overview

	ErbB3 gene analysis study	**Principal finding**	**References**
1	Breast (n=25) and lung (n=26) cancer tissues from United Kindom	No mutations detected	Stephens P, 2005, Davies H, 2005
2	208 tissues samples (100 colon, 60 breast, 48 lung) from Korea	One missense mutation (S846I) and one silent mutation (H828H) in kinase domain	Jeong 2006
3	254 established tumor cell lines	9 mutations, G1064E in all samples, 8 other mutation (S1119C, L1177I, N126K, R667H, P1142H, R611W, R1077W and R1089W); none located in kinase domain.	Ruhe, 2007
4	188 lung adenocarcinomas in USA	3 mutations in extracellular domain	(Ding et al. 2008)
5	Genecard collection	*24 SNPs, 4 in kinase domain: S717L, I744T, D758H, A962T	Gene card

*There are 24SNPs/Variants of ErbB3 reported in the ErbB3 GeneCard. They are S20Y, P30L, V105G, T204I, S385N, -429P, L436L, R449I, V530V, L594L, L634L, R683W, S717L, I744T, D758H, A962T (red indicates SNPs located in the kinase domain), K998R, M1055I, R1116R, S1119C, R1127H, L1177I, T1254K, G1271S. These notations are based on the precursor ErbB3, prior to cleavage of the signal peptide. They should be adjusted by -19 to match to the E933Q notation.

1.8 Signal transduction in membrane microdomains

In the past decade, there has been intense interest in roles for membrane microdomains in signal propagation through EGFR family members, as well as GPCRs and immunoreceptors such as the TCR, BCR and FcεRI and others (Edidin 1997; Insel et al. 2005; Luo et al. 2008). These domains have been called "lipid rafts" (Brown & London, 1995); more recently, the Wilson and Davis laboratories proposed the term "protein islands" to emphasize the role of proteins in regulating microdomain organization (Lillemeier et al. 2006). The existence of membrane microdomains was originally proposed based on biochemical analyses of detergent-solubilized, sucrose density fractionated membranes. To avoid the complications introduced by detergents, the UNM laboratories of Wilson and Oliver refined the "rip-flip" method of preparing plasma membrane sheets on EM grids (Wilson et al. 2000; Wilson et al. 2001; Wilson et al. 2004; Wilson et al. 2007; Xue et al. 2007; Yang et al. 2007). These native membrane preparations can be labeled with gold probes recognizing specific proteins (and lipids) and imaged by transmission electron microscopy (TEM). Together with Steinberg (UNM Mathematics and Statistics Dept), the laboratory group has developed a set of computer-aided tools for automated image analysis and statistical analysis of gold particle distributions (Wilson et al. 2004; Zhang et al. 2006; Wilson et al. 2007; Yang et al. 2007; Zhang et al. 2008). *Importantly, this technology offers an unprecedented level of resolution for viewing membrane microdomain organization, revealing the size and changing composition of rafts during signaling.*

1.9 Central hypotheses for this dissertation project

Traditional models of ErbB signal transduction are based upon the prediction that receptors form homo- and hetero-dimers following ligand binding. However, the characteristics of individual family members influence both dimer composition and receptor fate. For example, ErbB1 homodimers are readily formed in the presence of ligand but ErbB1-ErbB2 heterodimers are considered to be equally favored if ErbB2 is also expressed in the cell (Wiley et al. 2003). ErbB2, which is thought to be always in the extended conformation, is considered to be a poor homodimerizing receptor but favored for heterodimerization with any other ErbB (ErbB1, 3, 4) when they bind ligand. ErbB1 homodimers are rapidly endocytosed, while ErbB1-ErbB2 heterodimers are internalized much slower than ErbB1 homodimers (Lidke et al. 2004). The signaling output from homodimers and heterodimers is significantly different, since the phosphorylated cytoplasmic tails of the ErbB family recruit both distinct and partially overlapping sets of signaling proteins.

In this work, we consider the hypothesis that membrane spatial organization influences the dimerization behavior of ErbB family members. This work builds on previous observations that ErbB receptors are non-randomly distributed in the plasma membrane and, in at least some cell types, that ligand activation leads to clusters that are sufficiently large enough to visualize by fluorescence microscopy (Nagy et al. 1999; Nagy et al. 2002; Pike 2005). Anderson and colleagues suggested that signaling by ErbB1 might be regulated in part by residency of resting receptors in caveolae, followed by ligand-induced movement out of these specialized domains with eventual endocytosis

in coated pits. We predicted that novel insight could be gained by using the high resolution electron microscopy method developed in our laboratory. We set out to map the topography of ErbB receptors in SKBR3 cells, derived from an aggressive breast cancer tumor and frequently used as a model system in ErbB signaling (Agus et al. 2002; Sergina et al. 2007; Cai et al. 2008). This cell line expresses very high numbers of ErbB2 (over 2 million), abundant EGFR (~200,000) and intermediate levels of ErbB3. We also evaluated the A431 cell line, that overexpresses ErbB1 (2-4 million) and expresses very little of the other ErbBs, as well as Chinese Hamster Ovary (CHO) cells into which we introduced VFP-chimeras of ErbB family members. Biochemical assays were performed in tandem with the EM studies, allowing for correlation of ErbB distributions on resting and activated membranes with receptor phosphorylation state, kinase activity and recruitment of adaptor proteins. As described in **Chapter 2**, our spatial and biochemical studies raise doubts about the commonly presumed extent of heterodimerization and support our hypothesis that membrane organization plays a role in regulating ErbB signal transduction.

In the course of the membrane topography studies in SKBR3 cells, we made several intriguing observations that led us to focus on ErbB3 in the second phase of work. As discussed above, ErbB3 is traditionally considered to have neglible tyrosine kinase activity. In evaluating ErbB3 dimerization partners using an *in vitro* tyrosine kinase assay, we found that ErbB3 immunoprecipitates from SKBR3 breast cancer cells contained Heregulin-inducible tyrosine kinase activity despite barely-detectable levels of coprecipitating ErbB1 or ErbB2. We further discovered that these cells express two ErbB3 alleles, wildtype (WT) and a single kinase domain substitution (E933Q).

Therefore, we hypothesized that the unexpected ErbB3 tyrosine kinase activity might be attributed to the E933Q mutation, possibly through increased association of the ErbB3 tail with a cytoplasmic tyrosine kinase or through restoration of ErbB3's own integral tyrosine kinase activity. As a model system, we compared the signaling capabilities of ErbB3 (WT) and ErbB3 (E933Q) using stably-transfected CHO cells. Our work, described in full in **Chapter 3**, suggests that the E933Q mutation does not restore unexpected ErbB3 kinase activity. Instead, we found that it leads to enhanced signaling through the ErbB3-PI3K-AKT cell survival pathway by converting a portion of receptors to a high affinity state. Although we have been unable to definitively resolve the question of whether the robust kinase activity in ErbB3 immune complexes is attributed to an associated tyrosine kinase, a prominent 50kDA tyrosine-phosphorylated protein remains a candidate for coupling to ErbB3 in SKBR3 (but not CHO) cells. This work has led to revision of the original hypothesis. We now propose that the E933Q mutation may fall into a general class of RTK mutations that can alter signaling by influencing ligand affinity, consistent with previous descriptions of EGFR mutations L834R and ΔL723-P729insS (Choi et al. 2007). Based upon studies using 2C4 antibodies that block ErbB2 heterodimerization, we also hypothesize that ErbB3 signaling can be partially independent of ErbB2 and therefore may represent a new therapeutic target.

Chapter 2

Mapping ErbB Receptors on Breast Cancer Cell Membranes During Signal Transduction

Published in ***Journal of Cell Science,* 2007, 120: 2763-2773**

2.1 Summary

Distributions of ErbB receptors on membranes of SKBR3 breast cancer cells were mapped by immunoelectron microscopy. The most abundant receptor, ErbB2, is phosphorylated, clustered and active. Kinase inhibitors ablate ErbB2 phosphorylation without dispersing clusters. Modest coclustering of ErbB2 and EGFR, even after EGF treatment, suggests that both are predominantly involved in homointeractions. Heregulin leads to dramatic clusters of ErbB3 that contain some ErbB2 and EGFR and abundant PI 3-kinase. Other docking proteins, Shc and STAT5, respond differently to receptor activation. Levels of Shc at the membrane increase 2-5 fold with EGF while preassociated STAT5 becomes strongly phosphorylated. These data suggest that the distinct topography of receptors and their docking partners modulates signaling activities.

2.2 Introduction

The ErbB family consists of four related receptors, ErbB1 (EGFR/Her1), ErbB2 (Neu/Her2), ErbB3 and ErbB4 (Yarden et al. 2001; Warren et al. 2006). These receptors are single-pass transmembrane proteins with an extracellular ligand binding domain and a cytoplasmic tail containing an integral tyrosine kinase domain and multiple tyrosine

phosphorylation sites. Upon ligand binding, the ErbB receptors form homo or heterodimers that are trans-phosphorylated by their active kinase domains. Exceptions are ErbB3, that has very poor kinase activity, and ErbB2, that does not bind ligands. Once phosphorylated, all of the ErbB receptors serve as docking sites for the recruitment of cytoplasmic adaptor proteins and enzymes, initiating signaling cascades that control multiple cellular processes.

Mutations, gene amplifications and protein overexpression of ErbB family members are all linked to carcinogenesis (Roskoski 2004). In particular, ErbB2 is overexpressed in ~30% of all breast cancers and is correlated with poor prognosis (Kraus et al. 1987; DiGiovanna et al. 2005). Importantly, the cooperative interplay between multiple ErbB family members profoundly influences neoplastic transformation and survival (Alimandi et al. 1995; Harari et al. 2000; Tikhomirov et al. 2004). Current models suggest that ErbB2 is the preferred heterodimerizing partner for other ErbBs, with relatively poor homodimerizing capabilities. This is particularly intriguing based upon recent structural studies of ErbB receptors (Burgess et al. 2003). The extracellular domain of EGFR, ErbB3 and ErbB4 have a closed conformation that unfolds upon ligand binding (Burgess et al. 2003; Bouyain et al. 2005). Because ErbB2 constitutively assumes an open conformation, it seems possible that ErbB2 needs to be sequestered from other copies of itself -- or from the ligand binding ErbBs -- to prevent premature signaling. In light of this complexity, the development and use of new, specific therapies tailored to inhibit ErbB targets present both an opportunity and a challenge (Rowinsky 2004).

Signal transduction through ErbB receptors begins at the plasma membrane. Many studies implicate membrane microdomains (lipid rafts, membrane rafts) in signaling via EGFR and other receptors with integral tyrosine kinase activity. Anderson's group provided early evidence that EGF receptors localize to caveolae, considered by many to be a specialized lipid raft structure (Smart et al. 1995). According to one model, EGFR moves out of caveolae following stimulation with EGF (Mineo et al. 1999). Other work has suggested that non-caveolar lipid rafts might sequester EGF receptors, influence their dimerizing and ligand binding properties, or mediate endocytosis (Nagy et al. 2002; Ringerike et al. 2002; Roepstorff et al. 2002; Pike et al. 2005; Puri et al. 2005). Sophisticated fluorescence imaging techniques have documented the large scale clustering of ErbB receptors (Nagy et al. 1999; Ichinose et al. 2004) and demonstrated that EGFR exhibits more restricted diffusion than ErbB2 (Orr et al. 2005). These diverse findings point to the need to better understand the nanoscale relationships of ErbB receptors in the membranes of normal and malignant cells.

Immunoelectron microscopy of native membrane sheets has proven to be a powerful technique for mapping the dynamic behavior of activated FcεRI and BCR, two tyrosine kinase-linked immunoreceptors (Wilson et al. 2000; Wilson et al. 2001; Wilson et al. 2004; Kim et al. 2005). Immunoelectron microscopy has also been applied to the study of Ras isoforms, demonstrating the distinct membrane localization properties of H-Ras and K-Ras (Prior et al. 2003). In the present study, we apply this method to map the topography of ErbB receptors and several of their signaling partners in cultured SKBR3 breast cancer cells. Our results show distinct patterns of membrane clustering for the

different ErbBs. They also reveal distinct recruitment behavior and topographical relationships of ErbBs for different signaling adaptors and enzymes.

2.3 Materials and Methods

Cell lines. SKBR3 cells were obtained from ATCC and grown according to their guidelines. CHO cells stably transfected with EGFR-GFP, erbB2-mYFP or erbB3-mCitrine (Lidke et al. 2004) were gifts of Thomas M. Jovin and Donna Arndt-Jovin (Max Planck Institute). CHO cells were cultured in DMEM, 10% FBS (Hyclone) with pen-strep and L-glutamine.

Reagents. Epidermal growth factor (EGF) was from Biomedical Technologies (Stoughton, MA). Recombinant Heregulin β was from US Biological (Swampscott, MA). AG1478 was from Alexis Biochemicals (San Diego, CA); AG879, PD153035, PP2 and staurosporin were from Calbiochem (LA, Jolla, CA). EGFR specific antibodies were EGFR.1 (Calbiochem, La Jolla, CA) and 610016 (BD Transduction Laboratories). ErbB2 specific antibodies were RB9040 (Labvision), SC-08 (Santa Cruz Biotechnology, CA) and MS-325 (Labvision). ErbB3 SC-285 and SC-415 antibodies, p85 SC-423 antibodies and STAT5 SC-838 antibodies were also from Santa Cruz. Shc 610081 antibodies were from BD Transduction. p85 06-497 antibodies were from UBI (Lake Placid, NY). Anti-phospho694 STAT5 and anti-phospho-ErbB antibodies were from Cell Signaling. HRP-conjugated PY20 was from BD Transduction.

Western blotting and immunoprecipitation analysis. Cells were serum starved (2 hr) then stimulated with ligands. After a PBS rinse, cells were solubilized in cold NP-40 lysis buffer (150 mM NaCl, 50 mM Tris/HCl pH 7.2, 1% NP-40, 5 µg/ml Leupeptin, 5 µg/ml antipain, 1 mM $NaV0_4$, 1 mM PMSF). Lysates were clarified by centrifugation. Protein concentrations were measured by BCA protein assay (Pierce). Supernatants were mixed with 5x sample buffer for SDS-PAGE or used directly for immunoprecipitations. For IP, supernatants were preincubated with Trueblot anti-mouse or anti-rabbit Ig beads (Ebioscience, San Diego, CA), followed by transfer to tubes containing specific antibodies and overnight incubation at 4°C. After 4 washes in lysis buffer, 2× reducing Laemlli buffer was added to beads for SDS-PAGE and subsequent transfer to nitrocellulose membranes. Blocked membranes were probed with 1^o and HRP-conjugated 2^o antibodies, followed by detection of bands by the ECL method (Pierce).

Cytosol/Membrane Fractionation. Cells were serum starved (2 hr); where indicated, inhibitors were added for last hr prior to addition of agonist. Cells were transferred to 4^oC, rinsed with PBS, scaped off and briefly sonicated; unbroken cells and debris were sedimented by microcentrifugation (10 min). Cloudy supernatants were subjected to ultracentrifugation (100,000 x g, 1 hr, 4^oC) to yield membrane and cytosol fractions. Membrane pellets were dissolved in cold NP-40 lysis buffer. Protein concentrations in fractions were determined by BCA assay to normalize samples prepared for SDS-PAGE.

In vitro tyrosine kinase assays. K-LISA EAY kits (Calbiochem, La Jolla, CA) were used to measure kinase activity in receptor immunoprecipitates. Receptors were immunoprecipitated (using EGFR.1 for EGFR or RB9040 for ErbB2) and aliquots of

precipitate-slurry transferred to replicate wells of K-LISA strips. Strips were incubated with and without inhibitors, washed and read on a spectrofluorimeter, according to the manufacturer's protocol.

Flow cytometry to quantify surface expression of EGFR, ErbB2 and ErbB3. Cells were detached with Tris-EDTA/PBS (Sigma) and labeled for 1 hr at 4^{o}C with saturating amounts of FITC-conjugated antibodies against EGFR (sc-120 FITC), ErbB2 (sc-23864 FITC) or ErbB3 (sc-23865 FITC). Calibration beads (Quantum Simply Cellular, Anti-Mouse IgG, Banglabs) were labeled in parallel for each condition. After PBS rinses, samples and beads were analysed by FACScan (BD Bioscience). Receptor numbers were determined based upon the calibration curve generated from the bead standards.

Preparation of Plasma Membrane Sheets and Gold Labeling for TEM. Detailed methods are described in earlier papers (Wilson et al. 2000; Wilson et al. 2001; Wilson et al. 2004). A recent chapter (Wilson et al. 2007) reports both FRAP and single particle tracking experiments demonstrating that PFA fixation immobilizes membrane proteins prior to labeling. In brief, cells were cultured on 15 mm round, clean glass coverslips. After incubation at 37^{o}C +/- stimuli, cells on coverslips were fixed in 0.5-2% PFA (10 min, RT), inverted onto EM grids and ripped. The stronger (2% PFA) fix was used when cells were prelabeled from the outside with immunogold reagents. In all cases, EM grids were incubated in 2% PFA for an additional 20 min after ripping. Grids were glow-discharged and coated with formvar and poly-L-lysine. Washed membranes were labeled from the inside by incubating sequentially with 1^{o} antibodies and gold-conjugated 2^{o} reagents. Sheets were post-fixed with 2% glutaraldehyde (20 min, RT), stained with

tannic acid and uranyl acetate and digital images acquired on an Hitachi H-7500 transmission electron microscope. At least 10 images were taken, from at least 2 separate experiments, for each condition.

Mapping & Analyzing Gold Particle Distributions. Digital images (6.8 megapixel) were analysed using a customized ImageJ plugin to find and count coordinates of 5 and 10 nm particles automatically (Zhang et al. 2006) . Coordinates were analyzed using the Hopkins test for clustering (Jain et al. 1988; Wilson et al. 2004; Zhang et al. 2006). The Ripley's K bivariate function was used to evaluate co-clustering (Haase, 1995; Wilson *et al.,* 2004; Zhang *et al.,* 2005). Markov Random Field simulations were used to account for hidden receptors (Zhang et al. 2008).

2.4 Results

ErbBs cluster when expressed individually in transfected CHO cells

We began this study by establishing the clustering behavior of ErbB family members in the absence of other family members. We used stably transfected CHO cells that lack endogenous EGFR or ErbB3 and have only minute amounts of endogenous ErbB2. Transfectants expressing visible fluorescent protein-fusion chimeras of ErbB2 and ErbB3 were flow-sorted to enrich in cells expressing either high or low numbers of each receptor on the cell surface. The $CHO^{EGFR\text{-}GFP}$ cell line is clonally derived and was not amenable to flow sorting.

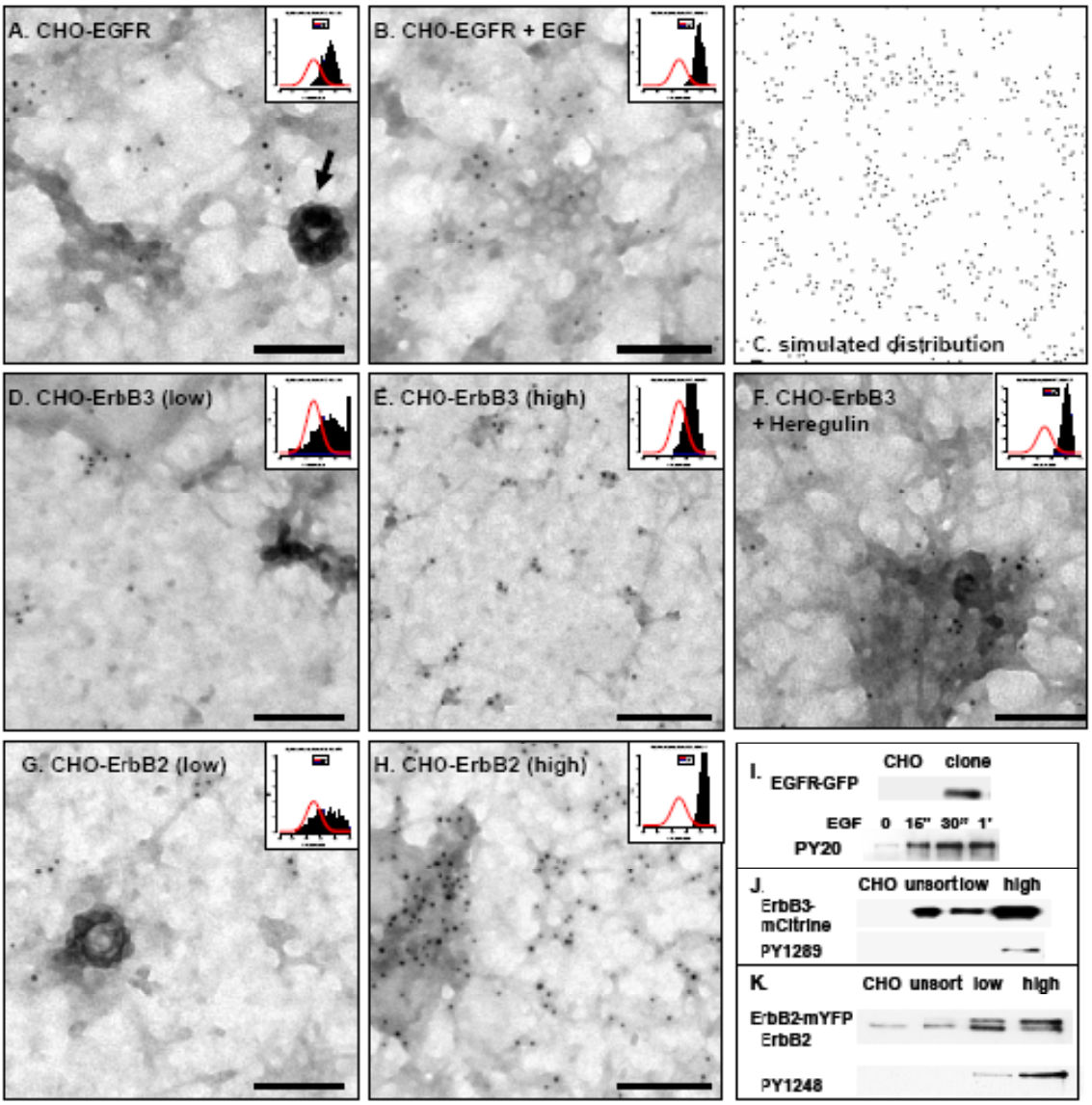

Figure 2.1. ErbB receptors cluster when expressed in CHO cells. Membrane sheets were prepared from CHO cells transfected with EGFR-GFP (A,B), ErbB3-mCit (D-F) or ErbB2-mYFP (G,H) and labeled with specific primary antibodies, followed by secondary antibodies conjugated to 5 nm colloidal gold.CHO-EGFR-GFP cells in (B) were stimulated for 2 min with 20 nM EGF. CHO-ErbB3-mCit cells in (F) were stimulated for 5 min with 3.2 nM Heregulin. EGFR was labeled from the outside with GR-15 antibodies; ErbB3 was labeled from the inside with sc-285 antibodies; ErbB2 was labeled from the inside with RB9040 antibodies. Bars = 0.1 micron. Data in (C) show estimated cluster size and distribution for EGFR in resting cells expressing 80,000 receptors on the cell surface, as determined by Markov Random Field computer simulations. Data in (I) show that only the transfected CHO-EGFR-GFP cells express EGFR; lower panel shows EGFR phosphorylation status before and after addition of 20 nM EGF. Data in J-K report the endogenous levels of ErbB3 (none) or ErbB2 (very low) in parental CHO cells and the levels of chimericreceptors in transfected cells before and after flow sorting; lower panels in each figure report levels of basal phosphorylation in serum starved cells using phosphotyrosine-specific antibodies. Inserts: Hopkins clustering test results. Shifts to the right of the red line indicate that receptors are significantly clustered.

Results in Figure 2.1A show membrane sheets prepared from resting $CHO^{EGFR-GFP}$ cells and labeled from the outside with GR15 anti-EGFR antibodies, followed by 5 nm gold-conjugated secondary antibodies. A coated pit, lacking gold label, is marked with an arrow. This image shows that EGFR is preclustered. The inset in Figure S1 confirms the clustered state of receptors using the Hopkins statistical test for random distributions (Wilson et al. 2004). There were low levels of EGFR tyrosine phosphorylation in resting cells; as expected, EGF (20 nM) led to a rapid increase in phosphorylation (Fig. 2.1I). However, addition of EGF to transfected CHO cells did not markedly change EGFR cluster size (Fig. 2.1B). All results were confirmed by the Hopkins test (insets).

Previous work using the immunogold technique has demonstrated that labeling efficiency rarely approaches 100%. We find that labeling with small gold probes (3-5 nm) typically yields the best results, while labeling with larger probes (10 nm) is markedly less efficient. In double labeling procedures (see Fig. 2.4-2.5, 2.7-2.10), experiments are typically repeated by reversing the sizes of gold to validate co-clustering results. In single labeling procedures, we optimize results by using only small gold probes. In both cases, it is useful to apply computer simulation methods to reconstruct complete data from incomplete data sets. Figure 2.1C shows results of applying Hidden Markov Random Field modeling (Zhang et al, submitted) to simulate the complete distribution of EGFR on the surface of transfected $CHO^{EGFR-GFP}$ cells. This image corrects mathematically and spatially for underlabeling. Assuming 80,000 EGFR/cell, we estimated that 39% and 54% of the EGFR were labeled with 5 nm anti-EGFR gold particles before and after EGF, respectively. The predicted average size of EGFR clusters on the surface of SKBR3 cells is about 7 receptors, although the sizes ranged

from singlets to as many as 80 receptors. We found no significant difference in cluster size before and after activation with EGF.

ErbB3 and ErB2 are also found in small clusters on the surface of transfected CHO cells. Following flow sorting, we compared the average cluster size on cells expressing low (Figure 2.1 D) and high (Fig. 2.1 E, F) levels of ErbB3 or low (Fig. 2.1 G) and high (Fig. 2.1 H) levels of ErbB2. Samples of the sorted cells were also lysed and solubilized proteins were separated by SDS-PAGE, followed by immunoblotting with anti-ErbB3 or anti-ErbB2 antibodies (Fig. 2.1J-K). Results in Figure 2.1D and 2.1E show that ErbB3 cluster size on the surface of resting CHO cells is largely independent of expression levels. Remarkably, the addition of Heregulin (also known as neuregulin 1) leads to formation of significantly larger ErbB3 clusters on the CHO surface (Fig. 2.1F). Consistent with neglible kinase activity of ErbB3 (Guy et al. 1994; Sierke et al. 1997), overexpression alone results in barely detectable phosphorylation of the ErbB3 cytoplasmic tail at tyrosine 1289 (Fig. 2.1J). Addition of Heregulin to $CHO^{ErbB3\text{-}mCit}$ cells also results in a very slight increase in ErbB3 tyrosine phosphorylation (not shown). This might be explained if, as proposed in one early report (Guy et al. 1994), ErbB3 is only a poor kinase and not a completely dead kinase. Alternatively, the very low endogenous expression of ErbB2 may support small amounts of kinase-competent ErbB3-ErbB2 heterodimers.

In contrast to the other family members, ErbB2 has no known ligand. We noted that, although most clusters in CHO cells overexpressing ErbB2-mYFP remain small, occasional very large clusters containing 50-100 gold particles are observed. In addition,

analysis of ErbB2 in a population flow-sorted for high expressors showed that overexpression alone leads to substantial ErbB2 tyrosine phosphorylation, demonstrated using anti-PY1248 antibodies in Figure 2.1 K. This result is consistent with the concept that high levels of receptors override the relatively poor homodimerizing capabilities of ErbB2 (Penuel et al. 2002; Garrett et al. 2003), leading to productive and active homodimers.

Biochemical analysis of endogenous ErbB family members in SKBR3 cells

Having established that each of the three ErbB receptors inherently cluster on CHO cells, we turned to a cancer relevant cell model system where multiple family members are co-expressed. We chose the SKBR3 breast cancer cell line, that has exceptionally high levels of endogenous ErbB2 (>2,750,000), intermediate levels of EGFR (<200,000) and modest levels of ErbB3 (<70,000). ErbB4 is undetectable in this cell line. These values were determined by quantitative flow cytometry (not shown) and confirmed by western blotting (Fig. 2.2E). Biochemical studies, reported in Figure 2.2A, established high basal levels of ErbB2 phosphorylation and some detectable ErbB3 phosphorylation, even after serum starvation. As expected, EGF led to EGFR phosphorylation (Fig. 2.2A) and an increase in EGFR kinase activity (Fig. 2.2B, left), but produced little change in ErbB3 phosphorylation. Although a change in ErbB2 phosphorylation was barely detectable after EGF addition (see Fig. 2.2D), there was a transient increase in kinase activity associated with ErbB2 immunoprecipitates at 1 min of EGF treatment (Fig. 2.2B, right).

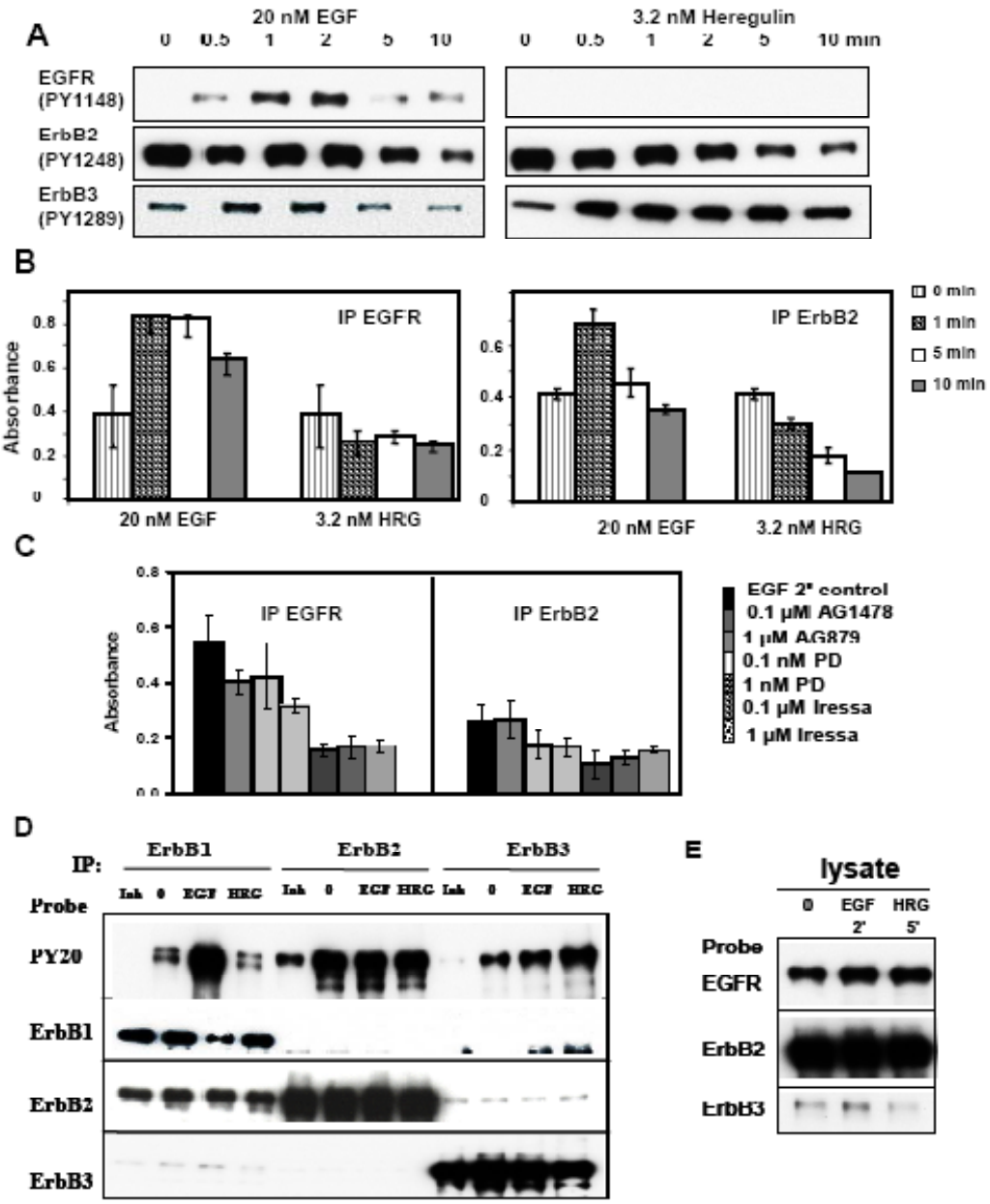

Figure 2.2. Biochemical analysis of endogenous ErbB family members in SKBR3 cells. A) Tyrosine phosphorylation status of ErbB receptors in SKBR3 cells after 2 hours serum starvation ("0") or after indicated time course of treatment with either EGF (20 nM) or Heregulin (3.2 nM). B) Kinase activity associated with EGFR or ErbB2 immunoprecipitates prepared from resting, EGF- or Heregulin-treated cells, measured *in vitro* by K-LISA. C) Effects of kinase inhibitors on EGFR or ErbB2 kinase activity, measured by K-LISA in immunoprecipitates prepared from cell lysates after 2 min stimulus with 20 nM EGF. K-LISA values are corrected for baseline color development typical in IgG controls. D) Co-precipitation assay for ErbB heterodimerization. Where indicated, cells were stimulated with 20 nM EGF or 3.2 nM Heregulin, followed by lysis with 1% NP-40 and immunoprecipitation using EGFR, ErbB2 or ErbB3-specific antibodies. Samples were subjected to SDS-PAGE, followed by immunoblotting with ErbB-specific antibodies. E) Immunoblotting of equal amounts of SKBR3 lysates (10 □g of protein each lane) to document the relative levels of all three ErbB3 family members.

Results in Figure 2.2C show the effects of putative EGFR-selective inhibitors (AG1478, PD153035, Iressa) and ErbB2-selective inhibitors (AG879) on *in vitro* kinase activity. The same drugs are tested for effects on EGF- and Heregulin-stimulated tyrosine phosphorylation in intact cells in Figure 2.3. In general, higher concentrations were required to inhibit phosphorylation in culture than in the *in vitro* kinase assay, presumably due to limited cellular uptake of the drugs. EGFR and ErbB3 were highly sensitive to AG1478 and ErbB2 was particularly sensitive to AG879. Continuing studies used a combination of AG1478 and AG879 to ablate phosphorylation of all three receptors.

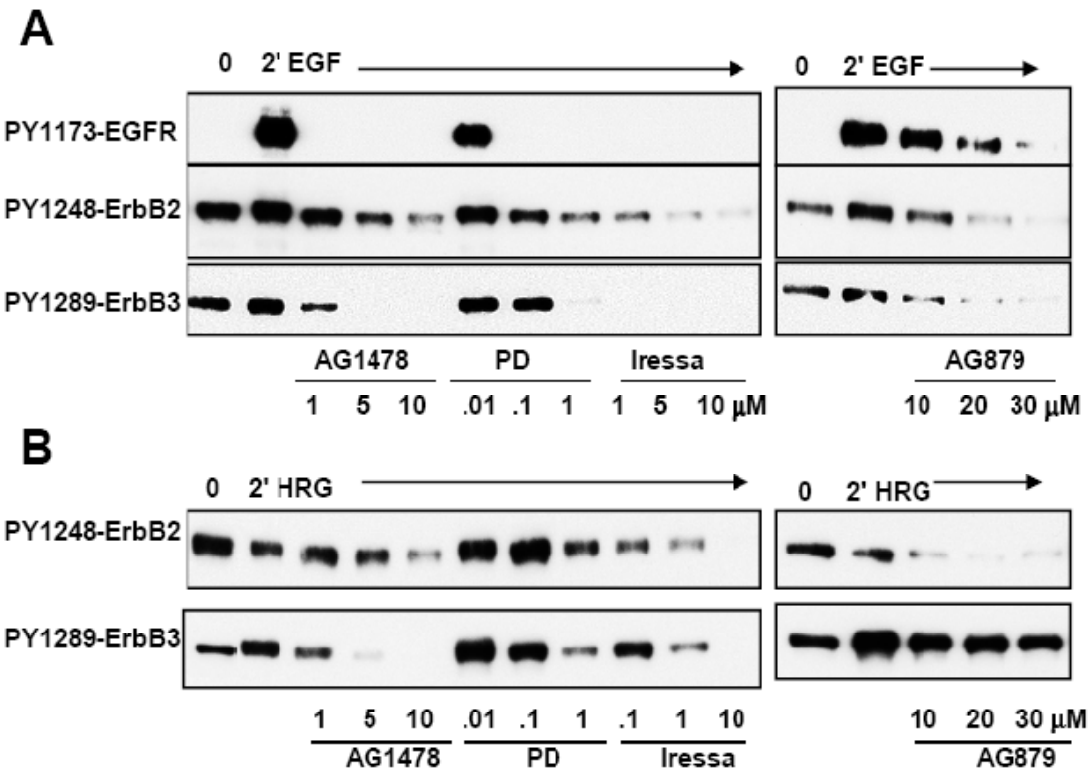

Figure 2.3. Effects of kinase inhibitors on receptor phosphorylation status. Where indicated, cell permeable inhibitors AG1478, AG879, PD153035 or Iressa were applied to cell cultures for 2 hours prior to lysis. Labels indicate samples that were stimulated for 2 min with 20 nM EGF or 3.2 nM Heregulin. Aliquots of lysates were subjected to SDS-PAGE, followed by immunoblotting with phospho-specific antibodies.

A co-immunoprecipitation assay was performed, using NP-40 detergent lysates, as a biochemical method to evaluate heterodimerization between the ErbB family members in SKBR3 cells. Figure 2.2D shows that this method yields data that are difficult to interpret. For example, ErbB1 immune complexes contain significant amounts of ErbB2 (and very little ErbB3). This may reflect pre-formed dimers, since the amount of ErbB2 coprecipitating does not change with EGF treatment, or that the dimers form after membrane lysis. In contrast, when the experiment was performed in reverse by immunoprecipitating ErbB2, the immune complexes contained barely detectible ErbB1 or ErbB3. ErbB3 immune complexes contain a small amount of ErbB2 and essentially no ErbB1. In this experiment, probing of immune complexes with anti-phosphotyrosine antibodies detects ligand-dependent activation of ErbB1 and ErbB3 (Fig. 2.2D, top panel). The double band detected by PY20 blotting of ErbB1 precipitates is consistent with co-precipitation of ErbB2, that migrates slightly slower in SDS-PAGE than ErbB1. We can conclude that some ErbB1/ErbB2 heterodimers *do* occur. However, the reliability of measuring dimerization by immunoprecipitation depends strongly on the antibodies used and can be markedly impacted by the choice of detergent. Based upon these results, we chose to use double labeling protocols on native membrane sheets to evaluate the proximity of ErbB family members, before and after ligand addition (see Fig. 2.4 and 2.5, below).

Limited co-localization of endogenously expressed ErbBs in breast cancer cell membranes.

We first examined the clustering state of ErbB2 on SKBR3 cells. As predicted from the work of Lisanti and co-workers (Koleske et al. 1995), these highly transformed cells have

few or no caveolae. Like high expressor CHO cells, the surface of serum starved SKBR3 is studded with ErbB2 clusters (Fig. 2.4A). ErbB2 cluster size proved remarkably refractory to interventions. Cluster size does not change after 1 hr treatment with AG1478 and AG879 to block ErbB2 phosphorylation (Fig. 2.4B). ErbB2 cluster size also does not change after the addition of EGF that would be predicted to initiate the formation of both EGFR homodimers and EGFR/ErbB2 heterodimers (Fig. 2.4C). Results in Figure 2.4D-F show membrane sheets that were double labeled for ErbB2 and phospho-ErbB2 (PY1248). All of the ErbB2 clusters in serum-starved cells contain label marking the presence of phosphorylated receptor and there is little or no change after the addition of EGF (Fig. 2.4E). Based upon Markov Random Field simulations that account for underlabeling in the EM approach (demonstrated in Fig. 2.1C), we estimate that the average ErbB2 cluster contains about nine receptors. In the lower panel of this figure, we document the multiple spatial statistics approaches we used to confirm these visual impressions. Figure 2.4G shows the Hopkins test used to prove that ErbB2 distribution in Figure 2.4A is significantly non-random. Figure 2.4 H shows the full range of ErbB2 cluster sizes in a group of 5 images from the same experiment as Figure 2.4A (resting cells). Like CHO cells, resting SKBR3 cells have occasional very large ErbB2 clusters with over 50 particles (last bar, Fig. 2.4H); these very large clusters do not contain a higher ratio of phosphorylated receptor (Fig. 2.4F). Figure 2.4I applies the Ripley's bivariate test to show that the labels for ErbB2 and phospho-ErbB2 are statistically co-clustered. Thus, although ErbB2 clusters in SKBR3 cells all contain a significant fraction of phosphorylated, active ErbB2, the driving force for cluster formation is clearly not its phosphorylation state.

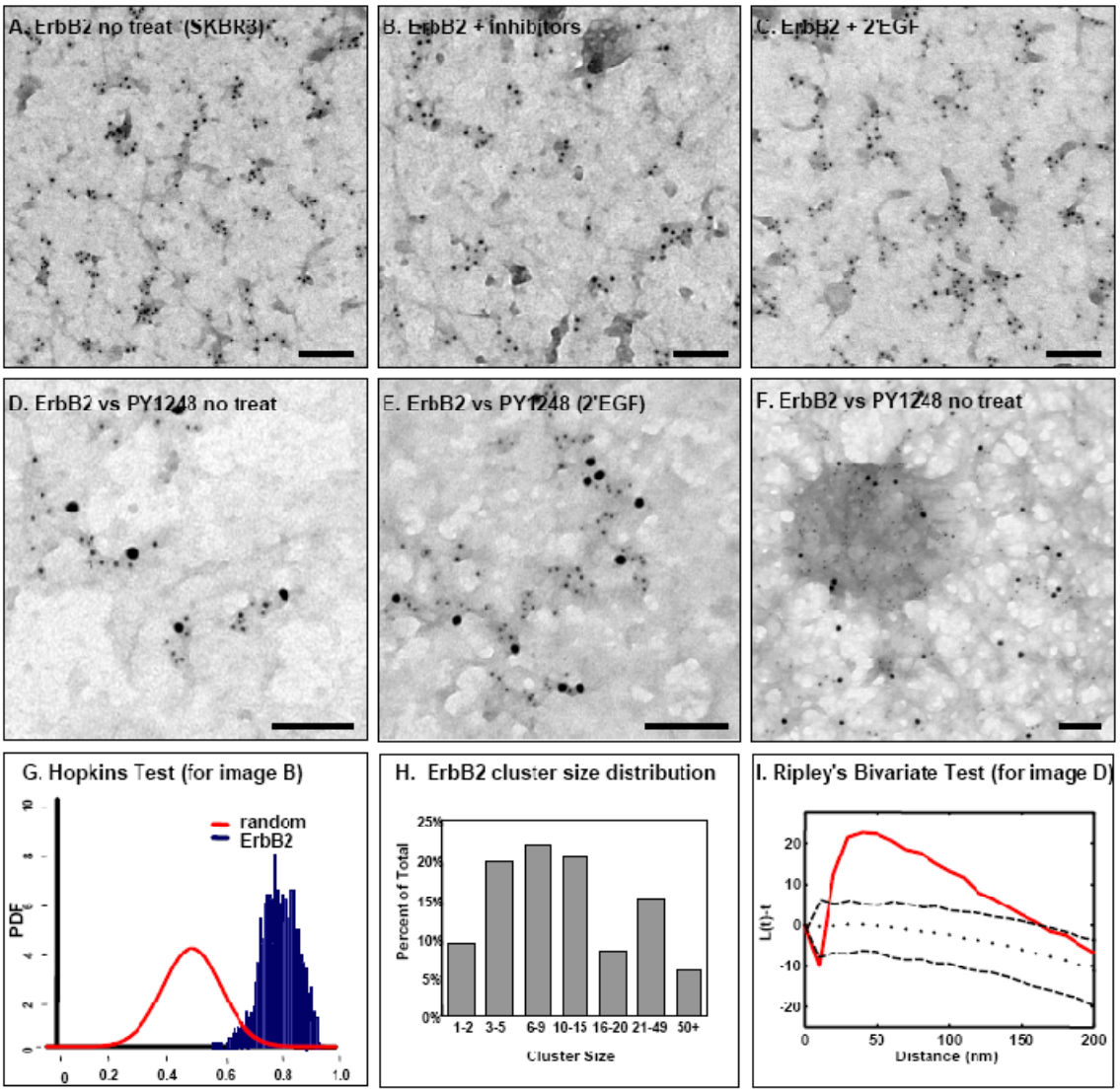

Figure 2.4. ErbB2 clustering in SKBR3 cells. Membrane sheets were prepared from serum starved cells (A, D, F), from cells pretreated with the combination of 1 µM AG1478 + 20 µM AG879 for 2 hrs (B), or from cells that were serum starved, then stimulated with 20 nM EGF for 2 min (C, E). Distributions of ErbB2 were determined by immunogold labeling from the inside using RB9040 primary antibodies and 5 nm gold-conjugated secondary antibodies. In D-F, membranes were also double labeled with 10 nm gold reagents to detect phosphorylated tyrosine 1248 in the ErbB2 cytoplasmic tail. G) Hopkins test is positive for ErbB2 clustering (applied to the data in image 2A). H) Range of cluster size for resting ErbB2 in 5 images from the same experiment in 2A. I) Positive Ripley's test for coincidence of label for pan-specific anti-ErbB2 antibodies vs phospho-specific ErbB2 antibodies. Bars = 0.1 micron.

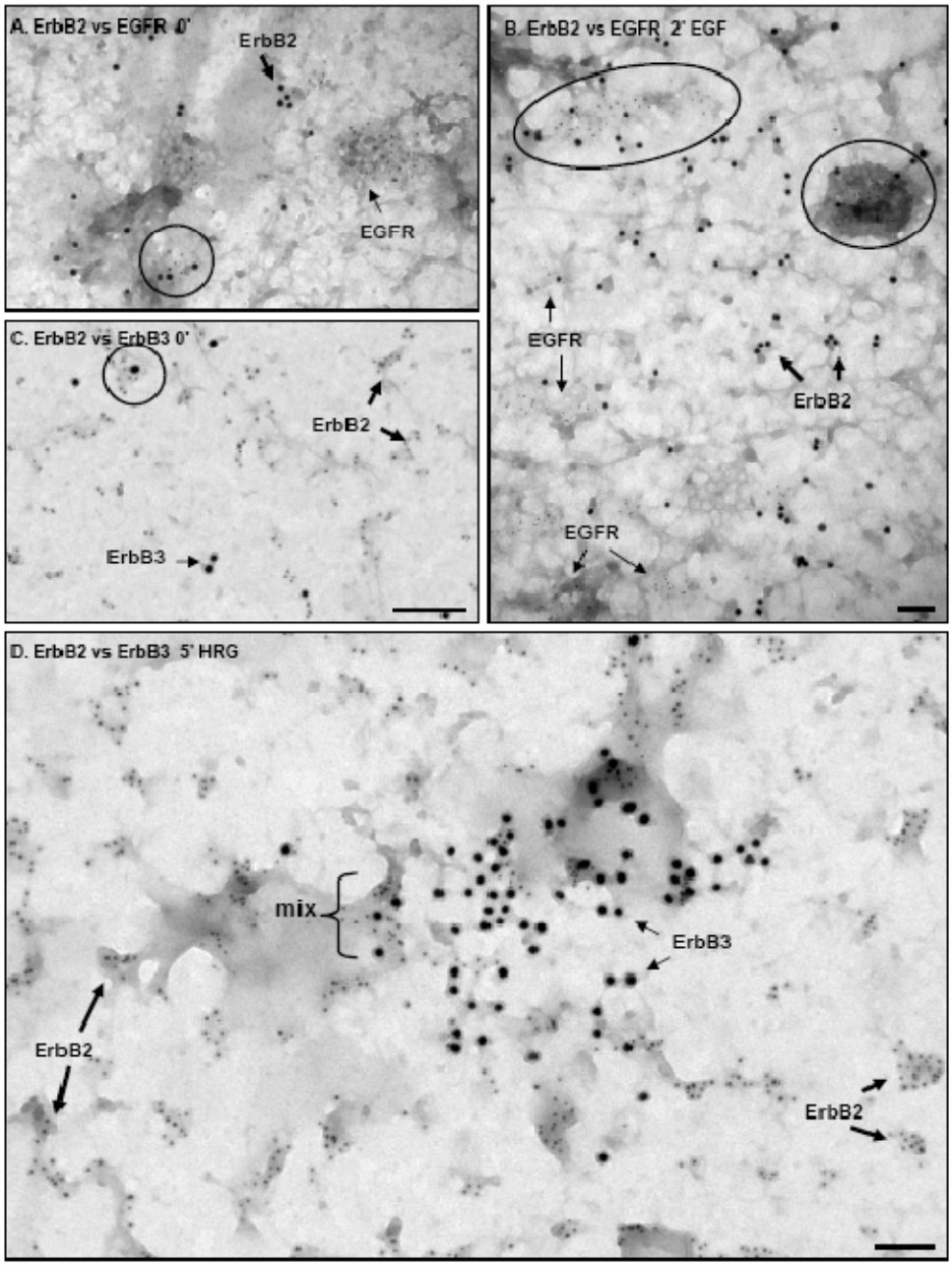

Figure 2.5. Analysis of ErbB2 co-clustering with EGFR and ErbB3 in SKBR3 cells. Membrane sheets were prepared from serum starved cells (A, C) or from cells that were serum starved and then stimulated with either 20 nM EGF for 2 min (B) or 3.2 nM Heregulin for 5 min (D). Sheets in (A, B) were double labeled from the inside with antibodies to ErbB2 (10 nm gold) and EGFR (5 nm); Sheets in (C, D) were double labeled from the inside for ErbB2 (5 nm) and ErbB3 (10 nm). Circles in (A-C), as well as the bracket in (D), indicate co-clusters of ErbB2 with either EGFR or ErbB3. Labeled arrows point to clusters containing only a single species of ErbB receptor. Bars = 0.1 micron.

A central goal was to determine if these three family members behave in a coordinated or independent manner, when they are expressed together in the cancer cell. In Figure 2.5, membrane sheets were double labeled for ErbB2 versus EGFR or ErbB3, with and without their ligands. Figure 2.5A shows that SKBR3 cells generally maintain distinct clusters of ErbB2 and EGFR (arrows) before the addition of EGF, although occasional co-clusters can be observed (circles). This image fails the Ripley's statistical test for co-clustering (Fig. 2.6). Furthermore, of 6 images analyzed from this data set, only one passed the Ripley's co-clustering test.

Figure 2.5B shows the results of double labeling membrane sheets from cells stimulated for 2 min with EGF. This image weakly passes the Ripley's test for co-clustering (Fig. 2.6), which is explained by two prominent co-clusters (circles in Fig. 2.5B) as well as many segregated clusters containing only EGFR or ErbB2 alone. Segregation of the two receptor clusters was more prominent than mixing, since only 30% of the images passed the Ripley's test for co-clustering in the EGF-treated data set. We speculate that the distinct spatial distributions reflects low amounts of EGF-induced heterodimerization.

Figure 2.5C shows that most ErbB2 and ErbB3 also cluster independently in resting cells (arrows), with occasional co-clusters (circle in Fig. 2.5C). Only 1 of 5 images passed the Ripley's co-clustering test. The most striking result, however, is the dramatic clustering of ErbB3 after 5 min treatment with Heregulin (Fig. 2.5D). In this image, the large gold particles marking ErbB3 form a large, dispersed cluster that is over 400 nm wide. Small gold particles marking ErbB2 span the entire membrane sheet (bold arrows), with some of these clusters falling within the larger ErbB3 cluster (bracket). It is important to note

that the EM assay establishes only proximity and is not a direct measure of dimerization. However, these “mixed clusters" indicate the opportunity for heterodimers of ErbB2 and ErbB3 to form. Furthermore, the mixing is of sufficient magnitude to pass the Ripley’s test for co-clustering (see Fig. 2.6). Because of the wide distribution of ErbB2, the impression from these experiments is that *ErbB2 is neither excluded, nor specifically recruited, to the ErbB3 patch.* It appears that, with 2.7 million ErbB2 receptors, abundance alone is sufficient to ensure that the large ErbB3 patches will contain some ErbB2.

We also evaluated membranes double-labeled for EGFR and ErbB3. We found very little co-clustering in resting membranes (not shown). We found the large ErbB3 clusters induced by Heregulin do have some EGFR interspersed through the cluster. However, these images fail the Ripley’s test for co-clustering. A representative micrograph, along with the Ripley’s analysis, is shown in Figure 2.7. Thus, although there is also potential for ErbB3-EGFR heterodimers in these clusters, it appears that ErbB3 clusters also do not specifically recruit EGFR.

Figure 2.4

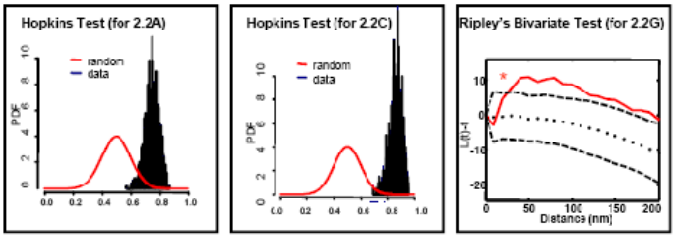

Figure 2.5

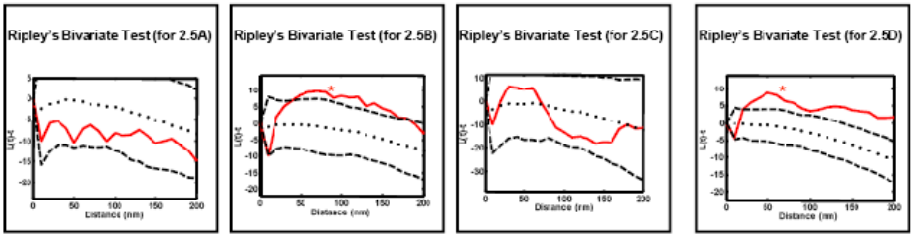

Figure 2.8

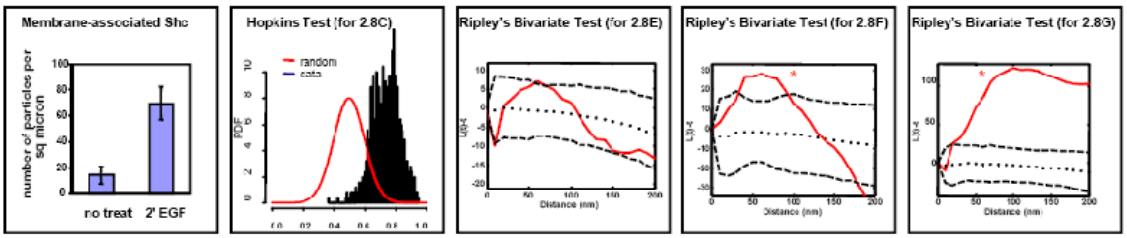

Figure 2.9

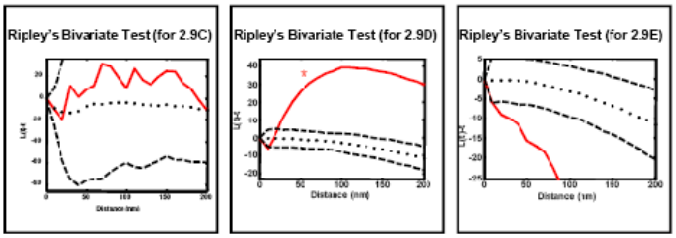

Figure 2.10

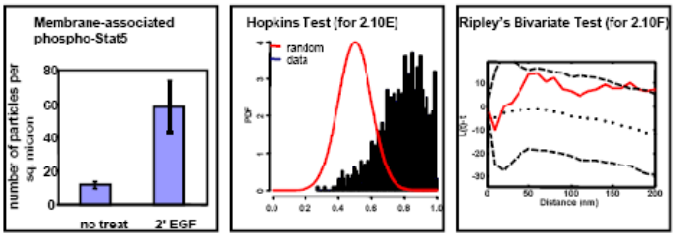

Figure 2.6. Summary of spatial statistics performed for figures in the main text. The Hopkins test is used to evaluate clustering of a single molecular species, where distributions to the right of the red line indicates significant difference from nonrandom. The Ripley's bivariate test evaluates co-clustering between 2 species. In these graphs, co-clustering is indicated only when the experimental values for *L(t)-t* (solid red line) fall above the boundaries predicted for pairwise sets of random points (dashed lines). Positive examples are marked with an asterick.

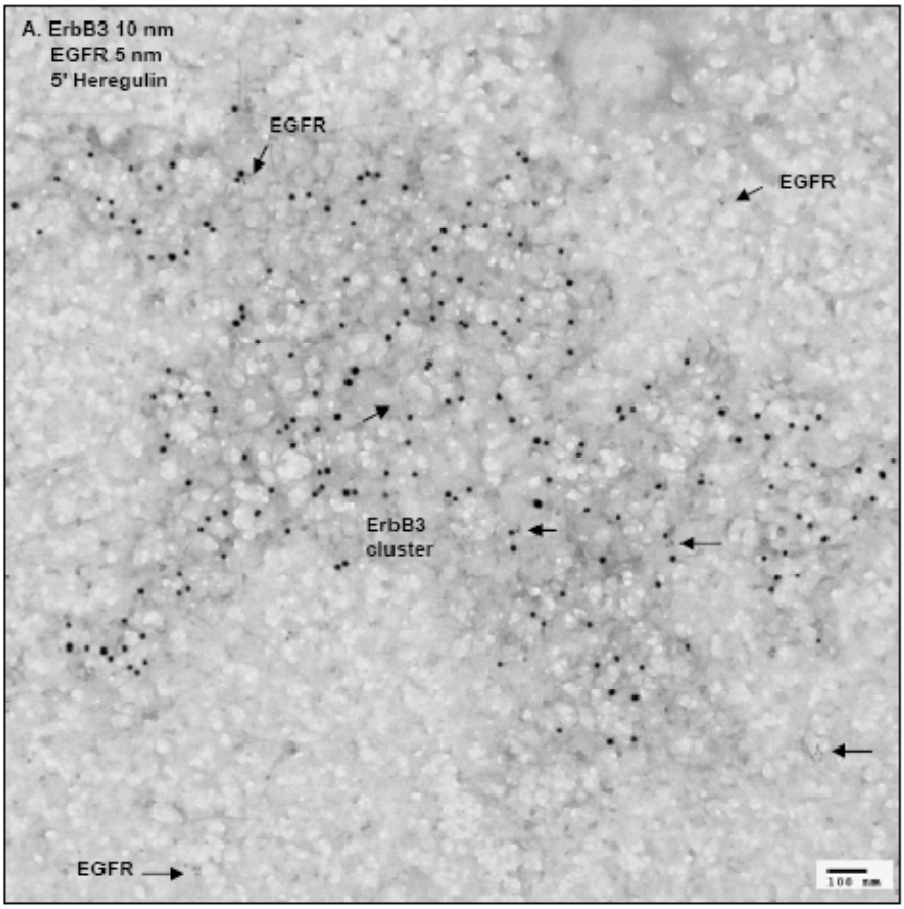

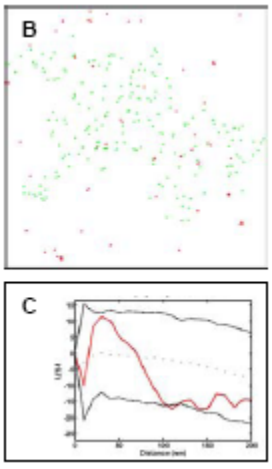

Figure 2.7. **EGFR randomly distributed with ErbB3**. A) Membrane sheet prepared from SKBR3 cells after 5 min treatment with Heregulin, then double-labeled for ErbB3 (large gold) and EGFR (small gold). Arrows point to isolated clusters of EGFR distributed across the image. A very large cluster of ErbB3 is in the center. B) Digital representation of the same image, where ErbB3 are represented by green dots and EGFR by red dots. C) Ripley's analysis of the same image, where the value for L(t)-t (solid red line) falls within the confidence interval and fails the Ripley's test. This indicates that, that although some EGFR can be found within the larger ErbB3 clusters, the EGFR label is randomly distributed with respect to ErbB3.

Three downstream signaling molecules – Shc, PI 3-kinase and STAT5 – have distinct recruitment behavior and topographical relationships to ErbBs.

It is well established that specific phosphotyrosines in the cytoplasmic tails recruit cytoplasmic adaptors and downstream effectors to active ErbB receptors (Jorissen et al. 2003). The general model is that these proteins reside in the cytoplasm and are recruited to the membrane following phosphorylation of specific tyrosine on receptor tails. Here, we evaluated the spatial and kinetic relationships of three of these proteins, Shc, PI 3-kinase and STAT5, with the membrane and with the individual ErbB receptors, generating evidence for distinct recruitment behaviors for the different signaling proteins.

Figure 2.8 reports results of experiments directed at Shc, an adaptor that binds strongly to EGFR phosphopeptides (Schulze et al., 2005). When evaluated *in vitro*, Shc is also capable of binding phosphopeptides derived from the ErbB2 tail (Schulze et al., 2005). Simple cell fractionation experiments revealed the presence of two isoforms of Shc in crude cytosol and membrane fractions from SKBR3 cells (Fig. 2.8A). The smaller p46 isoform of Shc was primarily cytosolic regardless of treatment. In contrast, resting membranes contained significant amounts of the larger p52 isoform of Shc (Shc-p52). Shc-p52 membrane association was reduced by treatment with tyrosine kinase inhibitors and increased by incubation with EGF. Cytosolic Shc-p52 was correspondingly increased by tyrosine kinase inhibitors and reduced by incubation with EGF. In comparison with EGF, Heregulin caused a smaller loss of cytosolic Shc-p52 and a correspondingly modest gain in membrane-associated Shc-p52. The electron micrographs in Figures 2.8B,C

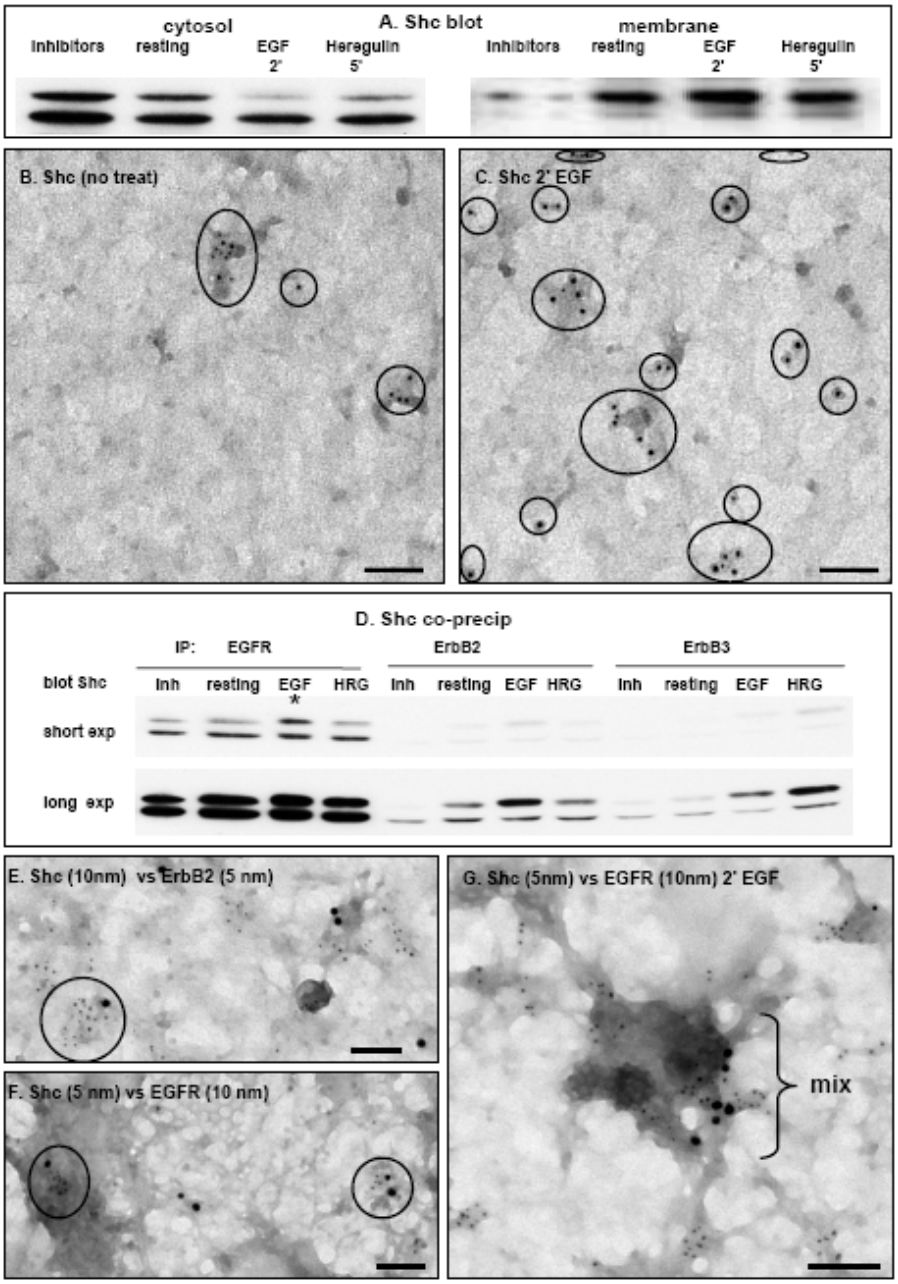

Figure 2.8. Membrane recruitment of Shc following EGF treatment. A) SKBR3 cells were serum starved (resting), treated for 1 hour with a combination of 1 μM AG1478 + 20 μM AG879, or serum starved and stimulated for 2 min with 20 nM EGF or 5 min with 3.2 nM Heregulin, followed by fractionation to yield crude cytosol and membrane fractions. Samples were subjected to SDS-PAGE and immunoblotting with pan-reactive anti-Shc antibodies. (B,C, E-G). Membrane sheets were prepared from serum starved cells (B, E, F) or EGF-simulated cells (C,G) and either singly labeled with 5 nm gold reagents recognizing Shc or double labeled for Shc and either ErbB2 or EGFR, as indicated by labels on each image. Circles in B,C highlight singly-labeled clusters of Shc in these membranes. Circles in E,F show co-clusters of Shc with ErbB2 or EGFR in serum-starved cells. Bracket in G indicates co-cluster of Shc with EGFR after 2 min EGF treatment. (D). Immunoblotting evidence for the coprecipitation of Shc with EGFR and, to a much lesser extent, with ErbB2 and ErbB3. Treatment of cells is indicated by labels for each lane. Bar = 0.1 micron.

confirm the recruitment of Shc to plasma membranes of EGF-treated cells. For the experiment shown here, the average number of gold particles marking Shc in resting cells was 15 per sq micron (Fig. 2.8B, circles). After 2 min of EGF treatment, this increased 4 fold to an average of 70 gold particles per sq micron (Fig. 2.8C, circles; plot in Fig. 2.6). When evaluated in multiple experiments, we routinely found 2-5 fold increases in Shc at the membrane of EGF-treated cells.

The association of Shc with ErbB isoforms is presented in Figures 2.8D-G. A significant amount of Shc-p52 coprecipitates with EGFR from resting and inhibitor-treated cells (Fig. 2.8D). EGF treatment causes a marked increase in the association of Shc-p52 with EGFR. This recruitment is readily observed on short exposure of the blot to film (marked with an * in Fig. 2.8D). Longer exposure of the blot to film permits detection of additional Shc association with the very abundant ErbB2 (again with an increase in Shc-p52 bound after EGF treatment) and with ErbB3 (with an increase in Shc-p52 bound after Heregulin or EGF treatment). In Figure 2.8D, anti-ErbB immunoprecipitates also contain the smaller p46 isoform of Shc, in amounts that are relatively unaffected by treatment conditions. Since Shc-p46 is primarily cytosolic (Figure 2.8A), we speculate that this Shc-p46 may have bound to receptor tails following the lysis procedure, creating an appearance of co-association that is not supported by independent methods.

Experiments with membrane sheets confirmed the coclustering of Shc with ErbB2 (Fig. 2.8E) and EGFR (Fig. 2.8F) in membranes prepared from serum-starved cells. Shc-EGFR coclustering, and adjacency of the co-clusters to coated pits, were both prominent features of EGF-activated membranes (Fig. 2.8G). This is consistent with work by

Sorkin (Huang et al., 2004) and others showing that EGFR is predominantly taken up by clathrin-mediated endocytosis. When evaluated by the Ripley's co-clustering test, a majority of images from both resting and activated cells passed the test for colocalization of activated EGFR with Shc (see example, Fig. 2.6). Thus a portion of Shc-p52 preassociates with ErbB family members in a phosphorylation-dependent (tyrosine kinase inhibitor-sensitive) manner and a further portion is recruited from the cytosol to receptors following a ligand-induced increase in phosphorylation. Shc-p46 plays no apparent role in ErbB signaling in SKBR3 cells.

PI 3-kinase is perhaps the most important binding partner of activated ErbB3 (Soltoff, et al, 1994; Hellyer et al., 2001) and it is generally considered to be a poor binding partner for other ErbB receptors. The biochemical experiments in Figure 2.9A show that a significant amount of p85 is preassociated with crude membrane fractions and is not changed by treatment of cells with tyrosine kinase inhibitors. In addition, neither ligand significantly changes the ratio of p85 between membrane and cytosolic fractions. Figure 2.9B examines the association of p85 with different receptors. Only anti-ErbB3 coprecipitates significant amounts of p85 from serum-starved cells (Fig. 5B). p85 is displaced from ErbB3 with tyrosine kinase inhibitors, indicating dependence on ErbB3 phosphorylation (see Fig. 2.9B). Addition of Heregulin leads to a marked increase in p85 in ErbB3 immunoprecipitates. Electron micrographs of membrane sheets prepared from resting cells show that most p85 is present in small clusters that are widely dispersed across the membrane inner surface, sometimes near ErbB3 (bold arrow, Fig. 2.9C) or along cable-like structures that may represent elements of the cortical cytoskeleton (small

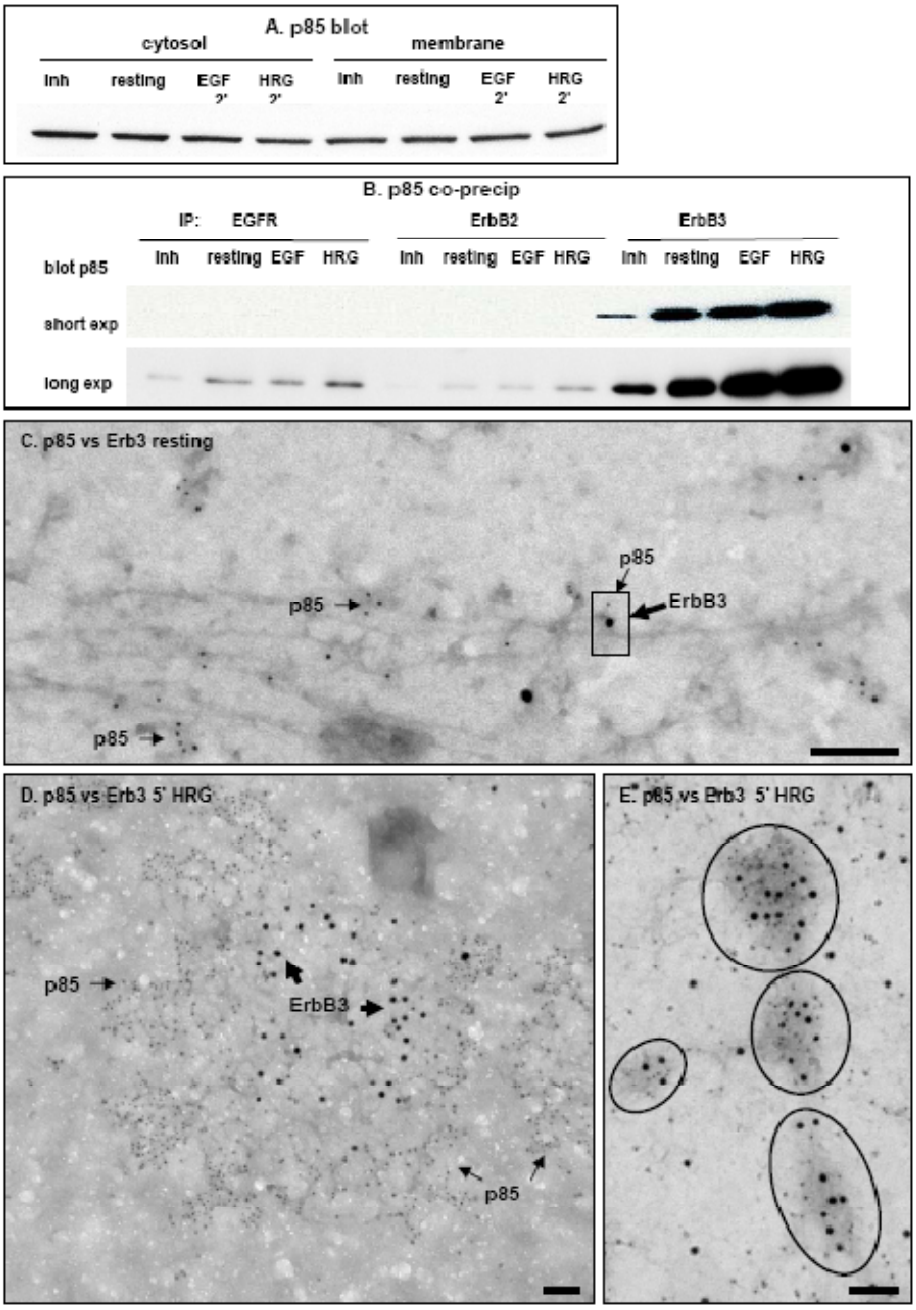

Figure 2.9. Redistribution of membrane-associated PI 3-kinase in Heregulin-stimulated SKBR3 cells. A) Cytosol and membrane fractions were prepared from treated and untreated SKBR3 cells, as described in the legend to Fig. 4. Samples were subjected to SDS-PAGE and immunoblotting with anti-p85 antibodies. B) Immunoblotting evidence for the coprecipitation of p85 with ErbB3 (and very little coprecipation with EGFR or ErbB2). Treatment of cells is indicated by labels for each lane. Membrane sheets in (C-E) were prepared from serum starved cells (C) or cells treated for 5 min treatment with 3.2 nm Heregulin (D,E); membranes were then double labeled for p85 (5 nm gold) and ErbB3 (10 nm). Bold arrows in C,D point to examples of ErbB3 label and fine arrows to examples of p85 label. Circles in (E) show multiple co-clusters of ErbB3 and p85. Bar = 0.1 micron.

arrows, Fig. 2.9C). This image fails the Ripley's test for colocalization (Fig. 2.6). After Heregulin treatment, dramatic co-clustering of p85 with ErbB3 was often seen (circled clusters in Fig. 2.9E). Co-localization was confirmed by the Ripley's test (See Fig. 2.6). In addition, we observed novel bull's eye structures in these membranes (Fig. 2.9D), with ErbB3 clusters in the center (large gold) that are surrounded by heavy labeling of p85 (small gold). In this case, the downward projection of the red line in the Ripley's test indicates a strong deviation from normal (Fig. 2.6). In summary, we see that PI 3-kinase is markedly recruited to ErbB3 clusters in activated cells, probably from the pool of inherently membrane-associated enzyme. Heregulin can also induce formation of a unique membrane domain around ErbB3 clusters, that is distinguished here by a ring of PI 3-kinase.

Finally, Figure 2.10 examines STAT5 association with the membranes of SKBR3 cells. Like Shc, STAT5 is a preferred binding partner of activated EGFR (Olayioye et al., 1999; Kloth et al., 2002). However, fractionation experiments (Fig. 2.10A) showed very little change in the overall levels of STAT5 in the membrane and cytosol fractions after EGF (or Heregulin) treatment and treatment with the tyrosine kinase inhibitor cocktail failed to displace STAT5 from the membrane. As expected, EGF led to phosphorylation of STAT5 within 30 sec (Fig. 2.10C) and to the appearance of the phospho-STAT5 dimer in both the cytosolic and membrane fractions (Fig. 2.10A).

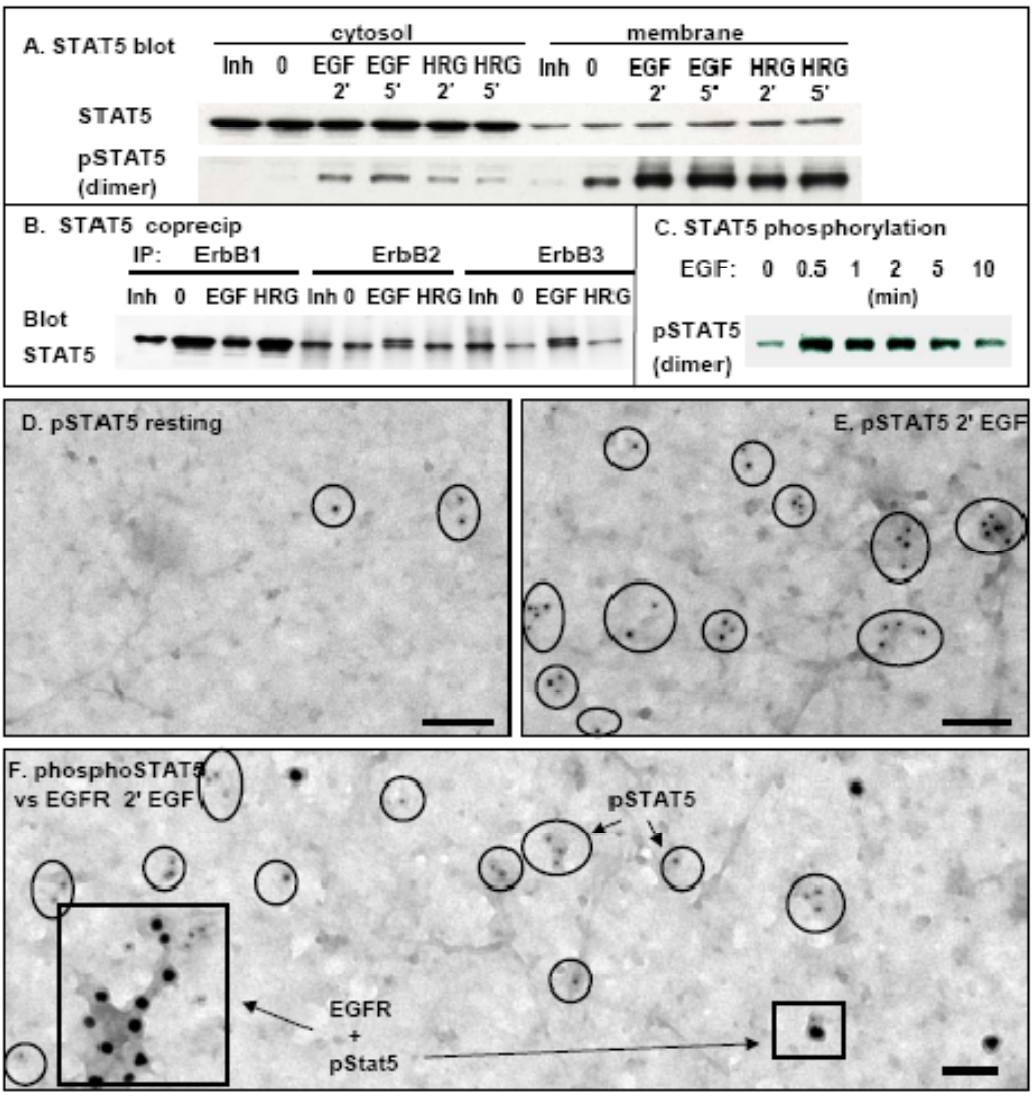

Figure 2.10. Rapid tyrosine phosphorylation of membrane-associated STAT5 with EGF treatment. A) Cytosol and membrane fractions were prepared from treated and untreated SKBR3 cells, as described in the legend to Fig. 4. Samples were subjected to SDS-PAGE and immunoblotting with anti-STAT5 antibodies. B) Immunoblotting evidence for the coprecipitation of STAT5 with EGFR and, to a lessor extent, to ErbB2/ErbB3. Treatment of cells is indicated by labels for each lane. C) Immunoblotting with anti-STAT5 PY694 antibodies demonstrates the time course of STAT5 phosphorylation in response to 20 nM EGF. Membrane sheets in (D-F) were prepared from serum starved SKBR3 cells (D) or after 2 min of treatment with 20 nM EGF (E,F). Sheets in (E,D) were singly labeled with 5 nm gold reagents that specifically recognize STAT5 when phosphorylated on tyrosine 694; circles help to demonstrate that there is marked increase in the amount of phospho-STAT5, but not the general pool of STAT5, after EGF treatment. The membrane sheet in (F) was double labeled for phospho-STAT5 (5 nm gold) and EGFR (10 nm). Boxes serve to mark the few co-clusters of EGFR and phospho-STAT5 in EGF-treated membranes. Bar = 0.1 micron.

STAT5 coprecipitated with all three receptors, and EGF led to the appearance of a slightly slower migrating form, presumably representing phosphorylated STAT monomer (Fig. 2.10B). The persistent ability to coprecipitate STAT5 with all three receptors after treatment with tyrosine kinase inhibitor cocktail indicates that STAT5 association is not dependent upon receptor phosphorylation.

Membrane sheet experiments confirmed similar levels of STAT5 labeling on both resting and EGF-treated membranes (not shown) and documented that cell activation increased STAT5 phosphorylation. As shown in Figure 2.10D, SKBR3 membranes prepared from serum-starved cells showed negligible binding of gold particles marking phospho-STAT5 (<11.8 particles per sq micron). After 2 min of EGF treatment (Fig. 2.10E), there was a dramatic increase in the amount of phospho-STAT5 label (>58.3 particles per sq micron). These results are also depicted in a bar graph in Fig. 2.6. Double labeling experiments showed that this phospho-STAT5 was not preferentially associated with activated EGFR (Fig. 2.10F). In this micrograph, phospho-STAT5/EGFR co-clusters are marked with boxes and the more abundant, dispersed clusters of phospho-STAT5 are highlighted with circles; this image fails the Ripley's test for co-clustering (Fig. 2.6). Thus, STAT5 appears to associate inherently with ErbB isoforms and the principal effect of EGF appears to be the rapid tyrosine phosphorylation of preassociated STAT5 and the redistribution of phospho-STAT5 to separate membrane microdomains.

2.5 Discussion

Variability of ErbB receptor expression is considered to be an important factor in breast cancer prognosis (Rowinsky et al., 2004). Because dimerization is a key step in ErbB receptor activation, we propose that fine-scale membrane organization also contributes importantly to the oncogenic signaling process. We evaluated the spatial relationships of three family members (EGFR, ErbB2 and ErbB3), when expressed alone in transfected CHO cells and when co-expressed endogenously at high levels in a breast cancer line. This spatial information was acquired using immunoelectron microscopy of native membrane sheets, providing snapshots of receptors and their signaling partners at nanometer scale resolution.

We show that each of the ErbB receptors clusters independently when expressed in stably transfected CHO cells, even at very low expression levels. We observed large increases in cluster size for ErbB3 after ligand treatment but not in EGFR or ErbB2. EGF-induced changes in EGFR or ErbB2 cluster size have been reported by others using fluorescence microscopy techniques (Nagy et al. 1999; Ichinose et al. 2004). We suggest that differences in cell type, cell culture conditions and/or antibodies used to detect receptors may explain the discrepancy. In the course of these experiments, we ruled out the use of several commercial antibodies, originally raised against one ErbB family member but with significant crossreactivity against other ErbBs. This has been a subject of some controversy in the literature (DiGiovanna et al. 2005; Karlin et al. 2005). A few EGFR antibodies are also conformation specific, which might lead to significant changes in labeling after EGF treatment (DiGiovanna 1997; Johns et al. 2004).

It is significant that ErbB2 clusters are dominant features of the membrane in these breast cancer cells. ErbB2 is inherently clustered in resting cells and these clusters label with phospho-specific antibodies (Fig. 2.4). Since few ErbB2 clusters in serum-starved cells mix with other ErbB receptors, a high proportion of ErbB2 signaling must be driven by homointeractions. We note that clustering is not dependent on phosphorylation because treatment with tyrosine kinase inhibitors does not change cluster size. We speculate that high densities of ErbB2 may drive dimer formation despite its reportably poor homodimerizing capability (Burgess et al., 2003).

The relatively low incidence of co-clustering between different ErbB receptors in resting cells suggests segregation as one mechanism to minimize premature formation of heterodimers, while potentially favoring rapid homodimerization of EGFR and ErbB3 upon treatment with their respective ligands. This is puzzling to consider for ErbB3, that is generally considered to be dependent upon heterodimerization with other ErbBs for initiation of signaling. We do not presently offer an explanation for the segregation of individual ErbB clusters. Possibilities include unique "lipid shell" preferences for the individual receptor species (Anderson et al. 2002) or occupancy in different "protein islands" (Lillemeier et al. 2006). Consistent with the latter hypothesis, most receptors occupy dark regions of the membrane that are a hallmark feature of the protein island hypothesis (Lillemeier et al. 2006). Another alternative is that clustering could be mediated by weak homotypic interactions between the receptors themselves. Recent evidence suggests that ErbB3 can form "conformationally inactive" oligomers through binding interactions distinct from the dimerization interface identified in crystal structures of the ligand-bound (extended) ErbBs (Kani et al. 2005). It has been estimated

that up to 14% of EGFR is oligomerized prior to growth factor binding (Martin-Fernandez et al. 2002). These oligomerized receptors may be autoinhibited through structural conformations, such as the electrostatic interaction of unphosphorylated tails with acidic lipids in the plasma membrane, a model proposed by McLaughlin and colleagues (McLaughlin et al. 2005).

The fact that we detect segregation in the crowded ErbB2 landscape is remarkable. Although co-clustering is not a direct measurement of dimerization, it *is* a direct measurement of proximity. We found that only 30% of the images double-labeled for EGFR and ErbB2 passed the Ripley's test for co-clustering. Thus, a majority of EGFR in EGF-stimulated SKBR3 cells are likely to be participating in homotypic, not heterotypic, interactions. Relevant to this argument, previous work has suggested that the heterodimerization of ligand-bound EGFR with ErbB2 results in a slower internalization rate for EGFR, possibly resulting in prolonged and aberrant signaling at the cell surface (Wang et al. 1999; Lidke et al. 2004).

We hypothesize that, under more normal expression levels, segregation may be a powerful tool to limit heterodimerization of EGFR and ErbB2. Our work also has important implications for computational models that attempt to predict biological outcomes in both normal and oncogenic settings. Most models have assumed EGFR-EGFR homodimers and EGFR-ErbB2 heterodimers are favored equally (Hendriks et al. 2003). In cells expressing over 2 million ErbB2, Hendricks'model would predict that >80% of ligand-bound EGFR would occur in heterodimers. If this were the case, essentially all EGFR clusters should have also contained ErbB2. We did not observe this.

Docking partners, including Shc, PI 3-kinase and STAT5 are critical for coupling growth factor signals to downstream activation pathways. Textbook models suggest that receptor phosphorylation results in recruitment of these partners from the cytoplasm and that dissociation occurs upon receptor dephosphorylation. Remarkably, none of the proteins studied here follow this model in detail. Shc-p52 is the closest. A portion of Shc-p52 preassociates with all ErbB family members in a phosphorylation-dependent (tyrosine kinase inhibitor-sensitive) manner and a further portion is recruited from the cytosol to receptors following a ligand-induced increase in phosphorylation. PI 3-kinase deviates more strongly from the classic model. Heregulin strongly increases ErbB3-bound PI 3-kinase without appearing to increase total PI 3-kinases in membrane fractions. This suggests that the ErbB3-associated PI 3-kinase in activated cells derives mostly from a pool of inherently membrane-associated enzyme and not from the cytosol. STAT5 appears to associate inherently with EGFR and the principal effects of EGF appears to be the rapid tyrosine phosphorylation of preassociated STAT5 and its redistribution to separate membrane microdomains. There is precedent for this unexpected topographical behavior in the case of LAT, a transmembrane protein of mast cells that is phosphorylated by Syk and immediately redistributes to membrane domains away from Syk and its partnering receptor, FcεRI (Wilson et al., 2001).

The dramatic reorganization of ErbB3, together with PI 3-kinase, in Heregulin-treated SKBR3 cells is of particular interest. Early studies in human mammary carcinomas (Alimandi et al., 1995) implicated the ErbB3/PI 3-kinase pathway as a critical step in neoplastic transformation and a previous report using fluorescence imaging showed the first indications that the two signaling molecules co-patch on the cell surface (Gillham et

al., 1999). We found that the formation of large ErbB3 complexes occurred over a somewhat slow time course (5 min), compared to the kinetics of receptor phosphorylation (peaks at 1-2 min; see Fig. 2.2). The large clusters of ErbB3 contained no visible clathrin structures, consistent with slow internalization. PI 3-kinase mixed readily with smaller ErbB3 clusters (Fig. 2.9E) and was also sometimes found within the larger ErbB3 clusters. However, it also was seen as a distinctive ring around large ErbB3 clusters (Fig. 2.9D). Because the other ErbBs are neither recruited into, nor restricted from, the large ErbB3 clusters, we assume that the unique spatial relationships between ErbB3 and p85 is dynamic and not restricted by a corral (Tomishige et al., 1998). It is likely to only be incidentally similar to the immunological synapse that also forms a bull's eye (Bromley et al., 2001). The p85 that associates with activated ErbB3 appears to derive from a membrane-associated pool. Further study is needed to identify the binding sites involved in anchoring p85 to the membrane in resting cells.

In summary, high resolution imaging has documented several unique aspects of ErbB signaling. Most notably, we implicate segregation of ErbB family members as a potential way to limit heterodimerization to levels much lower than currently predicted. The discovery of three distinct membrane recruitment and topographical patterns for specific signaling proteins associated with ErbB signal propagation, none exactly following the conventional model, needs to be considered in future models of growth factor signaling in the context of breast and other cancers.

Chapter 3

ErbB2-dependent and independent mechanisms amplify ErbB3 signal transduction: Roles for membrane organization and E933Q mutation in ErbB3 activity

In preparation for submission to ***Cancer Cell***

3.1 Summary

EGFR and ErbB2 are important cancer therapeutic targets. ErbB3, a family member with impaired kinase activity, has been implicated in tumor escape from therapy. Our work suggests that at least three mechanisms amplify ErbB3 signaling and render it partially independent of its preferred heterodimerizing partner, ErbB2. First, robust tyrosine kinase activity in ErbB3 immunoprecipitates from Heregulin-stimulated SKBR3 cells suggests that ErbB3 may compensate for its poor catalytic capabilities by association with an unknown cytoplasmic tyrosine kinase. Second, we discovered that SKBR3 cells express two alleles, wildtype and a single kinase domain substitution (E933Q). At low ligand concentrations, ErbB3(E933Q) expressing CHO cells showed 2-3 fold higher receptor phosphorylation and increased p85 and AKT activation that cells expressing ErbB3(WT). Most wild type receptors bind Heregulin with a affinity (124±4nM) although a tiny fraction (<1%) exhibit high affinity. ErbB3(E933Q) receptors distinctly show two populations, with 5% high affinity (0.23±0.6nM) and 95% low affinity (105±31nM). Finally, electron microscopy studies show that essentially all ErbB3 redistributes into dramatic p85-positive signaling domains after treatment of CHO cells

with Heregulin, even when expressed at 2-3 fold higher levels than ErbB2. Dramatic increases in ErbB3 clustering is a common feature of Heregulin-treated E933Q transfectants but also observed in Heregulin-treated WT cells. The propensity to form clusters may be related to ErbB3's highly restricted motion, with mobile fractions of only 59% and 32% for WT and E933Q respectively. These results suggest that multiple mechanisms contribute to ErbB3's critical roles in tumor survival and, further, that ErbB3 and its cytosolic partners are potential therapeutic targets.

3.2 Introduction

Epidermal growth factor receptor (EGFR/ErbB1) and ErbB2 are members of the ErbB family and are important molecular targets for cancer therapy (Wieduwilt et al. 2008). ErbB3, a close family member considered to have very poor kinase activity, has received less attention as a cancer therapeutic target. However, recent studies have shown that ErbB3 is a critical factor in the escape from therapies targeting other ErbBs in lung and breast cancer (Engelman et al. 2007; Sergina et al. 2007). Increased ErbB3 mRNA or ErbB3 protein levels correlate with poor prognosis in multiple human cancers, including those of breast, ovaries, prostate, gastrointestinal and lung (Sithanandam et al. 2008). Investigation of the novel aspects of ErbB3 signaling will advance our understanding of its role in cancer and may identify it as a new target for cancer therapy.

Early studies of bovine ErbB3 and rat ErbB3 led to the conclusion that ErbB3 is either a "weak" (Guy et al. 1994) or "dead" kinase (Sierke et al. 1997). This widely held view has been supported by analysis of the primary sequence of ErbB3's kinase domain, where

substitutions involve key amino acids involved in the catalytic reactions of ErbB1 and other related tyrosine kinases (Zhang et al. 2006). The classic model of ErbB3 signaling assumes that ligand binding permits heterodimerization with kinase-competent ErbB family members, particularly ErbB2, which then leads to transphorylation of YXXM motifs in the ErbB3 and recruitment of PI 3-kinase. However, a recent report in the context of lung cancer supports the notion that ErbB3 can heterodimerize with other membrane receptors, such as MET, leading to signaling that is independent of other ErbB receptors (Engelman et al. 2007). Others have suggested that ErbB3 evades tyrosine kinase inhibitors that block other ErbBs via compensatory changes in Akt-mediated negative feedback regulation and/or substrate evasion (Sergina et al. 2007) .

Oncogenic mutations in ErbB1, ErbB2 and ErbB4 are well established (Paez et al. 2004; Lee et al. 2006; Soung et al. 2006). Lung adenocarcinomas harboring mutations in the ErbB1 kinase domain strongly correlate with positive clinical response to gefitinib (Iressa) and erlotinib (Tarceva) (Paez et al. 2004). ErbB2 and ErbB4 kinase domain mutations have also been detected in lung, gastric, colorectal and breast carcinomas (Stephens et al. 2004; Lee et al. 2006; Soung et al. 2006). Collectively, these studies indicate that the kinase domains of the ErbB family play important roles in human carcinogenesis. ErbB3 kinase domain mutations have been reported to be relatively rare in lung, breast and colon carcinomas (Jeong et al. 2006). In a systematic study of the tyrosine kinase transcriptome in 254 established tumor cell lines, ErbB3 amino acid substitutions were found, but all were located outside the kinase domain (Ruhe et al. 2007). However, at least four amino acid substitution or SNPs in the ErbB3 kinase domain are expected in Genecard (http://www.genecards.org/cgi-bin/carddisp.pl?

gene=Erbb3). The potential contributions of these ErbB3 substitutions have not been studied, presumably because of the assumption that changes within a pseudokinase domain would be insignificant.

In evaluating ErbB3 dimerization partners using an *in vitro* tyrosine kinase assay, we found that ErbB3 immunoprecipitates from SKBR3 breast cancer cells contained Heregulin-inducible tyrosine kinase activity. Since negligible amounts of ErbB2 are present in ErbB3 immune complexes, we searched for potential cytoplasmic kinase partners without success. We further discovered that these cells express two ErbB3 alleles, wildtype (WT) and a single kinase domain substitution (E933Q). We compared the signaling capabilities of ErbB3 (WT) and ErbB3 (E933Q) using stably-transfected CHO cells, that express modest levels of endogenous ErbB2. Our comprehensive approach includes ligand binding studies, electron microscopy and live cell imaging, as well as phosphorylation kinetics in the absence and presence of ErbB2 blocking reagents. We show that Heregulin leads to activation and global reorganization of ErbB3, even when expressed at levels exceeding those of ErbB2. Approximately 30-50% of ErbB3's phosphorylation is retained during 2C4 treatment, that blocks dimerization with ErbB2. Remarkably, the E933Q substitution increases ligand sensitivity and amplifies the ErbB3-PI3K-AKT signaling pathway.

3.3 Materials and Methods

Cell lines. SKBR-3 cells were obtained from ATCC and grown according to their guidelines. Parental CHO cells and their stable transfectants were cultured in DMEM,

10% FBS (Hyclone) with penicillin-streptomycin and 2 mM L-glutamine.

Reagents. Epidermal growth factor (EGF) was purchased from Biomedical Technologies (Stoughton, MA). Recombinant Heregulin 1-β1 was from US Biological (Swampscott, MA). AG879, PD153035, PP2 and staurosporin were from Calbiochem (LA, Jolla, CA). EGFR specific antibodies were EGFR.1 (Calbiochem) and 610016 (BD Transduction Laboratories, Los Angeles, CA). Humanized ErbB2 blocking antibody pertuzumab (2C4) was a gift from Genentech (San Francisco, CA) to Dr. D. Jovin (Gottingen, Germmany). ErbB2 specific antibodies RB9040 and MS-325 were from Labvision (Fremont, CA); ErbB2 antibodies SC-08, ErbB3 antibodies SC-285 and SC-415, and p85 antibodies SC-1637, SC-423 were from Santa Cruz (Santa Cruz, CA); and p85 06-497 antibodies were from UBI (Lake Placid, NY). Antibodies for phospho-(Y1289)-ErbB3, phosphor-(S473)-Akt and total Akt were from Cell Signaling, while HRP-conjugated PY20 antibodies were from BD Transduction.

Sequencing ErbB3 tyrosine kinase domain in SKBR3 cells and other cell lines. Messenger RNA was extracted using the RNeasy Mini Kit (QIAGEN, (chartsworth, CA)) from SKBR3 cells or other cells. Two pairs of primers were designed to span the entire ErbB3 tyrosine kinase domain: 5'-CTC TGG ACC CCA GTG AGA AG-3' and 5'-GGG AGT ACA AAT TGC CAA GG-3'; 5'-GGT CAG CCA CAC CAA AAT CT-3' and 5'-CAG ATA CCG TGG TGG GTC TC-3'. The ErbB3 tyrosine kinase domain was amplified by RT-PCR using a QIAGEN One-step RT-PCR kit. The PCR products were separated by agarose gel electrophoresis, extracted with the QIAquick gel extraction kit (QIAGEN) and sequenced using above two pairs of primers.

Site-directed mutagenesis and transfection. The human v-erb-b2 homolog 3 (ERBB3) WT gene was introduced into the pcDNA6V5HIS-A vector by Jovin and colleagues (Lidke et al. 2004); its sequence was identical to that in Genbank #NM_001982. A G to C mutation was produced at nt 3047 of that sequence (nt 2853 of the coding sequence). PAGE-purified mutagenesis primers of the sense strand with the G to C change (CAAGTGTTGGATGATTGA TCAGAACATTCGCCCAAC) and its reverse complement was obtained from Invitrogen (Carlsbad, CA). Site-directed mutagenesis was performed using the Stratagene Quik-Change Site-Directed Mutagenesis kit following the manufacturer's protocol, with 12 cycles of amplification. Methylated, non-mutated template DNA was removed by DpnI digestion, XL1-Blue bacteria were transformed with the products, and the bacteria were plated on X-gal LB ampicillin plates. White colonies were picked and DNA was amplified using Templiphi (GE Healthcare Life Sciences) rolling-circle reactions. The products were sequenced using primers upstream of the desired mutation. The sequence of the remaining portion of the gene and the promoter were verified with six additional sequencing primers; no other nucleotide changes were found. WT or E933Q-mCitrine plasmids were introduced into CHO cells using lipofectamine 2000 (Invitrogen). The antibiotic blasticidine (7μg/ml) was used for selection. Transfectants expressing visible ErbB3-mCitrine were sorted by Moflo, followed by selection of colonies in 96 well plates. Colonies expressing ErbB3-mCitrine on the cell surface were selected by fluorescence microscopy and used for the study.

Western blotting and immunoprecipitation analysis. Cells were serum-starved (2 hr) then stimulated with ligands, with or without pretreatment with 2C4 antibodies or kinase inhibitors; concentrations of inhibitors are reported in the figure legends. After a PBS

rinse, cells were solubilized in cold NP-40 lysis buffer (150 mM NaCl, 50 mM Tris-HCl pH 7.2, 1% NP-40, 5 µg/ml leupeptin, 5 µg/ml antipain, 1 mM $NaVO_4$, 1 mM PMSF). Lysates were clarified by centrifugation. Protein concentrations were measured by BCA protein assays (Pierce, Rockford, IL). Supernatants were mixed with 5x sample buffer for SDS-PAGE or used directly for immunoprecipitation. For IP, supernatants were preincubated with Trueblot anti-mouse or anti-rabbit Ig beads (Ebioscience, San Diego, CA), followed by transfer to tubes containing specific antibodies and overnight incubation at 4°C. After 4 washes in lysis buffer, 2× reducing Laemlli buffer was added to beads for SDS-PAGE and subsequent transfer to nitrocellulose membranes. Blocked membranes were probed with primary and HRP-conjugated secondary antibodies, followed by detection of bands by the ECL method (Pierce).

***In vitro* tyrosine kinase assays.** K-LISA EAY kits (Calbiochem, La Jolla, CA) were used to measure kinase activity in ErbB3 immunoprecipitates. Receptors were immunoprecipitated and aliquots of precipitate-slurry transferred to replicate wells of K-LISA strips. Strips were incubated in the presence or absence of inhibitors, washed and read on a spectrofluorimeter according to the manufacturer's protocol.

TranSignal phosphotyrosine profiling (SH2 PY) array. TranSignal phosphotyrosine profiling arrays were purchased from Panomics (Redwood city, CA). SKBR3 cells were serum-starved (2 hr) then stimulated with 12 nM Heregulin for 2min. Cell lysates were prepared as for Western Blotting (above) and then incubated with blocked membrane. Washed membrane were incubated with ErbB3 or ErbB2 specific antibodies, followed

by HRP-conjugated second antibody. Reactive spots were visualized by the ECL method (Pierce).

Affinity measurements by flow cytometry. Heregulin 1-β1 EGF domain (R&D systems, Minneapolis, MN) was conjugated with Alexa fluor 647 using the Alexa Fluor 647 Microscale protein labeling kit (Invitrogen), resulting in a dye to ligand labeling molar ratio (MR) of 1.3. Adherent, serum-starved CHO-ErbB3 (WT) and CHO-ErbB3(E933Q) cells were harvested using 1xTris-EDTA (Sigma, Santa Louis) in PBS and resuspended in 0.1%BSA/PBS at density of 2x 10^6 cells/ml. Aliquots of 1x10^5 cells in 50µl were used to measure the binding of fluorescent HRG (0.1nm-300nM, 1 hr 4^{o}C), with or without 1 hr preincubation with 1mM unlabeled ligand as a competitive blocker. Equilibrium binding data were collected with the Becton-Dickinson FACS Calibur flow cytometer (Sunnyvale, CA).

Preparation of plasma membrane sheets and gold labeling for TEM. Detailed methods are described in earlier papers (Wilson et al. 2000; Wilson et al. 2001; Wilson et al. 2004; Wilson et al. 2007). In brief, cells were cultured on 15 mm round, clean glass coverslips. After incubation at 37^{o}C with or without stimuli, cells on coverslips were fixed in 0.5-2% PFA (10 min, RT), inverted onto EM grids (grids were previously glow-discharged and coated with formvar and poly-L-lysine) and ripped. EM grids were then incubated in 2% PFA for an additional 20 min. Washed membranes were labeled from the inside by incubating sequentially with 1^o antibodies and gold-conjugated 2^o reagents. Sheets were post-fixed with 2% glutaraldehyde (20 min, RT), stained with tannic acid and uranyl acetate and digital images acquired on an Hitachi H-7500 transmission

electron microscope. For each condition, at least 10 images were taken from at least 2 separate experiments.

Mapping and analyzing gold particle distributions. Digital images (6.8 megapixel) were analysed using a customized ImageJ plugin to find and count coordinates of 5 and 10 nm particles automatically (Zhang et al., 2005). Coordinates were analyzed using the Hopkins test for clustering (Jain et al. 1988; Wilson et al. 2004; Zhang et al. 2006). The Ripley's K bivariate function was used to evaluate co-clustering (Haase 1995; Wilson et al. 2004; Zhang et al. 2006).

Fluoresence recovery after photobleaching (FRAP). Experiments were performed on an LSM 510META confocal microscope with a 63x1.4 NA oil immersion objective. Serum-starved (2 hr) CHO-ErbB3 (WT)-mCit and CHO-ErbB3 (E933Q)-mCit cells were imaged at low power (500ms/image) with excitation at 488 nm. A region of interest (ROI, 2.5μm-diam circle) was selected on the bottom membrane of the cells and photobleached by increasing the laser to full power. FRAP data were analyzed by subtracting the background and corrected for photobleaching during image acquisition. Post-bleach curves were fit to obtain the recovery half-time. The half-time and circular geometry of the bleach region were used to calculate the diffusion coefficient, D, as described in Axelrod et al (Axelrod et al. 1976).

3.4 Results

Heregulin-induced tyrosine kinase activity in ErbB3 immunoprecipitates from SKBR3 cells.

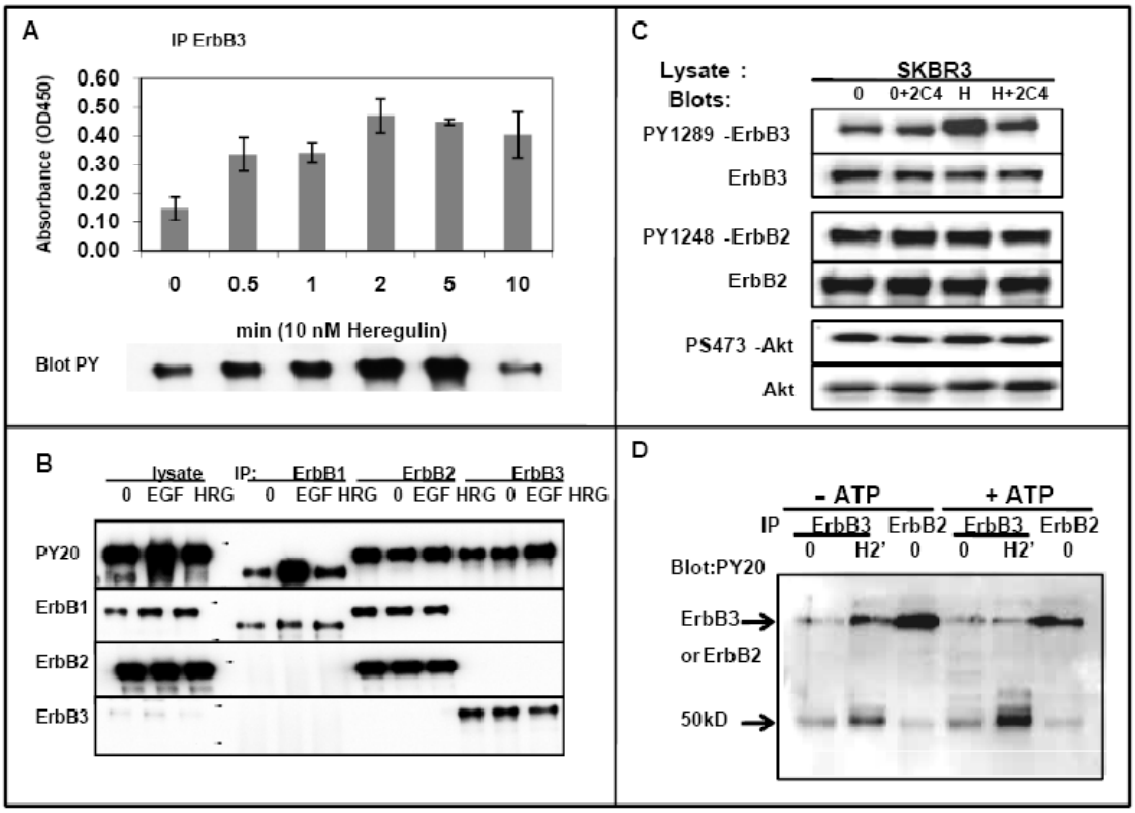

Figure 3.1 ErbB3 tyrosine kinase activity and the possible mechamism may contribute from ErbB2 and an unknown 50kD protein. (A) ErbB3 tyrosine kinase activity. ErbB3 was immunoprecipitated from SKBR3 cells after 2 hours serum starvation (0) or after the indicated time course of treatment with Heregulin (10nM). Immunoprecipitated ErbB3 was used to measure *in vitro* kinase activity by K-LISA (top panel) or subjected to SDS-PAGE, followed by immunoblotting with PY antibody (lower panel). (B) Immunoprecipitation assay for ErbB dimerization. Where indicated, cells were stimulated with 20nM EGF or 3.2nM heregulin, followed by lysis using 1% NP-40 and immunoprecipitation using ErbB1-, ErbB2- or ErbB3-specific antibodies. Samples were subjected to SDS-PAGE, followed by immunoblotting with ErbB-specific antibodies. (C) 2C4 inhibition of ErbB3 and Akt phosphorylation in SKBR3 cells. SKBR3 cells were serum-starved for 2hr (0), treated for 1hr with 100nM 2C4 (0+2C4), or serum starved and stimulated with 12nM Heregulin for 2min (H), or treated for 1hr with 100nM 2C4 and stimulated with 12nM Heregulin for 2min (H+2C4). Aliquots of lysates were separated by SDS-PAGE, followed by immunoblotting with phospho-specific antibodies or total ErbB3, ErbB2 and Akt. (D) A 50kD unknown protein co-IPs with ErbB3 not ErbB2 and is upregulated by Heregulin. SKBR3 cells were serum starved for 2hr (0), or serum-starved and stimulated with 12nM Heregulin for 2min (H2'), followed by immunoprecipitation of ErbB3 or ErbB2. Samples were subjected to SDS-PAGE and immunoblotting with HRP-PY20 antibody.

The bar graph in Figure 3.1A reports results of a tyrosine kinase assay performed using ErbB3 immune complexes isolated from resting and HRG treated SKBR3 cells, an aggressive breast cancer cell line with over 2 million ErbB2, tenfold fewer ErbB1 and less than 70,000 ErbB (Yang et al. 2007). HRG stimulation resulted in an increase in kinase activity in ErbB3 immunoprecipitates that was evident at 0.5 minutes and reached a maximum at 2 minutes. The anti-PY blot in Fig. 3.1A (lower panel) shows increases in ErbB3 phosphorylation in these samples, consistent with measurements of kinase activity. When identically prepared ErbB3 immune complexes were subjected to SDS-PAGE and blotting for ErbB1 or ErbB2, we failed to detect any significant co-precipitation of other ErbB family members (Fig. 3.1B). ErbB1 or ErbB2 immunoprecipitates served as positive controls in these experiments.

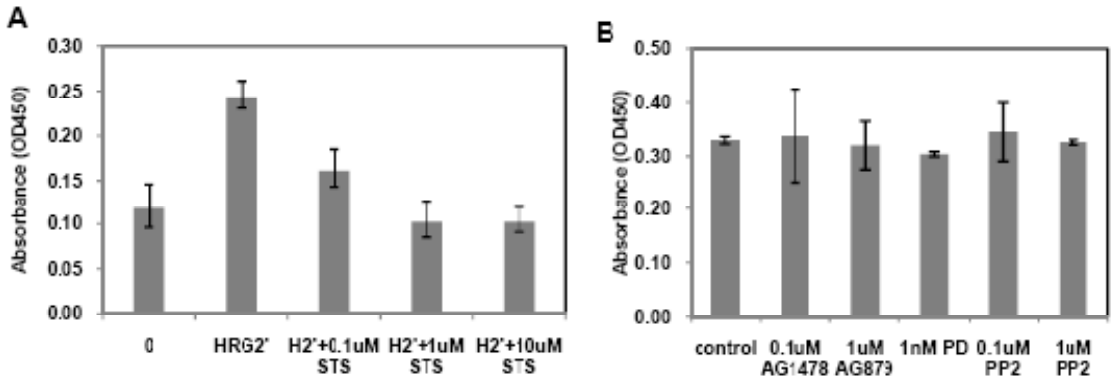

Figure 3.2. Effects of kinase inhibitors on ErbB3 kinase activity. ErbB3 activity was measured by K-LISA in ErbB3 immunoprecipitates prepared from cell lysates before or after 2 min stimulus with 12nM Heregulin. (A) *In vitro* kinase activity in ErbB3 immunoprecipitates (-/+ staurosporine as indicated). (B) *In vitro* kinase activity in ErbB3 immunoprecipitates (-/+ ErbB1 or ErbB2 inhibitors as indicated).

We also treated ErbB3 immunoprecipitates with a panel of kinase inhibitors. Although *in vitro* activity in ErbB3 immune complexes was blocked by addition of the broad specificity inhibitor, staurosporine (Fig 3.2A), there was negligible inhibition by ErbB1 or ErbB2 specific inhibitors (Fig 3.2B). However, a role for ErbB2 in ErbB3 activation

was supported by data shown in Figure 3.1C, showing that preincubation of SKBR3 cells with 2C4 monoclonal antibodies blocked Heregulin-stimulated phosphorylation of tyrosine 1289 on ErbB3 by ~50%. The humanized anti-ErbB2 treatment Pertuzumab, was derived from this antibody. These data suggest that ErbB2's association with ErbB3 may be transient or extremely sensitive to NP-40 detergents used for solubilization of membrane proteins. Importantly, the presence of tyrosine kinase activity in ErbB3 immune complexes cannot be attributed entirely to ErbB2.

Other sources of kinase activity in ErbB3 immune complexes were considered, including candidate proteins previously shown to associate with ErbB3 (Schulze et al. 2005; Jones et al. 2006). The cytoplasmic tyrosine kinases Src, Abl2, and Brk were not detected by western blotting (data not shown). Expression of MET receptor tyrosine kinase was not detected in SKBR3 cells, although it could be reliably blotted in lysates prepared from the human lung cell line used by Engleman et al. (2007). A commercial SH2 array was also used to screen for potential ErbB3 binding proteins in SKBR3 cells; this array includes SH2 domains containing proteins derived from thirteen cytoplasmic tyrosine kinases (Abl, Csk, BTK, Zap-70 and all members of the Src family). In this assay, we treated SKBR3 cells with Heregulin to induce ErbB3 phosphorylation, followed by preparation of detergent lysates. It should be noted that ErbB2 is strongly phosphorylated in these samples, presumably because its overexpression leads to homodimerization (Yang et al. 2007). We modified the manufacturer's protocol by incubating the arrays with the cell lysates, followed by washing and probing of the membranes for ErbB2 or ErbB3 receptors bound to SH2 domains containing proteins immobilized on the array. Results in Fig. 3.3C showed that SH2 domains from none of the 13 tyrosine kinases

represented on the array bound to phosphorylated ErbB3. Only the SH2-domain of the p85 subunit of PI 3-kinase, already well established as the primary binding partner for phosphorylated ErbB3, captured ErbB3 to a significant amount.

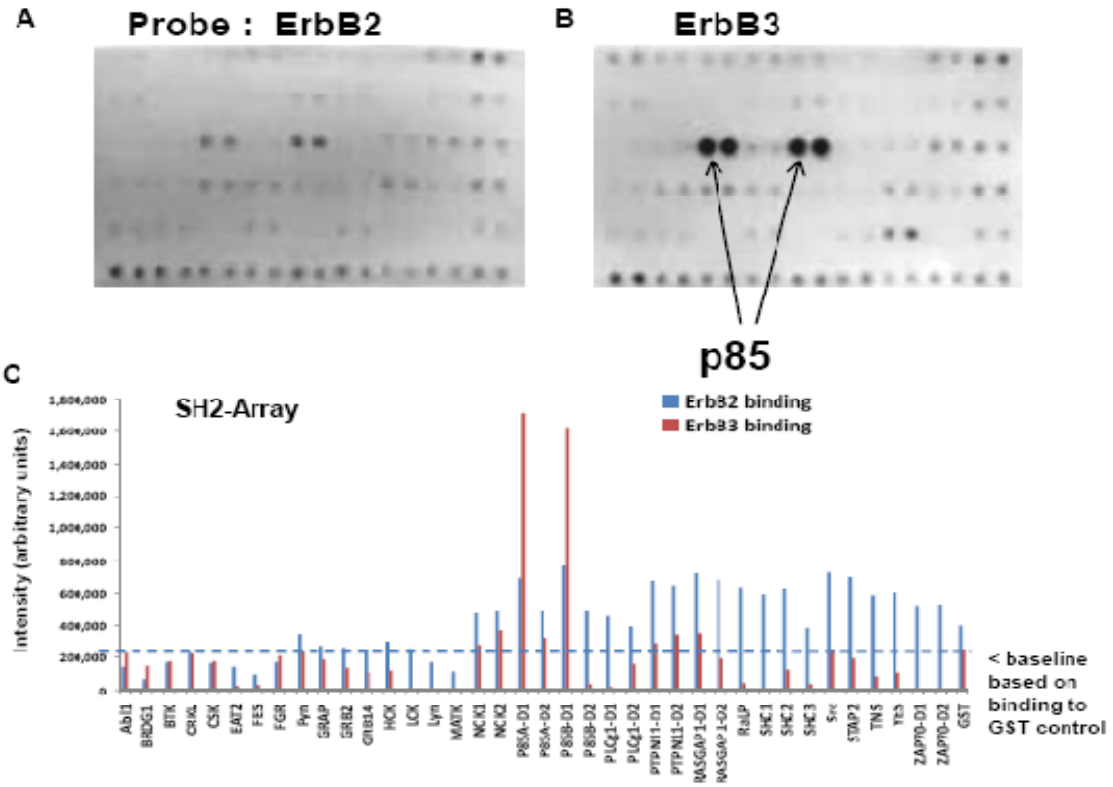

Figure 3.3. TranSignal phosphotyrosine profiling (SH2 PY) array SKBR3 cell lysates were prepared from cells after 2 min Heregulin treatment (12nM). SH2 array membranes were incubated with cell lysates, sequentially probed with ErbB2 (A) or ErbB3 (B) primary antibodies and HRP-conjugated second antibodies, and chemiluminescence signal was detected by the ECL method. (C) Quantitative data were acquired by using a Genegenome densitometer.

We next performed an *in vitro* kinase assay to improve the chances of detecting an associated kinase by autophosphorylation. Results in Figure 3.1D show that incubation of ErbB3 immune complexes with exogenous ATP resulted in *in vitro* tyrosine phosphorylation of both ErbB3 (band at 180 kDa) and an unknown band at ~ 50-52 kDa. Importantly, this 50-52kDa band was not detected in parallel *in vitro* kinase assays

conducted using ErbB2 immunoprecipitates (lanes labeled ErbB2, in Figure 3.1D). This band is weakly phosphorylated in ErbB3 immune complexes prepared from resting SKBR3 cells but intensely phosphorylated in the HRG-treated sample. This unknown protein remains a candidate for an ErbB3-associated kinase and its identity will be sought in future work using a mass spectrometry approach.

In order to determine the relative contribution of ErbB2 in ErbB3 activation, we compared ErbB3 PY1289 phosphorylation in cells treated with the antibody 2C4 to block ErbB2/ErbB3 heterdimerization (Figure 3.1C). Results show that 2C4 preincubation (100 nM, 1 hr) was able to block Heregulin-mediated upregulation of ErbB3 PY1289 and Akt PS473 by approximately 50%, but not ErbB2 phosphorylation at PY1248.

SKBR3 cells express two alleles of ErbB3, wildtype (WT) and a single kinase domain substitution (E933Q).

Concurrent with the biochemical studies, we considered the possibility that SKBR3 cells might express an activating mutation in the ErbB3 kinase domain. PCR-based sequencing was used to span the entire ErbB3 tyrosine kinase domain. We discovered that SKBR3 cells express two alleles, wildtype (WT) and a single kinase domain substitution (E933Q) (Fig. 3.4A). Site directed mutagenesis was then used to introduce this substitution into an existing vector for expression of a mCit-ErbB3 (WT) fusion protein. The two vectors were stably transfected into Chinese Hamster Ovary (CHO) cells and colonies selected for high surface expression of recombinant ErbB3 (images in Fig.3.4B,C).

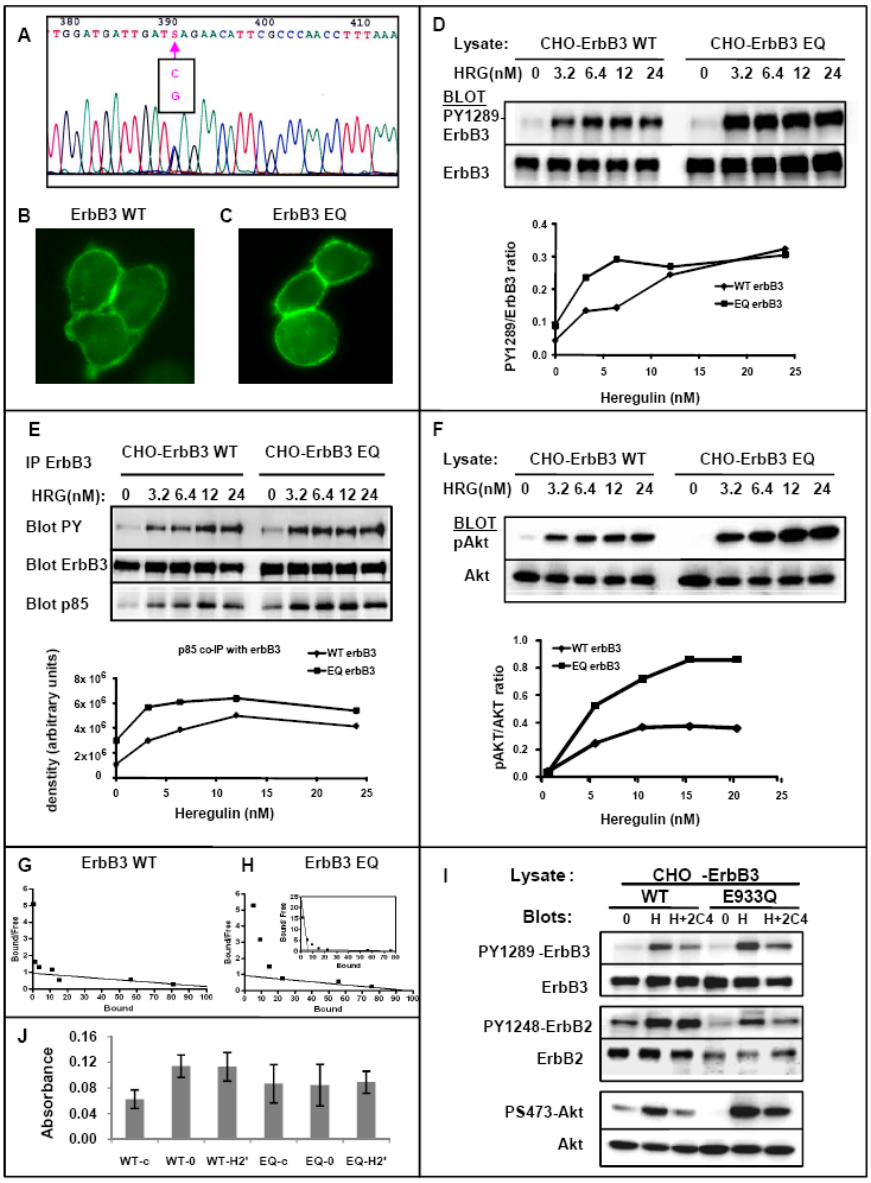

Figure 3.4 ErbB3 mutation in SKBR3 cells; ErbB3(WT) activate the PI3K/AKT signaling pathway and ErbB3(E933Q) amplifies this signaling pathway. (A) DNA sequencing shows that SKBR3 cells are heterozygous for ErbB3, expressing both wildtype (G391) and a form of ErbB3 with a point mutation in the tyrosine kinase domain (C391), E933Q. (B,C) Fluorescent picture show transfected ErbB3-mCit located at the CHO cell membrane, (WT in B and E933Q in C). (D) Western blotting showing that ErbB3 tyrosine phosphorylation (PY1289) status responds to different doses of Heregulin treatment. CHO transfected cells were serum starved for 2 hours (0) or treated with the indicated dose of Heregulin, cell lysate were subjected to SDS-PAGE, immunoblotting with ErbB3-PY1289 antibody. ErbB3 phosphorylation signal were quantified by densitometry (lower panel) (similar results were obtained from three repeated experiments). (E) p85 co-immunoprecipitated with ErbB3(E933Q) more than ErbB3(WT). (F) Western blotting shows Akt phosphorylation responds to Heregulin treatment. (G, H) Heregulin binding affinity with ErbB3 (WT in G) and (E933Q in H). (I) 2C4 inhibition of ErbB3 and Akt phosphorylation in CHO transfected cells. CHO cells were serum starved for 2hr (0), or serum starved and stimulated with 3.2nM Heregulin for 2min (H), or treated for 1hr with 100nM 2C4 and stimulated with 3.2nM Heregulin for 2min (H+2C4). Aliquots of lysates were subjected to SDS-PAGE, followed by immunoblotting with phospho-specific antibodies or total ErbB3, ErbB2 and Akt.

ErbB3(WT) activates the PI3K/AKT signaling pathway in CHO cells and ErbB3(E933Q) amplifies this signaling pathway.

As shown in Figure 3.4D (diamonds), introduction of ErbB3 (WT) into CHO cells results in dose-dependent increases in phosphorylation at PY1289. However, robust PY1289 phosphorylation of ErbB3 (E933Q) was consistently detected at the lowest concentration of Heregulin in the dose response series (N of 3 independent experiments). The upper line plot in Figure 3.4D (squares) documents our observation that ErbB3 (E933Q) showed *2 to 3 fold stronger* phosphorylation than ErbB3 (WT) at low ligand concentrations.

The robust phosphorylation of ErbB3(E933Q) in response to low doses of ligand has the potential to amplify signaling by increased recruitment of PI3-kinase. In Figure 3.4E, we evaluated whether ErbB3 immunoprecipitates from WT and E933Q transfectants would also show differential levels of co-precipitating p85, the regulatory subunit in the heterodimeric PI 3-kinase complex. Results show that the amount of p85 recovered in ErbB3 immune complexes paralleled the degree of phosphorylation of ErbB3 in the CHO transfectants, with more PI 3-kinase recovery at low ligand doses for ErbB3 (E933Q) than for ErbB3(WT). Results in Figure 3.4F show that cells expressing ErbB3(E933Q) also have a more robust activation of the serine/threonine kinase, AKT, as measured by phosphorylation of AKT S473. The phosphoAKT/total AKT ratio was higher at all time points after Heregulin stimulation of CHO cells expressing ErbB3(E933Q), compared to cells expressing the WT receptor.

These results suggested that the ErbB3 (E933Q) substitution renders the receptor more sensitive to low concentrations of ligand. This possibility was confirmed by measuring the binding affinity of fluorescent Heregulin to both sets of stable transfectants by flow cytometry. Results showed that ErbB3(WT) on CHO cells binds Heregulin with a predominantly an affinity of 124±4nM (Figure 3.4G); a minute fraction (<1%) appears bind with high affinity. In contrast, ErbB3(E933Q) receptors show two distinct populations, with 5% high affinity (0.23±0.6nM) and 95% low affinity (105±31nM) (Fig 3.4H).

The CHO cell model differs significantly from the SKBR3 cells model in two important respects: First, SKBR3 cells express at least 30 fold *more* ErbB2 than ErbB3 (Yang et al., 2008) while our CHO transfectants express about many fold *fewer* ErbB2 than ErbB3. We asked whether 2C4 treatment would block ErbB3 phosphorylation in transfected CHO cells. As shown in Figure 3.4I, 2C4 again blocked the Heregulin-induced increased in PY1289-ErbB3 by about 50%, with similar results for the WT and E933Q forms of ErbB3. Second, the results of ErbB3 *in vitro* kinase activity using the K-LISA assay were dramatically different in CHO cells: there was no significant increase in tyrosine kinase activity in ErbB3 immune complexes after Heregulin treatment (Figure 3.4J). We speculate that CHO cells, unlike SKBR3 cells, lack a cytoplasmic tyrosine kinase partner for ErbB3.

Heregulin treatment leads dramatic clustering of both ErbB3 (WT) and ErbB3 (E933Q) on CHO cell membrane.

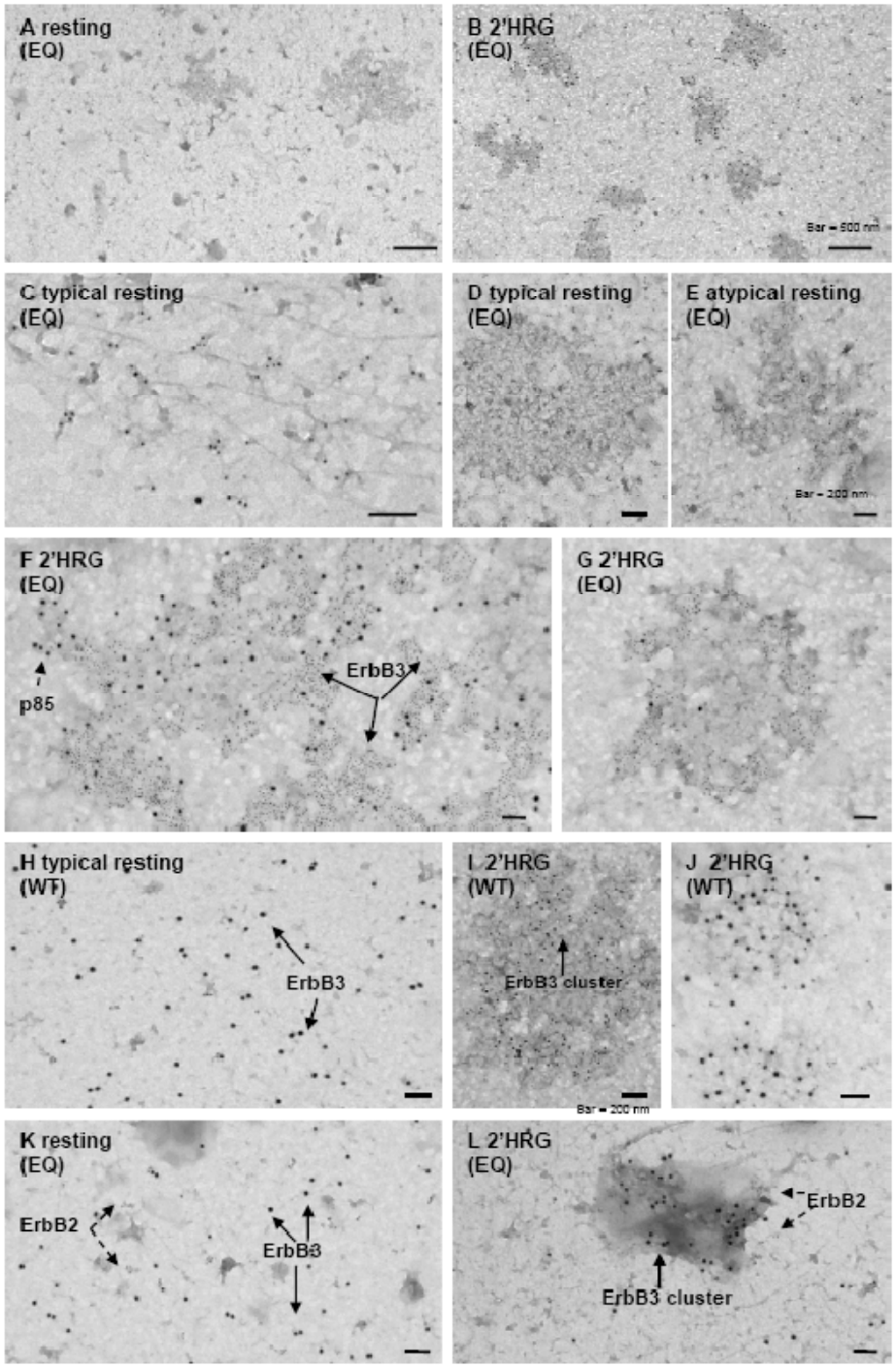

Figure 3.5 Redistribution of membrane-associated ErbB3 in Heregulin-stimulated CHO-ErbB3 (WT) and CHO-ErbB3(E933Q) cells. Transfected CHO cells were serum-starved for 2 hours (resting) or stimulated with 3.2nM Heregulin for 2-5min (2' HRG or 5' HRG). (A-G) Membrane sheets were prepared from CHO-ErbB3(E933Q) cells, then double labeled for ErbB3(5nM gold) and p85(10nM). (H-J) Membrane sheets were prepared from CHO-ErbB3(WT), then double labeled for ErbB3(10nM gold) and p85(5nM). (K. L) Membrane sheets were prepared from CHO-ErbB3(E933Q) cells, then double labeled for ErbB3(10nM gold) and ErbB2(5nM). Bars, 0.5μm for A and B, 0.2μm for D, E, I and J, 0.1μm for other images.

Our previous work in SKBR3 cells demonstrated that Heregulin treatment led to dramatic reorganization of endogenous ErbB3 in the plasma membrane. Large clusters of ErbB3 were observed on plasma membrane sheets ("rip-flips") prepared from activated SKBR3 cells, with concomitant recruitment of p85 to the clusters. Figure 3.5 shows results of this powerful electron microscopy approach to document the topographical distribution of activated ErbB3 when expressed in CHO cells. Membrane sheets were ripped from CHO transfectants, before or after HRG stimulation, and then incubated with immunogold reagents directed at either the cytoplasmic tail of ErbB3 or the p85 subunit of PI 3-kinase. The figure labels indicate the antigens recognized by pairs of 5 nm and 10 nm gold particles in these double labeling experiments. Fixation steps in this protocol ensure that the distribution of membrane proteins visualized with this method represent the native condition (Wilson et al. 2007).

In resting CHO cells expressing either ErbB3(E933Q) (Fig 3.5A) and or ErbB3WT (Figure 3.5H), ErbB3 is broadly distributed in small clusters. Notably, distinctive "dark patches" (arrows in Fig 3.5A, Figure 3.5D) in the images of resting membrane lack significant ErbB3 label. When seen at high magnification, the ErbB3 clusters are sometimes aligned with cable-like structures that may be elements of the cortical cytoskeleton (Fig. 3.5C).

Heregulin treatment leads to formation of dramatically large ErbB3 clusters (Figures 3.5B,F,G,I, J). p85 label is typically found in the center (Fig. 3.5J) or periphery (Fig. 3.5I) of these patches. In addition, a large fraction of the highly clustered ErbB3 was found in the distinctive "dark patches" that were empty of ErbB3 prior to Heregulin

stimulation. Spatial statistical analyses were applied to evaluate the extent of this redistribution in WT ErbB3 and mutant ErbB3-expressing cells. Numerous examples of ErbB3 (E933Q) were found where essentially every receptor on a membrane sheet was recruited to dark patches, despite the relatively low levels of ErbB2. Double labeling also showed that, unlike ErbB3, ErbB2 was not exclusively localized in the signaling patches (Figure 3.5K,L). These data suggest that ErbB3 can be recruited to signaling patches independent of ErbB2, possibly as a mix of ErbB2/ErbB3 heterodimers and ErbB3 homooligomers. It is notable that the massive recruitment of WT ErbB3 was only occasionally observed, consistent with the lower sensitivity of the WT ErbB3. Note that the EM studies were performed at a dose of 3.2 nM Heregulin to maximize the chances of observing differences using the microscopic assay.

ErbB3(WT) has a significant immobile population and the E933Q substitution results in an increased immobile fraction.

Previous work in other systems has demonstrated that the activation state of receptors is often closely tied to changes in diffusion. Fluorescence recovery after photobleaching (FRAP) is a powerful method to evaluate the diffusive properties of receptors in live cells. Using FRAP, we discovered that a larger fraction of fluorescent ErbB3(WT) has a mobile fraction (59%) compared to fluorescent ErbB3(E933Q), with a highly mobile fraction of only 32%. The data presented in Fig 3.6A show much faster recovery from photobleaching for mCit-ErbB3(WT) than mCit-ErbB3(E933Q). These data demonstrate another distinguishing feature of the E933Q substitution in ErbB3. They also suggest

that the ErbB3 reorganization documented by electron microscopy may be explained by local coalescence of slowly-diffusing clusters.

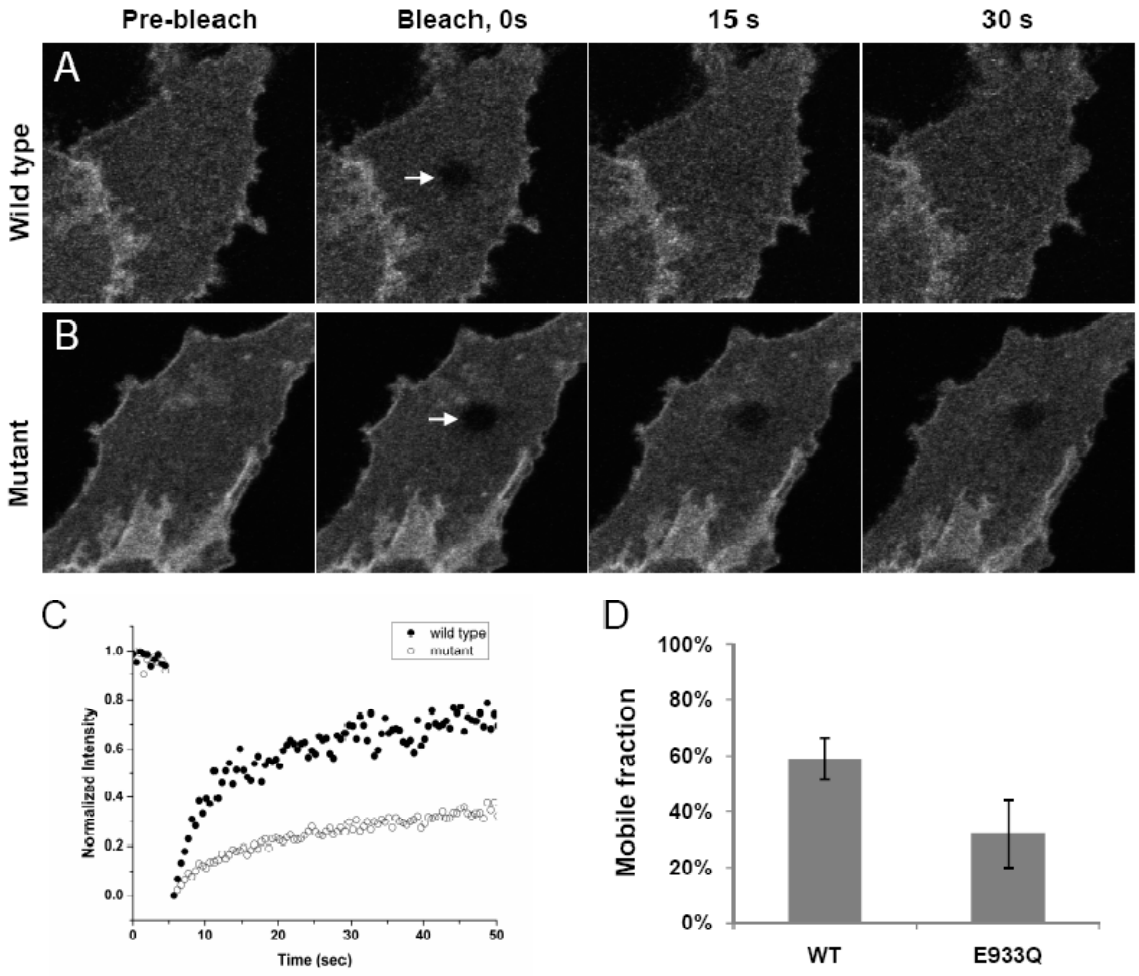

Figure 3.6. Example FRAP images for A) ErbB3(WT)-mCit and ErbB3(E933Q)-mCit expressed in CHO cells. Images have been background subtracted, corrected for photobleaching and gaussian filtered (σ_{xy}=1) corrected. C) Intensity traces from the bleach ROI (arrow) in A and B. D) Plot of mobile fraction for ErbB3(WT)-mCit (n=19) and ErbB3(E933Q)-mCit (n=20), P << 0.01.

3.5 Discussion

ErbB3, a member of epidermal growth factor receptor (EGFR/ErbB/HER) family, is unique in that it has only weak tyrosine kinase activity (Guy et al. 1994). In searching for an ErbB3 dimerization partner using an *in vitro* tyrosine kinase assay, we discovered that ErbB3 immunoprecipitates in SKBR3 breast cancer cells contain Heregulin-inducible tyrosine kinase activity. We further discovered that these cells express two ErbB3 alleles, wildtype (WT) and a single kinase domain substitution (E933Q). When mCitrine-fusion proteins of WT or E933Q ErbB3 were stably transfected into CHO cells, we demonstrated that WT ErbB3 upregulates the PI3K-AKT cell survival pathway through a mechanism that is only partially dependent on ErbB2. Remarkably, the E933Q substitutions in ErbB3 resulted in amplification of ErbB3 phosphorylation and coupling to the the PI3K-AKT pathway at low doses of ligand. This is the first report of a gain-of-function substitution in the kinase domain of ErbB3.

The widely-accepted mechanism for ErbB3 activation is that, upon ligand binding, ErbB3 forms heterodimers with other kinase-competent ErbB family member, especially ErbB2. Heterodimerization in turn leads to transphosphorylation of ErbB3's YXXM motifs and recruitment of PI 3-kinase. However, the possibility of ErbB3 activation independent of other ErbB receptors in ovarian cancers has also been reported (Beerli 1995, Campiglio 1999). We observed that ErbB3 activation is robust in transfected CHO cells, where it is expressed at least 2-3 times higher than endogenous ErbB2. In these cells, ErbB2 blocking antibodies (2C4) inhibit Heregulin-induced ErbB3 phosphorylation by only about 40%. Residual ErbB3 activation, in the absence of ErbB2 as a heterodimerizing

partner, may be attributed to ErbB3's own weak kinase activity or possibly to its association with an unknown cytoplasmic tyrosine kinase. Our future work is aimed at distinguishing these two possibilities.

In a systematic study of the tyrosine kinase transcriptome in 254 established tumor cell lines, Ruhe and colleagues reported that a single amino acid substitution (G1064E) of ErbB3 was common to SKBR3 cells and all other tumor cell lines evaluated in that study (Ruhe et al. 2007). The presence of G1064E mutation was also discribed in another early ErbB3 sequence study in the breast cancer cell line, MDA-MB-361 (Plowman et al. 1990). These studies suggest that G1064E is a common variant, not a mutation. However, the germline sequence for these tumors is not available for comparison. Eight other amino acid substitutions have also been noted as single incidences in a small subset of the tumor cell lines screened in the Ruhe study. These substitutions were S1119C, L1177I, N126K, R667H, P1142H, R611W, R1077W and R1089W; however, none of these additional substitutions were located in ErbB3 kinase domain. In the course of the current study, we sequenced the kinase domain (nucleotides 2259 to 3121) of four other ErbB3-expressing breast cancer cell lines (MCF7, T47D, MDA-MB-453 and BT474). All four of those cell lines express wildtype ErbB3. Nevertheless, public databases such as GENECARD report at least 24 amino acid sites for ErbB3 single polynucleotide polymorphisms (SNPs), including four in the kinase domain (S717L, I744T, D758H, A962T). For comparison to the E933Q substitution, which was numbered based upon the ErbB3 sequence minus the 19 amino acid signal peptide, these would represent S698L, I725T, D739H and A943T in the mature protein. To our knowledge, this is the first functional study of ErbB3 kinase domain mutations/substitutions and suggests that a

more extensive evaluation of the frequency of ErbB3 domain mutations in breast tumors is worthwhile.

The binding affinity of ErbB3 for the HRG1-β1 EGF like domain was measured previously by direct binding of I^{125}-HRG (EGF-like domain) to soluble ErbB3-IgG. In that study, a single binding site for wild type ErbB3 was reported, with a Kd of 5.4 nM (Jones et al. 1999). In a similar study, the binding of radiolabeled HRG to ErbB3 transfected COS-7 cells was measured, revealing a single class of HRG binding affinity and a Kd of 1.9± 0.3nM (Sliwkowski et al. 1994). These values differ from our measurements based upon flow cytometry and the use of fluorescent ligand (124±4nM for WT ErbB3). The EGF-like domain of HRG 1β was used in our study and both prior studies, although our protocol limited binding to one hour as opposed to overnight incubation in the Sliwkowski study. Our studies support the conclusion that WT ErbB3 displays only predominantly a single class of binding sites, with a barely-detectable high affinity population. However, we found that the mutant ErbB3 (E933Q) has two binding populations: a high affinity population (5%) and a low affinity population. This phenomenon is well known in the literature on the related family member, ErbB1/EGFR, where two classes of binding sites have been measured by several laboratories (Rousseau et al. 1995; Chung et al. 1997; Choi et al. 2007). It is difficult at present to propose a mechanism by which E933Q (or similar substitutions) might translate to changes in ligand affinity. By analogy with the integrins (Ginsberg et al. 2005), we speculate that kinase domain substitutions may facilitate a ligand-independent conformational change that increases the percentage of time the receptor is in the active state.

One unique feature of our studies is the direct visualization of ErbB3 "signaling clusters" by immunoelectron microscopy of membrane sheets. Our observations of ErbB3 redistribution in transfected CHO cells after Heregulin is reminiscent of our prior study in SKBR3 cells, where ErbB2 outnumbers ErbB3 by 50 fold. The situation is reversed in CHO cells, where ErbB3-mCFP are far more abundant than endogenous ErbB2. This is an important distinction, since we observed many cell membrane preparations where essentially every ErbB3(E933Q) receptor was recruited to the distinctive large signaling patches. Double labeling also showed that, unlike ErbB3, ErbB2 was not exclusively localized in the dark patches. Together, these data suggest that ErbB3 can be recruited to signaling patches independent of ErbB2, possibly as a mix of ErbB2/ErbB3 heterodimers and ErbB3 homooligomers. We point out that these studies also call for revision of the pre-oligomerization ErbB3 model of Landgraf and colleagues, where *preexisting* inactive ErbB3 oligomers are proposed to *dissociate* upon ligand binding to promote heterodimerization (Landgraf et al. 2000; Kani et al. 2005). We observed that ErbB3 clusters were small in resting cells, ranging in size from 1 to 7, followed by formation of clusters with hundreds of ErbB3 receptors after Heregulin treatment. If inactive ErbB3 oligomers exist, they must be composed of dimers or limited to only a few receptors per oligomer.

The CHO cell proved to be a fortuitous model system for studying membrane topography, since resting CHO cells are particularly rich in distinctive marginated "dark patches" that lack ErbB3 prior to ligand stimulation. These patches are morphologically unlike other known membrane domains, such as caveolae (Anderson et al. 2002), that have previously been implicated as destinations for signaling proteins (Carpenter 2000).

This suggests that the "dark patches" represent pre-existing membrane domains with properties that are attractive to activated receptors. They may represent specialized "protein islands", a hypothesis suggested by our prior work in T cells (Lillemeier et al. 2006). The molecular profile of these patches remains unidentified to date, although we found strong labeling for the p85 subunit of PI 3-kinase in the patches following HRG treatment. In data not shown, we determined that treatment of transfected CHO cells with the PI 3-kinase inhibitor, wortmannin, failed to inhibit the recruitment of ErbB3 or p85 to the patches. This indicates that the local synthesis of PIP_3 and other 3-phosphotidylinositols is not required for co-localization of ErbB3 receptors and PI-3K or for formation of the patches.

FRAP experiments reported in Figure 3.6 showed that large fractions of WT ErbB3 are poorly mobile, a property that is increased by the E933Q mutation. We postulate that this slow mobility may be due to association of the ErbB3 cytoplasmic tails with intracellular adaptor proteins or with cytoskeletal components. It would also be consistent with preexisting ErbB3 oligomers, which would diffuse slowly due to the larger size of the complex. As discussed above, if oligomers exist in resting cells, EM studies indicate that they must be limited to only a few receptors per oligomer. It is interesting to note that, despite their slow mobility, ErbB3 can redistribute into large clusters within minutes of HRG addition. A reasonable interpretation is that HRG-mediated ErbB3 reorganization occurs over relatively short distances, by coalescence of many small clusters or by trapping in the specialized domains imaged by electron microscopy.

Several issues are still not resolved in our studies. One of these is the mechanism of ErbB2-independent ErbB3 signaling. We propose two hypotheses for the mechanism of ErbB2-independent ErbB3 signaling. First, even WT ErbB3 may have residual kinase activity which can signal alone. Second, ErbB3 may recruit a cytoplasmic tyrosine kinase which promotes ErbB3 signaling. To test the first hypothesis, we plan to use ErbB2 SiRNA to further reduce the low levels of endogenous ErbB2 in CHO cells, then repeat our assays for ErbB3 tyrosine kinase activity and ErbB3 signaling. To test the second hypothesis, we plan to do a large scale immunoprecipitation of ErbB3, extract the 50Kd band and identify the protein by mass spectrometry.

In summary, we demonstrate that ErbB3 signals robustly to the PI3K-AKT cell survival pathway when artificially introduced into CHO cells, that express a small amount of endogenous ErbB2 and no other members of the ErbB family. HRG-dependent ErbB3 signaling in this model system is partially independent of ErbB2 and can be amplified by a novel gain-of-function mutation in the ErbB3 kinase domain. These results suggest that ErbB3 may have independent roles in tumor survival and is itself a potential cancer therapeutic target.

Chapter 4. Contributions for other co-author papers

Stochastic simulations of ErbB homo and heterodimerisation: potential impacts of receptor conformational state and spatial segregation

M.-Y. Hsieh, **S. Yang,** M.A. Raymond-Stinz, S. Steinberg, D.G. Vlachos, W. Shu, B. Wilson, J.S. Edwards

Published in ***IET Systems Biology*, 2008, 2: 256–272**

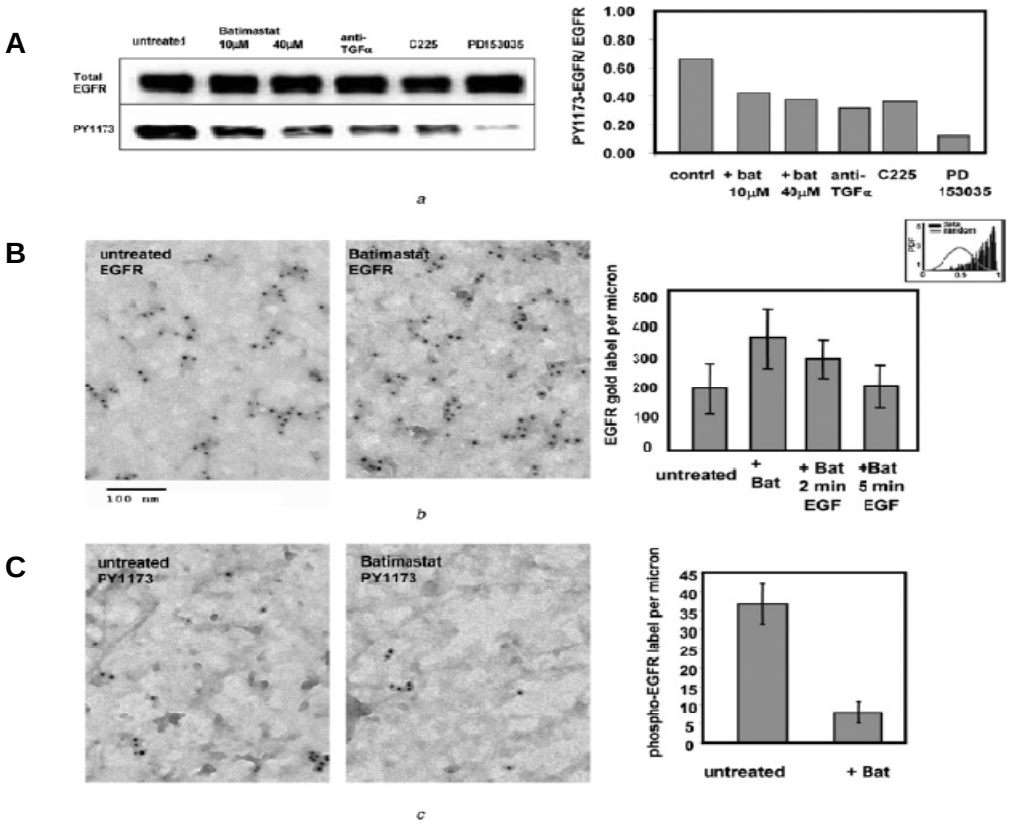

Figure 4.1 Experimental evidence for ligandless signalling by EGFR (A) Western blots show that EGFR phosphorylation in 'resting' A431 cells results from a combination of autocrine and ligand-independent stimulation. A431 cells were serum starved for 4 h, with or without treatments indicated. Lysates were harvested for SDS-PAGE and separated proteins transferred to nicrocellulose, followed by probing with antibodies to PY1173 or total EGFR. Bands were quantified by densitometry and plotted as ratios of PY1173/total EGFR. (B) TEM images of fixed membrane sheets prepared from untreated (serum-starved) or batimastat treated A431 cells (40 mM batimastat dose was used), followed by immunogold labelling to document clustering of EGFR. (C) Cell treatments were the same as in (B), but sheets were immunogold labelled with anti-PY1173 antibodies.

Spatio-Temporal Modeling of Signaling Protein Recruitment to EGFR

Ming-yu Hsieh, **Shujie Yang,** Mary Ann Raymond-Stinz, Alexandre Chigaev, Jeremy S. Edwards and Bridget Wilson

Submitted to PLos One

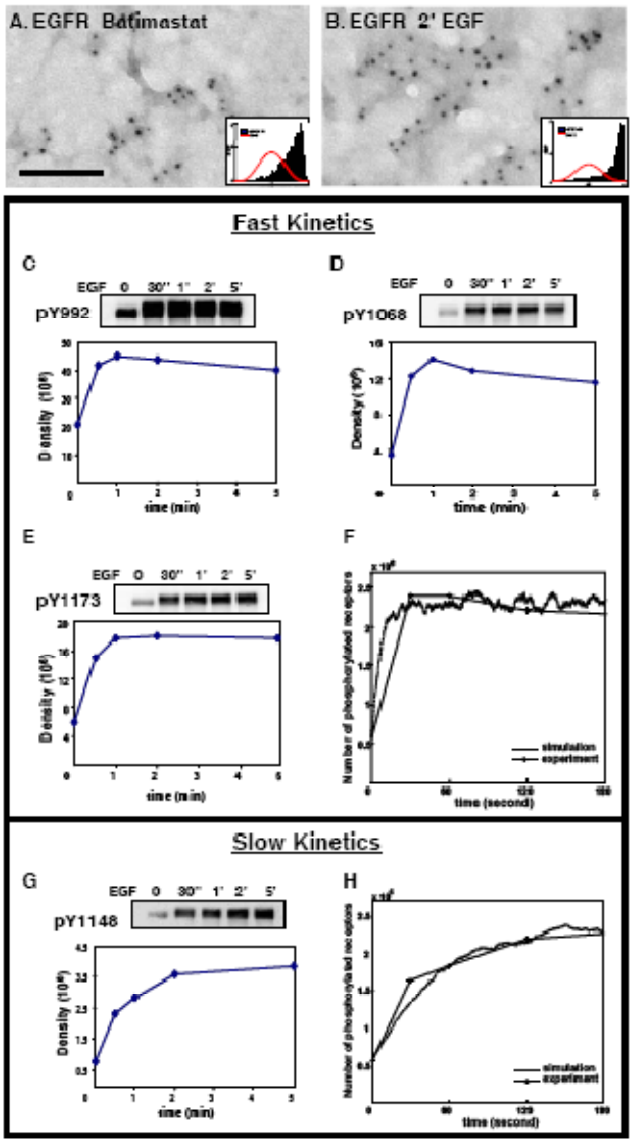

Figure 4.2 Analysis and simulation of EGFR tyrosine residues phosphorylation kinetics. A431 cells were serum-starved and treated with batimastat for "resting" condition shown in (A), or treated thereafter for 2 min with 20 nM EGF (B). "Rip-Flips" were prepared and membranes immunogold-labeled with anti-EGFR antibodies. Inset in both (A) and (B) confirms EGFR clustering by Hospkins test. Bars, 0.1 □m. Western blotting method was used to analyze phosphorylation kinetics of EGFR tyrosines (**C**) Y992, (**D**) Y1068, (**E**) Y1173, and (**G**) Y1148. Bands were quantified by densitometry and plotted as density of the bands. (**F**, **H**) Results of simulations (dashed lines) agree well with the "fast" kinetics and "slow" kinetics data (solid lines), using parameter values estimated by fitting to the data.

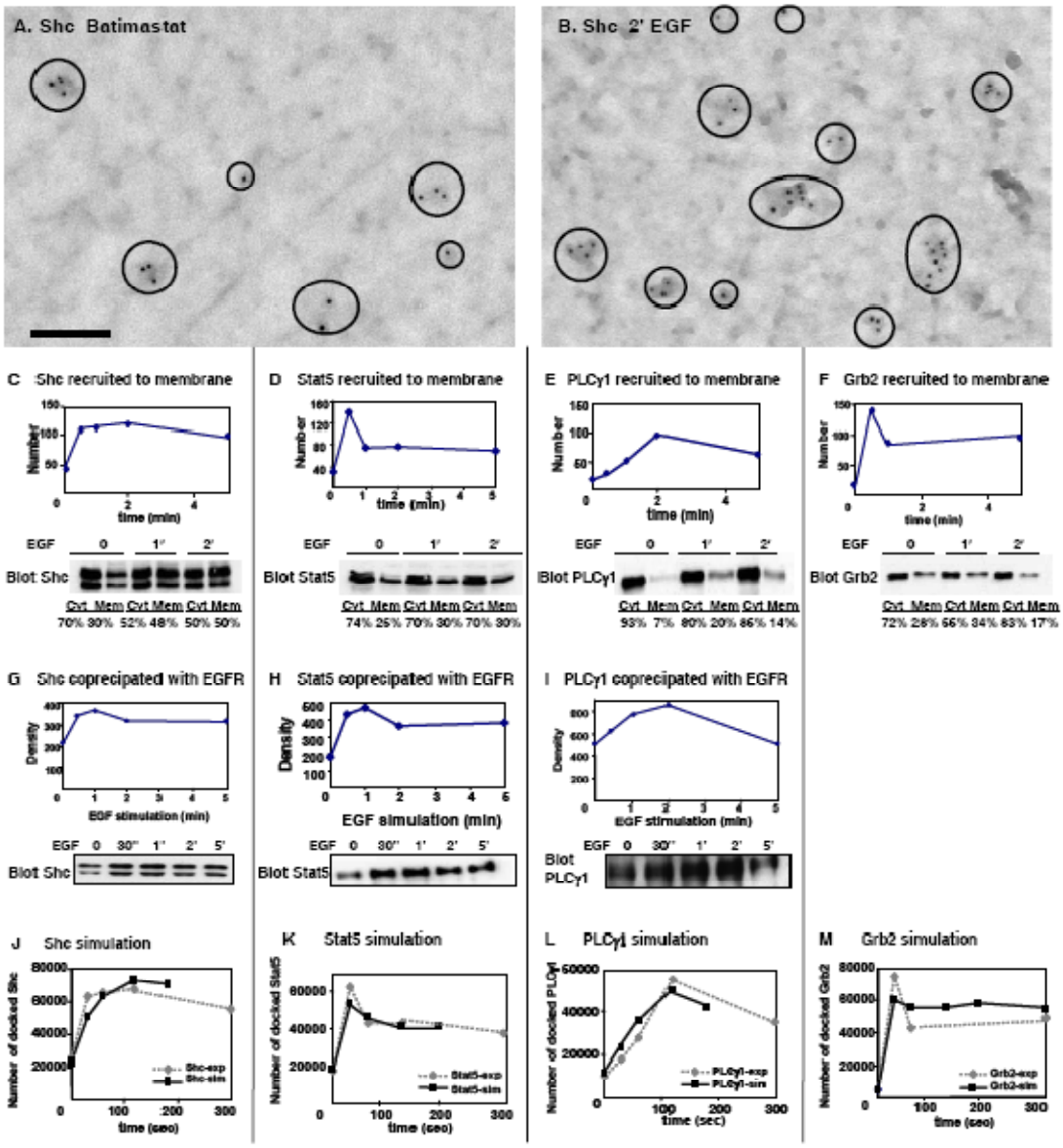

Figure 4.3 Analysis and simulation of the reaction kinetics between the four adaptors and EGFR. (**A-B**) Membrane sheets were prepared from serum-starved, batimastat-treated A431 cells without (A) or with EGF stimulation (**B**). Sheets were labeled with 5 nm gold reagents recognizing Shc. Circles in (**A, B**) highlight Shc label on these membranes. Bars, 0.1 μm. (**C-F**) Quantitative values of Shc, Stat5, PLCγ1, and Grb2 immunogold labeling on 3 μm^2 area of membrane, reported as an average of at least 10 membranes. Blots in **C-F** show results of fractionation experiments, where crude cytosol and membrane fractions were prepared, proteins separated by SDS-PAGE and membranes blotted for Shc, Stat5, PLCγ1 and Grb2. In (**G-I**), blots report co-precipitation of Shc, Stat5 and PLCγ1 with EGFR over a time course of EGF stimulation. Bands were quantified by densitometry and plotted as density of the bands. In (**J-M**), simulations of reaction kinetics between the four adaptors and EGFR using experiment-fitted values produce results (black solid line) similar to experimental data (grey dashed line).

Chapter 5. General Discussion

5.1 Insights into signaling from electron microscopy studies.

We have shown, for the first time, that there is partial segregation of ErbB family members on the plasma membrane. Data reported in Chapters 2, 3 and 4 show that we were able to observe and quantify the topographical relationships of ErbBs with each other and with several important signaling adaptors and enzymes. Although the immunoelectron microscopy method does not directly measure molecular associations, such as dimers, it does measure the proximity of molecules. This led to collaborative experiments between the experimental team (Wilson, Yang) and UNM mathematical modeling experts (Hsieh, Edwards) to attempt to estimate the impact of spatial segregation on ErbB dimerization patterns. The first phase of that work was recently published in IET Systems Biology (Hsieh et al. 2008) and a second manuscript is now under review. Biochemical and microscopy studies in support of these papers are provided in chapter 4, preceding this discussion. Importantly, computer simulations suggested that receptor clustering and partial segregation have significant implications for signaling. First, clustering of receptors creates high local densities that enhance the efficiency of adaptor coupling. Second, partial segregation of ErbB1 and ErbB2 (as demonstrated in Chapter 2, Fig. 2.5) suggests that homooligomers dominate, even when ErbB2 is in large excess over ErbB1. Figure 5.1 below, taken from Hsieh et al (2008), demonstrates how computer simulations support this conclusion. Third, overexpression of ErbB receptor overrides the need for receptor clustering by creating high overall densities. For ErbB1, this translates to promotion of ligand-independent signaling as

dimers form between receptors that flux between open and closed conformations. (See Figure 5.2 below, from Hsieh et al., 2008).

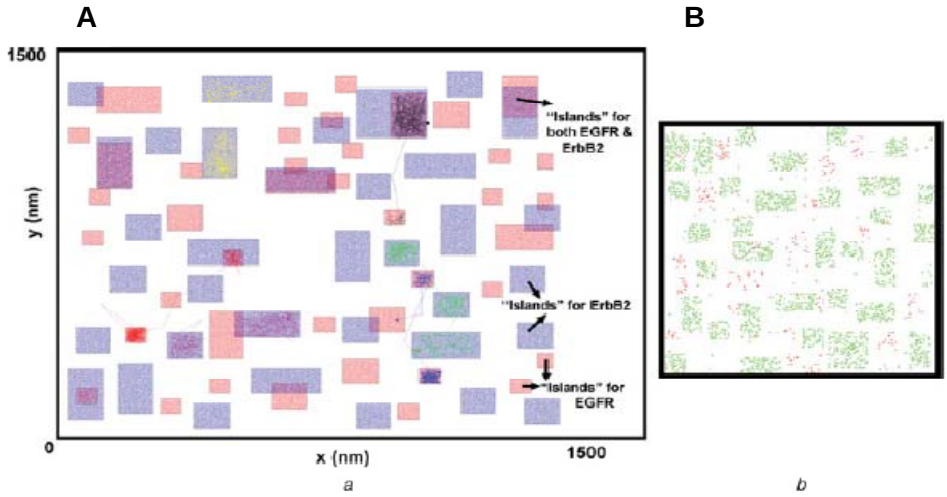

Figure 5.1 Simulation of partial ErbB family segregation using the protein island approach. (A) Thirty second trajectories of three EGFR (black, blue, and red) and three ErbB2 (green, yellow and pink) are plotted. EGFR is constrained in its preferred regions (red) and transverses other (blue regions, white area) fast and freely. Similarly, ErbB2 is constrained in its preferred regions (blue) and passes non-preferred regions unconstrained. (B) EGFR and ErbB2 are co-clustered at the areas where blue regions and red regions are overlapped.

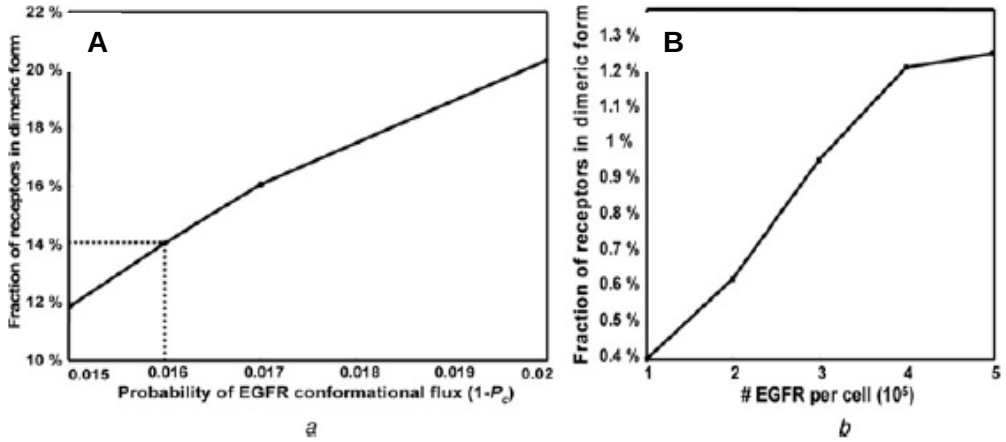

Figure 5.2 Estimation of the probability of EGFRs conformational flux. (A) Use of reported data to determine the probabilities of EGFR conformational flux. Stochastic simulations were initiated using a steadystate value of 14% oligomers (here assumed to be dimers) for unoccupied receptors, as reported in Martin-Fernandez et al. Results estimate that, under these conditions, each 'closed' receptor has a 0.016 chance to become open (Pc ¼ 0.984) (B) Increasing the density of EGFR leads to a higher percentage of active homodimers. Simulations in SPS predict that higher receptor densities will result in more frequent collisions between receptors in the open state, leading to a larger fraction of dimers in the absence of ligand.

Chapter 2, published in 2007 in the Journal of Cell Science, has already had impact on the field, as indicated by several recent citations. A comprehensive review of the ErbB family by Shepard highlighted our electron microscopy studies as part of its argument that ErbB2 is a rational target for cancer therapy (Shepard et al. 2008). A subsequent review by Sithanandam pointed to our observation of Heregulin-induced ErbB3 cluster formation as a hallmark of ErbB3 signaling (Sithanandam et al. 2008). Nagy, who has published a series of papers on light microscopic evaluation of ErbB receptor clustering (Nagy et al. 1999; Nagy et al. 2001; Nagy et al. 2002), cited our study in his recent Biophysical Journal paper (Szabo et al. 2008). Importantly, Nagy's work validates our findings by use of different, but complementary, microscopic techniques.

Pike and colleagues have also used light microscopy techniques to evaluate the mobility of EGFR/ErbB1 in live cells (Saffarian et al. 2007). Pike's studies were based upon fluorescence correlation spectroscopy (FCS), a technique that offers the capability to evaluate fluorescence associated with single and clustered receptors as they move through the focal volume. Pike found that, in the resting state, the majority of receptors (~70%) are monomeric. However, a significant fraction are dimers (~20%) or even higher order oligomers (less than 10%). This is consistent with our EM results that observed ErbB1 clusters in the resting state.

Our results differ from previous work. Anderson and colleagues suggested that signaling by ErbB1 might be regulated in part by residency of resting receptors in caveolae, followed by ligand-induced movement out of these specialized domains followed by endocytosis in coated pits. In 1995, Smart and colleagues in the Anderson group reported

EGFR was enriched in caveolae membrane fraction by using biochemical analyses of detergent-free, density gradient fractionated membranes. In 1999, Mineo in the same group reported EGFR was initially enriched in caveolae, but rapidly moved out of this membrane microdomain in response to EGF stimulation (Mineo et al. 1999). Again, this conclusion was based on biochemical analysis, not morphological observation. In 2002, Anderson summarize the different sizes of lipid rafts, range from 4nm to 700nm, based on many biochemistry or biophysical observation (for example molecular cross-linking, laser trap, depolarization FRET and single-particle tracking) in a review paper (Anderson et al. 2002). However, none of those methods have the ability to observe caveolae in high resolution like EM studies.

To determine if resting or activated receptors occupy caveolar membrane, we prepared plasma membrane sheets on EM grids by the "rip-flip" method, followed by labeling specific proteins (and lipids) on the native membrane preparations with gold probes and imaging by transmission electron microscopy (TEM) (Wilson et al. 2001; Wiley et al. 2003; Wilson et al. 2004; Wilson et al. 2007; Xue et al. 2007). We found that resting ErbB family members were not resident in structures resembling caveolae or clathrin-coated pits in SKBR3 cells.

We realize that the use of different cell lines may contribute to our disagreement with previous work. We have worked principally with an aggressive breast cancer cell line that lacks significant caveolae. Thus it is not surprising that we did not observe the residency of resting ErbB in caveolae-like structures. To better test the Anderson hypothesis, a cell system enriched with caveolae and clathrin would be a better model.

Landgraf also demonstrated the phenomenon of ErbB3 oligomerization in an *in vitro* biochemistry analysis by using the purified ErbB3 extracellular domain expressed in Drosophila S2 cells (Landgraf, 2000, Kani, 2005). This *in vitro* study concluded that ErbB3 formed inactive oligomers before Heregulin stimulation, and the oligomers were dissociated by Heregulin stimulation. Our conclusion from studies in native membranes is directly opposite. We observed ErbB3 clusters were small in resting cells, ranging in size from 1 to 7, followed by formation of large clusters with hundreds of ErbB3 receptors after Heregulin treatment. The radically different outcome of *in vitro* versus intact cell studies emphasizes the importance of validating results under physiological conditions. If inactive ErbB3 oligomers exist, they must be composed of dimers or limited to only a few receptors per oligomer.

We noted two patterns of association of PI 3-kinase with the ErbB3 signaling patches. PI3- kinase was either well mixed with ErbB3 or it showed a ring structure around ErbB3 clusters. The ring structure of PI 3-kinase suggests that PI 3-kinase may associate with another protein or lipid in the membrane after initial recruitment by ErbB3. This is a novel observation and potentially important. The p85 that associates with activated ErbB3 appears to derive from a membrane-associated pool. Further study is needed to identify the binding sites involved in anchoring p85 to the membrane in resting cells and activating cells.

The high resolution immunoelectron microscopy technique gives us "snapshots" of the ErbB signaling process. It provides only limited temporal information and it cannot directly measure dimerization. As a future direction, we propose to take advantage of the

quantum dot/single particle tracking approach developed by a colleague, Dr. Lidke. Dr. Lidke has already demonstrated the power of single particle tracking to follow EGFR dynamics (Lidke et al. 2004; Lidke et al. 2005). This technique offer the opportunities to watch receptor diffusion on the cell surface under different conditions (resting, after stimulation or inhibition with drugs), and to visualize direct receptor dimerization and receptor movement on the cell surface, as well as endocytosis or retrograde transport on the filopodia. This technique has the capability to resolve unanswered questions presented in this work, especially the proof that ErbB3 homodimers exist.

5.2 Kinase domain mutations in cancer are common in ErbB and other RTKs

To the best of our knowledge, the ErbB3 E933Q substitution described here is the first report of a functional ErbB3 alteration in a cancer cell lines. We found that cells expressing the E933Q form of ErbB3 are more sensitive to ligand stimulation than the cells expressing WT ErbB3 and that they amplify the ErbB3/PI3K/AKT cell survival pathway. We propose that this substitution fall within a general class of RTK mutations in the RTK kinase domain tail. In a study of 188 human lung adenocarcinomas, more than 1000 somatic mutation were found in 623 genes with known or potential relationships to cancer (Ding et al. 2008). As shown in figure 4.3, somatic mutations were found in five receptor families, including the ErbB family. A number of these mutations are located at near the carboxyl “end” of kinase domain. It suggesting that they are mutational “hot spot” with potentially similar effects.

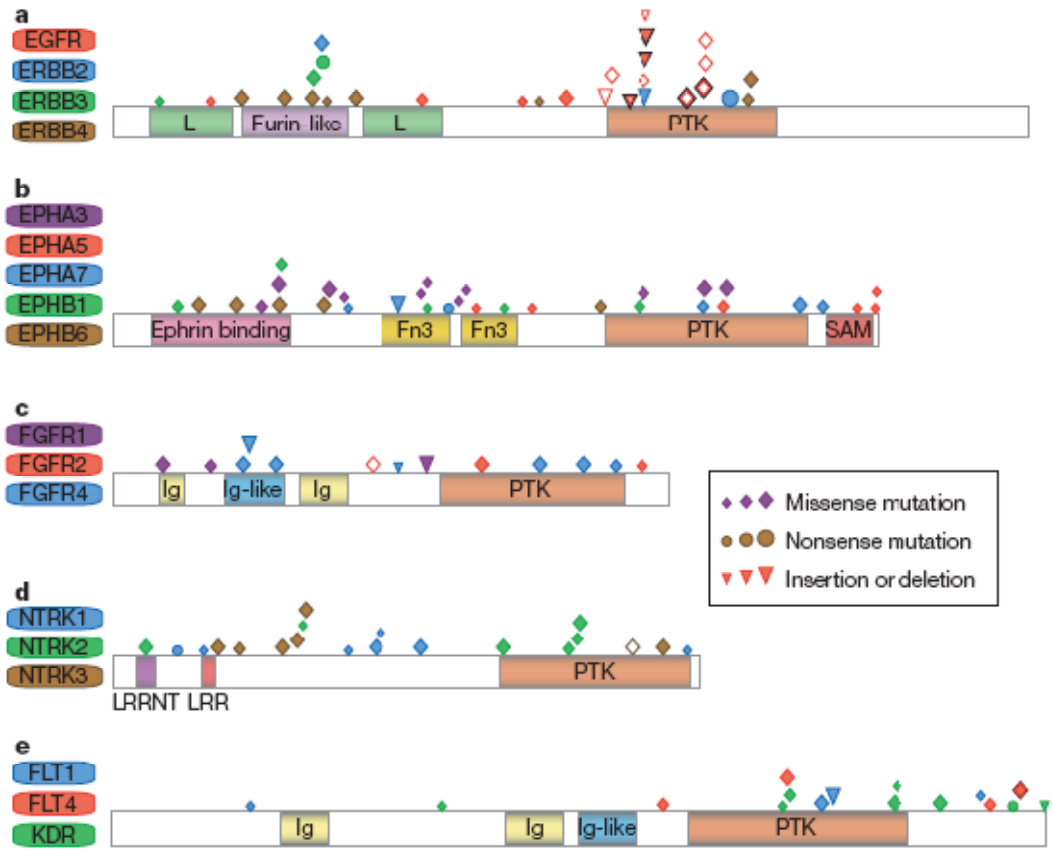

Figure 5.3 Diagrams of mutations found in the members of several receptor families in lung adenocarcinomas (from Nature, 2008, 455:1069-1075)

RTK mutations have been documented for many cases of cancer and have been linked to some outcomes of cancer therapy. EGFR mutations in lung cancer provide a striking example. In 2004, four important papers reported EGFR mutation in non-small cell lung cancer (NSCLC) (Baker 2004; Lynch et al. 2004; Paez et al. 2004; Sordella et al. 2004). These mutations include missense mutations (L834R, G965S) and deletion mutations (ΔL723-P729insS) that resulted in upregulation of the RAS/MAPK and STAT5 signaling pathways. Importantly, patients harboring these mutations account for only about 10-20% of all NSCLC cases and these patients show a 90-95% response rate to treatment with the

EGFR inhibitor, Gefitinib, compared to only 10-13% response rates in patients lacking EGFR mutations. Subsequent studies have demonstrated that this class of EGFR mutation results in ligand-independent receptor activation and changes in EGF ligand binding affinity. These results suggest a general concept to be tested in cells expressing WT and mutant forms of other RTKs.

It is interesting to speculate on why Gefitinib is so effective against lung cancer cells expressing these EGFR mutations. Since the precise somatic mutations vary between different patient samples, they are unlikely to be "initiating" mutations that drive the establishment of tumors. On the other hand, they may occur as secondary mutations that cells come to depend on for proliferation, leading to increased sensitivity to Gefitinib. Previously the term "Oncogene addiction" has been proposed to explain the apoptosis of cancer cells after suppression of a proliferative signal on which they have become dependent" (Weinstein 2002; Sordella et al. 2004). There are now initiatives in cancer genomics that attempt to map the frequency of somatic mutations in tumors, with the recognition that not all mutations contribute to the disease process. We believe that many more receptor kinase domain mutations are likely to be significant. Further study is warranted to evaluate potential new gain-of-function mutations. We further propose that full appreciation of ErbB3 kinase domain mutations will require screening of large (300-400 patients) tumor sets in breast, lung and endometrium. The additional ErbB3 mutations observed by others (Table 1.2) also still need to be characterized.

5.3 Implications of this work for current and future anticancer therapies

Therapeutic drugs targeting ErbB family members have achieved some degree of success for the treatment of breast, colon, lung, and pancreatic cancers. However, not all tumors respond to these therapeutic reagents and in many cases resistance eventually develops. Many resistance mechanisms have been proposed, including 1) a second EGFR resistant mutation, T790M, in lung cancer, 2) increased cell signaling through loss of PTEN or increased AKT activity and 3) alternative cell signaling mediated by ErbB family pathways through ligand (TGF-α, Heregulin) overexpression or by other receptor pathways like VEGF or IGFIR family. Therefore, new therapeutic strategies need be designed and tested for broader success at targeting ErbB in cancer.

Pertuzumab (Omnitarg, 2C4), a humanized monoclonal antibody targeting ErbB2, is one of the new generation cancer therapy reagents targeting ErbB family members. Early studies of pertuzumab in breast, colon and lung cancer cell lines demonstrated that 2C4 disrupts Heregulin mediated ErbB2-ErbB3 association and further blocks Heregulin mediated phosphorylation of ErbB2 and ErbB3, MAPK and Akt signaling pathway (Agus et al. 2002; Nahta et al. 2004; Sakai et al. 2007). Structural studies revealed that Pertuzumab binds the extracellular domain II of ErbB2 and prevents ligand-induced dimerization of ErbB2 with other ErbB family members (Franklin et al. 2004). It is currently in phase II and phase III clinical trials for several types of cancers (Johnson et al. 2006; Engel et al. 2007).

Our pertuzumab (2C4) data further confirm ErbB3 as a cancer therapy biomarker but raise a question about its mechanism of action. Based upon observations in Chapter 3, we propose that 2C4 does not block signaling by ErbB2 homodimers that form with overexpression. Rather, our data indicate that 2C4 blocks only ErbB2-dependent ErbB3 signaling and we predict therefore that response to pertuzumab should be dependent on ErbB3 expression. This idea is consistent with Lee-Hoeflich's findings that ErbB3 are critical for therapeutic response in ErbB2-overexpressed breast cancer cells (Lee-Hoeflich et al. 2008) .

Hsieh and Moasser proposed in a minireview in *British Journal of Cancer*: "the critical role of ErbB3 in cancer progression and drug resistance has two implications for future directions: …. ErbB3 is a much more suitable biomarker to guide the efficacy of treatments;…. identifies ErbB3 as a novel target for newer anti-cancer agents that can potentially overcome TKI resistance." (Hsieh et al. 2007).

One possible approach is to combine current chemotherapy with ErbB targeting agents, or to combine different ErbB targeting drugs, generating "pan-ErbB" drugs. One good "combination" strategy may be to employ drugs that target both ErbB and MET in ErbB TKI resistant NSCLC patient. The rationale for this suggestion is based on findings by Sergina and his colleagues (Sergina et al. 2007), that MET is amplified in about 20% of gefitinib-resistant lung cancer cell lines and is able to activate ErbB3 signaling and promote cell survival. Importantly, MET inhibition restores gefitinib sensitivity.

Therefore, simultaneous targeting of ErbB and MET should be an ideal strategy for future therapies aimed at overcoming TKI resistance due to ErbB3 tansactivation.

Another approach may be the use of ErbB3 SiRNA, as proposed by the Sithnandam and Anderson group in lung adenocarcinoma (Sithnandam, 2008). Humanized anti-ErbB3 antibody are also feasible drug and data on the antibody MM121 was presented at AACR 2008 by Kwok-Kin Wong (Dana-Farber Cancer Institute). Based on a literature search, a third approach is proposed here, using two natural drugs, Kahalalide F (KF) and Isoliquiritigenin (ISL). Although not intentionally designed to target ErbB3, these drugs proved to deplete ErbB3 (Janmaat et al. 2005; Jung et al. 2006; Shilabin et al. 2007). KF is a semisynthetic modification of a natural depsipeptides, with antitumor activity and antifungal activity. It induces necrosis-like cell death that involves depletion of ErbB3 and inhibition of Akt signaling. Currently KF has completed phase I trials and a phase II trial is in progress (Janmaat et al. 2005; Shilabin et al. 2007). ISL, a flavonoid found in licorice, shallots, and bean sprouts, is a potent anti-tumor promoting agent. ISL inhibits ErbB3 signaling in prostate cancer cells by reducing the protein and mRNA levels of ErbB3 in a dose-dependent manner, inhibiting HRG induced ErbB3 phosphorylation and binding with PI3K (Jung et al. 2006) .

As stated so eloquently by Shepard, “We believe that broader success in developing therapies directed at HER family members depends upon an increased appreciation for how these receptors consolidate signals from diverse sources and how they cooperate toward functional homeostasis in cancer cells.” (Shepard et al. 2008).

6. Acknowledgments

This work was supported by NIH grants R01 CA119232 and by the Oxnard Foundation. Use of the EM and flow cytometry facilities at the UNM SOM and CRTC, and NIH support for these cores, is gratefully acknowledged. Spatial statistics tools used here are available at http://cellpath.health.unm.edu/stmc/emtools/index.html.

7. Appendices. Abbreviations used

BRK (PTK6)	Breast tumor kinase (protein tyrosine kinase 6)
EGF	Epidermal growth factor
EGFR	Epidermal growth factor receptor
GPCR	G protein coupled receptor
HRG	Heregulin
MET	Hepatocyte growth factor
NRDP1	Neuregulin receptor degradation protein
PLCγ	Phospholipase Cγ
RTK	Receptor tyrosine kinase
STAT5	Signal transducer and activation of transcription 5

References

Agus, D. B., R. W. Akita, et al. (2002). "Targeting ligand-activated ErbB2 signaling inhibits breast and prostate tumor growth." Cancer Cell **2**(2): 127-37.

Alimandi, M., A. Romano, et al. (1995). "Cooperative signaling of ErbB3 and ErbB2 in neoplastic transformation and human mammary carcinomas." Oncogene **10**(9): 1813-21.

Anderson, R. G. and K. Jacobson (2002). "A role for lipid shells in targeting proteins to caveolae, rafts, and other lipid domains." Science **296**(5574): 1821-5.

Axelrod, D., D. E. Koppel, et al. (1976). "Mobility measurement by analysis of fluorescence photobleaching recovery kinetics." Biophys J **16**(9): 1055-69.

Baker, M. (2004). "EGFR inhibitors square off at ASCO." Nat Biotechnol **22**(6): 641.

Bouyain, S., P. A. Longo, et al. (2005). "The extracellular region of ErbB4 adopts a tethered conformation in the absence of ligand." Proc Natl Acad Sci U S A **102**(42): 15024-9.

Burgess, A. W., H. S. Cho, et al. (2003). "An open-and-shut case? Recent insights into the activation of EGF/ErbB receptors." Mol Cell **12**(3): 541-52.

Cai, Z., G. Zhang, et al. (2008). "Differential binding patterns of monoclonal antibody 2C4 to the ErbB3-p185her2/neu and the EGFR-p185her2/neu complexes." Oncogene **27**(27): 3870-4.

Carpenter, G. (2000). "The EGF receptor: a nexus for trafficking and signaling." Bioessays **22**(8): 697-707.

Choi, S. H., J. M. Mendrola, et al. (2007). "EGF-independent activation of cell-surface EGF receptors harboring mutations found in gefitinib-sensitive lung cancer." Oncogene **26**(11): 1567-76.

Chung, J. C., N. Sciaky, et al. (1997). "Heterogeneity of epidermal growth factor binding kinetics on individual cells." Biophys J **73**(2): 1089-102.

Citri, A. and Y. Yarden (2006). "EGF-ERBB signalling: towards the systems level." Nat Rev Mol Cell Biol **7**(7): 505-16.

Contessa, J. N., A. Abell, et al. (2006). "Compensatory ErbB3/c-Src signaling enhances carcinoma cell survival to ionizing radiation." Breast Cancer Res Treat **95**(1): 17-27.

Diamonti, A. J., P. M. Guy, et al. (2002). "An RBCC protein implicated in maintenance of steady-state neuregulin receptor levels." Proc Natl Acad Sci U S A **99**(5): 2866-71.

DiGiovanna, M. P. (1997). "Phosphorylation sensitivity of the commonly used anti-p185neu/erbB2 monoclonal antibody clone 3B5 suggests selective usage of autophosphorylation sites." Anal Biochem **247**(1): 167-70.

DiGiovanna, M. P., D. F. Stern, et al. (2005). "Relationship of epidermal growth factor receptor expression to ErbB-2 signaling activity and prognosis in breast cancer patients." J Clin Oncol **23**(6): 1152-60.

Ding, L., G. Getz, et al. (2008). "Somatic mutations affect key pathways in lung adenocarcinoma." Nature **455**(7216): 1069-75.

Edidin, M. (1997). "Lipid microdomains in cell surface membranes." Curr Opin Struct Biol **7**(4): 528-32.

Engel, R. H. and V. G. Kaklamani (2007). "HER2-positive breast cancer: current and future treatment strategies." Drugs **67**(9): 1329-41.

Engelman, J. A., K. Zejnullahu, et al. (2007). "MET amplification leads to gefitinib resistance in lung cancer by activating ERBB3 signaling." Science **316**(5827): 1039-43.

Fiddes, R. J., D. H. Campbell, et al. (1998). "Analysis of Grb7 recruitment by heregulin-activated erbB receptors reveals a novel target selectivity for erbB3." J Biol Chem **273**(13): 7717-24.

Franklin, M. C., K. D. Carey, et al. (2004). "Insights into ErbB signaling from the structure of the ErbB2-pertuzumab complex." Cancer Cell **5**(4): 317-28.

Garrett, T. P., N. M. McKern, et al. (2003). "The crystal structure of a truncated ErbB2 ectodomain reveals an active conformation, poised to interact with other ErbB receptors." Mol Cell **11**(2): 495-505.

Ginsberg, M. H., A. Partridge, et al. (2005). "Integrin regulation." Curr Opin Cell Biol **17**(5): 509-16.

Guy, P. M., J. V. Platko, et al. (1994). "Insect cell-expressed p180erbB3 possesses an impaired tyrosine kinase activity." Proc Natl Acad Sci U S A **91**(17): 8132-6.

Haase, P. (1995). "Spatial pattern analysis in ecology based on ripley's K function: introduction and methods of edge correction." journal of Vegetation Science **6**: 575-582.

Harari, D. and Y. Yarden (2000). "Molecular mechanisms underlying ErbB2/HER2 action in breast cancer." Oncogene **19**(53): 6102-14.

Hendriks, B. S., L. K. Opresko, et al. (2003). "Quantitative analysis of HER2-mediated effects on HER2 and epidermal growth factor receptor endocytosis: distribution of homo- and heterodimers depends on relative HER2 levels." J Biol Chem **278**(26): 23343-51.

Hsieh, A. C. and M. M. Moasser (2007). "Targeting HER proteins in cancer therapy and the role of the non-target HER3." Br J Cancer **97**(4): 453-7.

Hsieh, M. Y., S. Yang, et al. (2008). "Stochastic simulations of ErbB homo and heterodimerisation: potential impacts of receptor conformational state and spatial segregation." IET Syst Biol **2**(5): 256-72.

Hynes, N. E. and H. A. Lane (2005). "ERBB receptors and cancer: the complexity of targeted inhibitors." Nat Rev Cancer **5**(5): 341-54.

Ichinose, J., M. Murata, et al. (2004). "EGF signalling amplification induced by dynamic clustering of EGFR." Biochem Biophys Res Commun **324**(3): 1143-9.

Insel, P. A., B. P. Head, et al. (2005). "Caveolae and lipid rafts: G protein-coupled receptor signaling microdomains in cardiac myocytes." Ann N Y Acad Sci **1047**: 166-72.

Jain, K. A., U. M. Hamper, et al. (1988). "Comparison of transvaginal and transabdominal sonography in the detection of early pregnancy and its complications." AJR Am J Roentgenol **151**(6): 1139-43.

Janmaat, M. L., J. A. Rodriguez, et al. (2005). "Kahalalide F induces necrosis-like cell death that involves depletion of ErbB3 and inhibition of Akt signaling." Mol Pharmacol **68**(2): 502-10.

Jeong, E. G., Y. H. Soung, et al. (2006). "ERBB3 kinase domain mutations are rare in lung, breast and colon carcinomas." Int J Cancer **119**(12): 2986-7.

Johns, T. G., T. E. Adams, et al. (2004). "Identification of the epitope for the epidermal growth factor receptor-specific monoclonal antibody 806 reveals that it preferentially recognizes an untethered form of the receptor." J Biol Chem **279**(29): 30375-84.

Johnson, B. E. and P. A. Janne (2006). "Rationale for a phase II trial of pertuzumab, a HER-2 dimerization inhibitor, in patients with non-small cell lung cancer." Clin Cancer Res **12**(14 Pt 2): 4436s-4440s.

Jones, J. T., R. W. Akita, et al. (1999). "Binding specificities and affinities of egf domains for ErbB receptors." FEBS Lett **447**(2-3): 227-31.

Jones, R. B., A. Gordus, et al. (2006). "A quantitative protein interaction network for the ErbB receptors using protein microarrays." Nature **439**(7073): 168-74.

Jorissen, R. N., F. Walker, et al. (2003). "Epidermal growth factor receptor: mechanisms of activation and signalling." Exp Cell Res **284**(1): 31-53.

Jung, J. I., E. Chung, et al. (2006). "Isoliquiritigenin (ISL) inhibits ErbB3 signaling in prostate cancer cells." Biofactors **28**(3-4): 159-68.

Kamalati, T., H. E. Jolin, et al. (2000). "Expression of the BRK tyrosine kinase in mammary epithelial cells enhances the coupling of EGF signalling to PI 3-kinase and Akt, via erbB3 phosphorylation." Oncogene **19**(48): 5471-6.

Kani, K., C. M. Warren, et al. (2005). "Oligomers of ERBB3 have two distinct interfaces that differ in their sensitivity to disruption by heregulin." J Biol Chem **280**(9): 8238-47.

Karlin, J. D., D. Nguyen, et al. (2005). "Epidermal growth factor receptor expression in breast cancer." J Clin Oncol **23**(31): 8118-9; author reply 8119-20.

Kim, J. H., L. Cramer, et al. (2005). "Independent trafficking of Ig-alpha/Ig-beta and mu-heavy chain is facilitated by dissociation of the B cell antigen receptor complex." J Immunol **175**(1): 147-54.

Koleske, A. J., D. Baltimore, et al. (1995). "Reduction of caveolin and caveolae in oncogenically transformed cells." Proc Natl Acad Sci U S A **92**(5): 1381-5.

Kraus, M. H., P. Fedi, et al. (1993). "Demonstration of ligand-dependent signaling by the erbB-3 tyrosine kinase and its constitutive activation in human breast tumor cells." Proc Natl Acad Sci U S A **90**(7): 2900-4.

Kraus, M. H., W. Issing, et al. (1989). "Isolation and characterization of ERBB3, a third member of the ERBB/epidermal growth factor receptor family: evidence for overexpression in a subset of human mammary tumors." Proc Natl Acad Sci U S A **86**(23): 9193-7.

Kraus, M. H., N. C. Popescu, et al. (1987). "Overexpression of the EGF receptor-related proto-oncogene erbB-2 in human mammary tumor cell lines by different molecular mechanisms." Embo J **6**(3): 605-10.

Landgraf, R. and D. Eisenberg (2000). "Heregulin reverses the oligomerization of HER3." Biochemistry **39**(29): 8503-11.

Lee-Hoeflich, S. T., L. Crocker, et al. (2008). "A central role for HER3 in HER2-amplified breast cancer: implications for targeted therapy." Cancer Res **68**(14): 5878-87.

Lee, J. W., Y. H. Soung, et al. (2006). "Somatic mutations of ERBB2 kinase domain in gastric, colorectal, and breast carcinomas." Clin Cancer Res **12**(1): 57-61.

Lessor, T. J., J. Y. Yoo, et al. (2000). "Ectopic expression of the ErbB-3 binding protein ebp1 inhibits growth and induces differentiation of human breast cancer cell lines." J Cell Physiol **183**(3): 321-9.

Lidke, D. S., K. A. Lidke, et al. (2005). "Reaching out for signals: filopodia sense EGF and respond by directed retrograde transport of activated receptors." J Cell Biol **170**(4): 619-26.

Lidke, D. S., P. Nagy, et al. (2004). "Quantum dot ligands provide new insights into erbB/HER receptor-mediated signal transduction." Nat Biotechnol **22**(2): 198-203.

Lillemeier, B. F., J. R. Pfeiffer, et al. (2006). "Plasma membrane-associated proteins are clustered into islands attached to the cytoskeleton." Proc Natl Acad Sci U S A **103**(50): 18992-7.

Linggi, B. and G. Carpenter (2006). "ErbB receptors: new insights on mechanisms and biology." Trends Cell Biol **16**(12): 649-56.

Luo, C., K. Wang, et al. (2008). "The functional roles of lipid rafts in T cell activation, immune diseases and HIV infection and prevention." Cell Mol Immunol **5**(1): 1-7.

Lynch, T. J., D. W. Bell, et al. (2004). "Activating mutations in the epidermal growth factor receptor underlying responsiveness of non-small-cell lung cancer to gefitinib." N Engl J Med **350**(21): 2129-39.

Martin-Fernandez, M., D. T. Clarke, et al. (2002). "Preformed oligomeric epidermal growth factor receptors undergo an ectodomain structure change during signaling." Biophys J **82**(5): 2415-27.

McLaughlin, S., S. O. Smith, et al. (2005). "An electrostatic engine model for autoinhibition and activation of the epidermal growth factor receptor (EGFR/ErbB) family." J Gen Physiol **126**(1): 41-53.

Mineo, C., G. N. Gill, et al. (1999). "Regulated migration of epidermal growth factor receptor from caveolae." J Biol Chem **274**(43): 30636-43.

Nagy, P., A. Jenei, et al. (1999). "Activation-dependent clustering of the erbB2 receptor tyrosine kinase detected by scanning near-field optical microscopy." J Cell Sci **112 (Pt 11)**: 1733-41.

Nagy, P., L. Matyus, et al. (2001). "Cell fusion experiments reveal distinctly different association characteristics of cell-surface receptors." J Cell Sci **114**(Pt 22): 4063-71.

Nagy, P., G. Vereb, et al. (2002). "Lipid rafts and the local density of ErbB proteins influence the biological role of homo- and heteroassociations of ErbB2." J Cell Sci **115**(Pt 22): 4251-62.

Nahta, R., M. C. Hung, et al. (2004). "The HER-2-targeting antibodies trastuzumab and pertuzumab synergistically inhibit the survival of breast cancer cells." Cancer Res **64**(7): 2343-6.

Orr, G., D. Hu, et al. (2005). "Cholesterol dictates the freedom of EGF receptors and HER2 in the plane of the membrane." Biophys J **89**(2): 1362-73.

Paez, J. G., P. A. Janne, et al. (2004). "EGFR mutations in lung cancer: correlation with clinical response to gefitinib therapy." Science **304**(5676): 1497-500.

Penuel, E., R. W. Akita, et al. (2002). "Identification of a region within the ErbB2/HER2 intracellular domain that is necessary for ligand-independent association." J Biol Chem **277**(32): 28468-73.

Pike, L. J. (2005). "Growth factor receptors, lipid rafts and caveolae: an evolving story." Biochim Biophys Acta **1746**(3): 260-73.

Pike, L. J., X. Han, et al. (2005). "Epidermal growth factor receptors are localized to lipid rafts that contain a balance of inner and outer leaflet lipids: a shotgun lipidomics study." J Biol Chem **280**(29): 26796-804.

Plowman, G. D., G. S. Whitney, et al. (1990). "Molecular cloning and expression of an additional epidermal growth factor receptor-related gene." Proc Natl Acad Sci U S A **87**(13): 4905-9.

Prigent, S. A. and W. J. Gullick (1994). "Identification of c-erbB-3 binding sites for phosphatidylinositol 3'-kinase and SHC using an EGF receptor/c-erbB-3 chimera." Embo J **13**(12): 2831-41.

Prior, I. A., C. Muncke, et al. (2003). "Direct visualization of Ras proteins in spatially distinct cell surface microdomains." J Cell Biol **160**(2): 165-70.

Puri, C., D. Tosoni, et al. (2005). "Relationships between EGFR signaling-competent and endocytosis-competent membrane microdomains." Mol Biol Cell **16**(6): 2704-18.

Ringerike, T., F. D. Blystad, et al. (2002). "Cholesterol is important in control of EGF receptor kinase activity but EGF receptors are not concentrated in caveolae." J Cell Sci **115**(Pt 6): 1331-40.

Roepstorff, K., P. Thomsen, et al. (2002). "Sequestration of epidermal growth factor receptors in non-caveolar lipid rafts inhibits ligand binding." J Biol Chem **277**(21): 18954-60.

Roskoski, R., Jr. (2004). "The ErbB/HER receptor protein-tyrosine kinases and cancer." Biochem Biophys Res Commun **319**(1): 1-11.

Rousseau, D. L., Jr., J. V. Staros, et al. (1995). "The interaction of epidermal growth factor with its receptor in A431 cell membranes: a stopped-flow fluorescence anisotropy study." Biochemistry **34**(44): 14508-18.

Rowinsky, E. K. (2004). "The erbB family: targets for therapeutic development against cancer and therapeutic strategies using monoclonal antibodies and tyrosine kinase inhibitors." Annu Rev Med **55**: 433-57.

Ruhe, J. E., S. Streit, et al. (2007). "Genetic alterations in the tyrosine kinase transcriptome of human cancer cell lines." Cancer Res **67**(23): 11368-76.

Saffarian, S., Y. Li, et al. (2007). "Oligomerization of the EGF receptor investigated by live cell fluorescence intensity distribution analysis." Biophys J **93**(3): 1021-31.

Sakai, K., H. Yokote, et al. (2007). "Pertuzumab, a novel HER dimerization inhibitor, inhibits the growth of human lung cancer cells mediated by the HER3 signaling pathway." Cancer Sci **98**(9): 1498-503.

Schulze, W. X., L. Deng, et al. (2005). "Phosphotyrosine interactome of the ErbB-receptor kinase family." Mol Syst Biol **1**: 2005 0008.

Sergina, N. V., M. Rausch, et al. (2007). "Escape from HER-family tyrosine kinase inhibitor therapy by the kinase-inactive HER3." Nature **445**(7126): 437-41.

Shepard, H. M., C. M. Brdlik, et al. (2008). "Signal integration: a framework for understanding the efficacy of therapeutics targeting the human EGFR family." J Clin Invest **118**(11): 3574-81.

Shilabin, A. G., N. Kasanah, et al. (2007). "Lysosome and HER3 (ErbB3) selective anticancer agent kahalalide F: semisynthetic modifications and antifungal lead-exploration studies." J Med Chem **50**(18): 4340-50.

Sierke, S. L., K. Cheng, et al. (1997). "Biochemical characterization of the protein tyrosine kinase homology domain of the ErbB3 (HER3) receptor protein." Biochem J **322 (Pt 3)**: 757-63.

Sithanandam, G. and L. M. Anderson (2008). "The ERBB3 receptor in cancer and cancer gene therapy." Cancer Gene Ther **15**(7): 413-48.

Sliwkowski, M. X., G. Schaefer, et al. (1994). "Coexpression of erbB2 and erbB3 proteins reconstitutes a high affinity receptor for heregulin." J Biol Chem **269**(20): 14661-5.

Smart, E. J., Y. S. Ying, et al. (1995). "A detergent-free method for purifying caveolae membrane from tissue culture cells." Proc Natl Acad Sci U S A **92**(22): 10104-8.

Soltoff, S. P., K. L. Carraway, 3rd, et al. (1994). "ErbB3 is involved in activation of phosphatidylinositol 3-kinase by epidermal growth factor." Mol Cell Biol **14**(6): 3550-8.

Sordella, R., D. W. Bell, et al. (2004). "Gefitinib-sensitizing EGFR mutations in lung cancer activate anti-apoptotic pathways." Science **305**(5687): 1163-7.

Soung, Y. H., J. W. Lee, et al. (2006). "Somatic mutations of the ERBB4 kinase domain in human cancers." Int J Cancer **118**(6): 1426-9.

Stephens, P., C. Hunter, et al. (2004). "Lung cancer: intragenic ERBB2 kinase mutations in tumours." Nature **431**(7008): 525-6.

Szabo, A., G. Horvath, et al. (2008). "Quantitative characterization of the large-scale association of ErbB1 and ErbB2 by flow cytometric homo-FRET measurements." Biophys J **95**(4): 2086-96.

Tikhomirov, O. and G. Carpenter (2004). "Ligand-induced, p38-dependent apoptosis in cells expressing high levels of epidermal growth factor receptor and ErbB-2." J Biol Chem **279**(13): 12988-96.

Todd, D. G., R. B. Mikkelsen, et al. (1999). "Ionizing radiation stimulates existing signal transduction pathways involving the activation of epidermal growth factor receptor and ERBB-3, and changes of intracellular calcium in A431 human squamous carcinoma cells." J Recept Signal Transduct Res **19**(6): 885-908.

Wang, Z., L. Zhang, et al. (1999). "Endocytosis deficiency of epidermal growth factor (EGF) receptor-ErbB2 heterodimers in response to EGF stimulation." Mol Biol Cell **10**(5): 1621-36.

Warren, C. M. and R. Landgraf (2006). "Signaling through ERBB receptors: multiple layers of diversity and control." Cell Signal **18**(7): 923-33.

Weinstein, I. B. (2002). "Cancer. Addiction to oncogenes--the Achilles heal of cancer." Science **297**(5578): 63-4.

Wieduwilt, M. J. and M. M. Moasser (2008). "The epidermal growth factor receptor family: biology driving targeted therapeutics." Cell Mol Life Sci **65**(10): 1566-84.

Wiley, H. S., S. Y. Shvartsman, et al. (2003). "Computational modeling of the EGF-receptor system: a paradigm for systems biology." Trends Cell Biol **13**(1): 43-50.

Wilson, B. S., J. R. Pfeiffer, et al. (2000). "Observing FcepsilonRI signaling from the inside of the mast cell membrane." J Cell Biol **149**(5): 1131-42.

Wilson, B. S., J. R. Pfeiffer, et al. (2007). Electron microscopy methods to study membrane organization. Methods in Molecular Biology. T. McIntosh, Humana Press. **398:** 247-263.

Wilson, B. S., J. R. Pfeiffer, et al. (2001). "High resolution mapping of mast cell membranes reveals primary and secondary domains of Fc(epsilon)RI and LAT." J Cell Biol **154**(3): 645-58.

Wilson, B. S., S. L. Steinberg, et al. (2004). "Markers for detergent-resistant lipid rafts occupy distinct and dynamic domains in native membranes." Mol Biol Cell **15**(6): 2580-92.

Xue, M., G. Hsieh, et al. (2007). "Activated N-formyl peptide receptor and high-affinity IgE receptor occupy common domains for signaling and internalization." Mol Biol Cell **18**(4): 1410-20.

Yang, S., M. A. Raymond-Stintz, et al. (2007). "Mapping ErbB receptors on breast cancer cell membranes during signal transduction." J Cell Sci **120**(Pt 16): 2763-73.

Yarden, Y. and M. X. Sliwkowski (2001). "Untangling the ErbB signalling network." Nat Rev Mol Cell Biol **2**(2): 127-37.

Zhang, J., K. Leiderman, et al. (2006). "Characterizing the topography of membrane receptors and signaling molecules from spatial patterns obtained using nanometer-scale electron-dense probes and electron microscopy." Micron **37**(1): 14-34.

Zhang, J., S. L. Steinberg, et al. (2008). "Markov random field modeling of the spatial distribution of proteins on cell membranes." Bull Math Biol **70**(1): 297-321.

Zhang, X., J. Gureasko, et al. (2006). "An allosteric mechanism for activation of the kinase domain of epidermal growth factor receptor." Cell **125**(6): 1137-49.